Evolution of Postural Diversity in Primates as Reflected by the Size and Shape of the Medial Tibial Facet of the Talus

Doug M. Boyer,[1,2*] Gabriel S. Yapuncich,[1] Jared E. Butler,[3] Rachel H. Dunn,[4] and Erik R. Seiffert[5*]

[1]*Department of Evolutionary Anthropology, Duke University, Durham, NC 27708*
[2]*New York Consortium in Evolutionary Primatology (NYCEP), New York, NY*
[3]*Department of Anthropology and Archaeology, Brooklyn College, City University of New York (CUNY), Brooklyn, NY 11210*
[4]*Department of Anatomy, Des Moines University, Des Moines, IA 50312*
[5]*Department of Anatomical Sciences, Stony Brook University, Stony Brook, NY 11776*

KEY WORDS astragalus; calcaneus; prosimian; primate origins; strepsirrhine; grasp-leaping; pedal inversion; *Eosimias*

ABSTRACT *OBJECTIVES:* Comprehensive quantification of the shape and proportions of the medial tibial facet (MTF) of the talus (=astragalus) has been lacking for Primates and their closest relatives. In this study, aspects of MTF form were quantified and employed to test hypotheses about their functional and phylogenetic significance. The following hypotheses influence perceptions of primate evolutionary history but are due for more rigorous assessment: 1) A relatively large MTF distinguishes "prosimians" (strepsirrhines and tarsiers) from anthropoids and non-primate euarchontans; 2) the distinctive form of the "prosimian" MTF is a correlate of locomotor tendencies that emphasize use of vertical and small diameter supports in conjunction with inverted, abducted foot postures; and 3) the "prosimian" MTF form arose along the primate stem lineage and was present in the euprimate common ancestor.
METHODS: Three-dimensional (3D) scanning was used to create scale digital models of tali (n = 378 specimens, 122 species) from which three types of variables capturing aspects of MTF form were computed: 1) MTF area relative to body mass and ectal facet area; 2) MTF shape (elliptical vs. non-elliptical); and 3) MTF dorsal restriction on the talar body (i.e., extensive vs. minimal exposure of non-articular area). Data were analyzed using both phylogenetic and traditional comparative methods including Phylogenetic Generalized Least Squares, Ordinary Least Squares, ANCOVA, ANOVA, and Bayesian Ancestral State Reconstruction (ASR).
RESULTS: Extant "prosimians" are generally distinct from anthropoids and non-primate euarchontans in our quantitative representations of MTF form. MTF area (but not shape or dorsal restriction) correlates with fibular facet angle (FFa) of the talus, which has also been argued to reflect habitual pedal inversion. Among strepsirrhines, taxa that engage in grasp-leaping more frequently/effectively appear to have a relatively larger MTF than less acrobatic taxa. Directional models of evolutionary change better describe the phylogenetic distribution of MTF variation than do other models. ASR shows 1) little change in the MTF along the primate stem, 2) independent evolution of relatively large and dorsoplantarly deep MTFs in basal haplorhines and strepsirrhines, and 3) re-evolution of morphologies similar to non-euprimates in anthropoids.
CONCLUSIONS: Results support the hypothesis that differences in MTF form between anthropoids and "prosimians" reflect greater use of inverted foot postures and grasp-leaping in the latter group. Although fossil "prosimians" do not have the extreme MTF dimensions that characterize many extant acrobatic leapers, these variables by themselves provide little additional behavioral resolution at the level of individual fossils due to strong phylogenetic signal. ASR suggests that some specialization for use of inverted foot postures (as required in a fine-branch niche) and modifications for grasp-leaping evolved independently in basal strepsirrhine and haplorhine lineages. Am J Phys Anthropol 000:000–000, 2015.

The talus is the primary mechanical link between the leg and the foot. As such, it is often responsible for transmitting forces generated by the majority of an animal's body mass, and enabling mobility and/or providing stability during most locomotor and postural behaviors. The talus articulates proximally with both the tibia and fibula, two bones that rarely articulate with other (non-talar) tarsals in primates. The complex morphology of the talus, its relatively straightforward functional role in the ankle joint, and its prevalence in the fossil record make it a useful element for both functional and phylo-

Grant sponsor: NSF BCS; Grant number: 1317525; Grant sponsor: American Association of Physical Anthropologists Professional Development Grants (D. M. B. and E. R. S.); Grant sponsor: SBE-1028505 to S. G. B. Chester and E. Sargis, a Leakey Foundation Grant to S. G. B. Chester, a Wenner Gren grant to C. Orr, a Leakey Foundation grant to B. A. Patel, BCS-1074079 to A. Su and A. B. Demes, and DGE-0966166 to E. Delson and others.

*Correspondence to: Doug Boyer; Duke University, Department of Evolutionary Anthropology, Box 90383, Durham, NC 27708.
E-mail: doug.boyer@duke.edu or Erik R. Seiffert; Department of Anatomical Sciences, Health Sciences Center T-8 Stony Brook University, Stony Brook, New York 11776.
E-mail: erik.seiffert@stonybrook.edu

Received 31 October 2014; accepted 6 January 2015

DOI: 10.1002/ajpa.22702
Published online 00 Month 2014 in Wiley Online Library (wileyonlinelibrary.com).

genetic inferences (e.g., Gebo, 1986; Beard et al., 1988; Dagosto, 1988; Gebo, 1988, 1993, 2011; Marivaux et al., 2003; Boyer et al., 2010; Boyer and Seiffert, 2013).

While talar morphology is frequently invoked in phylogenetic assessments of fossil taxa (Gebo, 1985, 1986; Beard et al., 1988; Dagosto, 1988; Gebo, 1988, 1993, 2011; Franzen et al., 2009; Boyer and Seiffert, 2013), there has been relatively little quantification of the bone's most important distinguishing features (Dagosto, 1988; Gebo, 2011; Boyer and Seiffert, 2013). With the aid of micro-computed tomographic (CT) scanning and three-dimensional (3D) digital surface models, such quantification is now possible. For instance, Boyer and Seiffert (2013) published a comprehensive quantitative analysis of the talo-fibular facet slope among primates. In this case, quantitative data largely confirmed previous perspectives (e.g., Gebo, 1986), and revealed a clear divide between extant haplorhines and strepsirrhines in fibular facet orientation. Nonetheless, this approach also uncovered some unexpected patterns. For example, galagids have some of the shallowest talofibular facet slopes (i.e., more "horizontal" facets) among strepsirrhines, instead of an "intermediate" slope as suggested by Gebo (1986). Additionally, the earliest adapiforms and omomyiforms were found to be fairly similar to each other and exhibit haplorhine-like facet slopes, rather than conforming to extant strepsirrhine and haplorhine patterns, respectively (Gebo et al., 2012b).

The size and shape of the talar medial tibial facet (MTF) are other features that have been frequently cited as distinguishing "prosimians" and anthropoids (Gebo, 1986; Beard et al., 1988; Dagosto, 1988; Gebo, 1988, 1993) and as reflecting important functional variation, but the complex shape of this facet has precluded precise quantification. Gebo (1986, p. 423) originally noted the "talar facet for the tibial medial malleolus is dorsoplantarly narrow in anthropoids. In prosimians, the talar facet extends to the edge of the plantar talar body." He further suggested the narrowing of the anthropoid MTF is directly related to the distal migration of the talotibial ligaments. Dagosto (1990, p. 125) put these observations into a broader taxonomic context:

> "In most eutherians the medial talotibial facet is dorsoplantarly shallow, and *does not reach the plantar edge of the talus* [italics added]. Plesiadapiforms and anthropoids also exhibit this condition, while in nonanthropoid euprimates, the facet normally extends plantad to the edge of the talus."

Subsequent discussions have characterized the anthropoid MTF as simply "reduced" (Gebo, 1993; Gebo et al., 2000, 2001; Gebo, 2011). Importantly, differences in MTF form between "prosimians" and anthropoids have been linked to postural differences. Gebo (1993, p. 191) wrote:

> "In anthropoids, the reduced talar facet for the tibia and the steep lateral facet for the fibula indicate shorter bony prongs to hold the talus secure and lessened capabilities for foot abduction relative to tooth-combed prosimians."

In reference to fossil remains attributed to Eocene eosimiids, Gebo et al. (2000, p. 277) stated:

> "The reduction of both the medial talotibial facet and the calcaneocuboid joint surface suggests that there was less stability in sustained habitually inverted foot positions. This implies more frequent use of horizontal foot postures and probably horizontal supports in *Eosimias* than in prosimian primates."

Functional considerations

Despite frequent descriptions of MTF variation, explicit biomechanical explanations for how differences in behavior might select for noted differences in MTF form have not been thoroughly addressed. Though it seems clear that dorsoplantar depth of the MTF should correlate with malleolar length and that longer malleoli should lead to a more stable crurotarsal joint, it is unclear why shorter "bony prongs" holding the talus secure would reduce "stability in sustained habitually inverted foot positions" specifically. Dagosto (1985) focused on describing morphofunctional relationships of the strepsirrhine medial malleolus and tibial facet. She described how a medially rotated tibial malleolus with a convex distal articular surface aids in abduction and adduction during dorsiflexion and plantarflexion respectively in strepsirrhines. She and others (e.g., Gebo, 1993) have explained the utility of this mobility on vertical supports. However, a similarly detailed explanation for a dorsoplantarly taller medial malleolus (and MTF) is lacking.

Gebo (2011) proposed that the more horizontal (or "shallowly sloping") talofibular facet orientation in strepsirrhines improves the facet's ability to transmit forces generated by body mass. This increased ability to transmit force may be particularly important when the forelimbs are not available to help distribute load, as in orthograde postures. Boyer and Seiffert (2013) agreed with Gebo's (2011) proposal but suggested that behavioral tendencies other than orthogrady were also relevant. Specifically, Boyer and Seiffert (2013) emphasized the importance of more frequent use of relatively small diameter, midline supports in strepsirrhines compared with haplorhines (Fig. 1). They suggested that locomotion on narrow (and hence medially positioned) substrates leads to postures in which the knee is positioned laterally relative to the foot, and that some foot inversion is accomplished by this lateral (outward) inclination of the leg relative to the foot (note that such configurations also imply flexed knees and flexed, abducted thighs). Imagining a primate standing in a quadrupedal posture on a relatively small diameter horizontal support: As its knees are flexed and abducted (so the legs become more laterally inclined, and increasingly horizontal), a more shallowly sloping fibular facet will maintain a weight-bearing role over a greater range of inversion angles than a steeper one (Boyer and Seiffert, 2013: their Fig. 10).

If pedal inversion through leg rotation and thigh abduction is a common configuration in strepsirrhines, there are biomechanical implications for the medial malleolus and MTF: lateral shear along the lateral talar margin (expressed in the lateral tibial facet) and compressive force on the medial talar margin (expressed in the MTF) will both tend to be higher. In other words, among strepsirrhines, we would expect facets on the lateral margin of the talus to be transmitting proportionally less force, and facets on the medial margin (primarily the MTF) to be transmitting proportionally

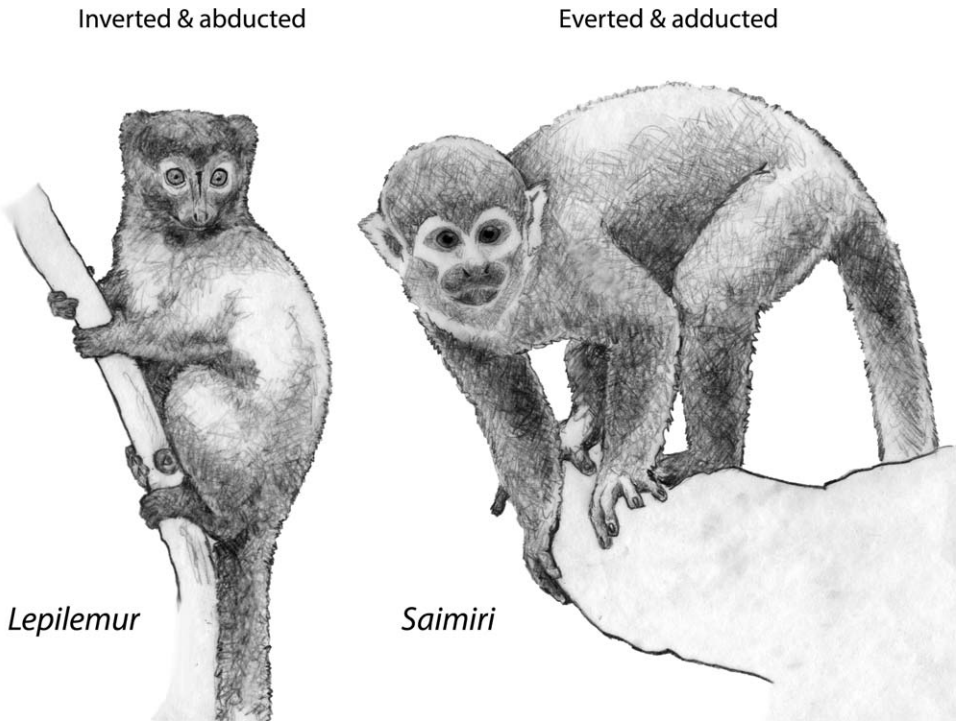

Fig. 1. Foot postures of "prosimians" (**left**) and anthropoids (**right**). Note the inverted, abducted foot in *Lepilemur* using small-diameter, inclined supports versus a more everted, adducted foot for *Saimiri*. In this study, we evaluate whether quantitative variation in the talar facets can be functionally correlated with such postural differences. Drawings by DMB.

more force. Increasing the area of contact between the medial malleolus and MTF would mitigate risks associated with both increased lateral shear and compressive force. Referring to this tradeoff, Yapuncich and Boyer (2014, p. 167) state that: "Explaining facet differences between strepsirrhines and haplorhines as consequences of habitual postural differences leads to the expectation that the MTF should also be larger in strepsirrhines than haplorhines at a given (body) size." If this functional explanation is correct, differences in facet area should be observed primarily in relation to body mass. Furthermore, just as use of inverted postures should emphasize the role of the MTF in weight-bearing, the use of more everted postures by anthropoids should emphasize more laterally positioned facets (such as the ectal [=posterior calcaneal] facet). Therefore, key differences between "prosimians" and anthropoids should be observable in the relative areas of MTF and ectal facets (EF).

Although predictions focusing on relative area of the MTF are easiest to articulate using a biomechanical premise, this is not how distinctions in MTF morphology between anthropoids and "prosimians" have previously been described by Gebo, Dagosto, and others as quoted above. Furthermore, our biomechanical premise may be incomplete or inaccurate. Therefore, any study quantifying variation in MTF morphology would be incomplete if it only examined scaling relationships of facet areas relative to body mass. Gebo (1986) and Dagosto (1990) both indicate that anthropoids have a more dorsoplantarly narrow facet (suggesting a different facet shape), as well as greater exposure of non-articular area on the medial aspect of the talar body. These are features that can be measured without direct reference to relative facet area and are incorporated with facet area measurements in the current study (see "Methods" section).

Evolutionary considerations

The functional variation described above has been invoked in scenarios of primate and anthropoid origins. Plesiadapiforms and non-primate euarchontans are generally characterized as differing from the earliest euprimates in having a more anthropoid-like MTF pattern (Dagosto, 1990), suggesting that these taxa lack "prosimian"-like locomotor patterns. If the "prosimian"-like MTF morphology was present in the common ancestor of extant primates, then euprimate origins may have been marked by an increased reliance on relatively smaller diameter and possibly more vertically oriented supports. Such behaviors are frequently associated with grasp-leaping (Napier and Walker, 1967; Szalay and Dagosto, 1980; Dagosto, 2007; Gebo, 2011; Boyer et al., 2013a,b) as exhibited by many extant "prosimians." The earliest known candidate stem anthropoids are middle Eocene eosimiids from China (Beard et al., 1996). Tali have been attributed to these taxa based on the presence of a relatively small MTF, and other features such as a steep-sided talo-fibular facet (Gebo et al., 2000, 2001; Boyer and Seiffert, 2013). This morphology, in combination with apparently primitive "prosimian" retentions (posterior trochlear shelf, narrow trochlea, and low neck angle), has been marshaled as evidence supporting a *reversal* to more pronograde quadrupedal locomotion in early anthropoids (Gebo et al., 2001), which was then

maintained to some degree in platyrrhines and catarrhines (Gebo, 1986, 1989a).

Addressing why early anthropoids may have switched to pronograde quadrupedalism, Gebo (1986) suggested a few alternative possibilities: 1) increased body size in the anthropoid stem lineage (making vertical locomotion more difficult [Hanna et al., 2008]), 2) a terrestrial phase, or 3) different available habitats. In the intervening decades, additional fossil evidence has helped rule out the first two possibilities. Postcrania of the earliest African anthropoids (Seiffert and Simons, 2001; Seiffert et al., 2010) and stem anthropoid eosimiids (Gebo et al., 2001) reveal characteristic anthropoid morphology in animals that are of diminutive body size and clearly arboreal. However, the Shanghuang fauna includes haplorhine and stem anthropoid primates of such unexpectedly small size (Gebo, 2004; Gebo et al., 2012a) that decreased body size should also be considered as a possible explanation for the development of anthropoid traits. If the anthropoid stem lineage underwent prolonged evolution toward smaller body size, then the supports that earlier and larger-bodied anthropoids had typically used would be relatively large when compared with the smaller bodies of later "dwarfed" stem anthropoids; life in such an arboreal environment might then translate into tendencies toward using these relatively large supports. The use of relatively large supports would be expected to reduce opportunities for strong hallucal grasping, thereby diminishing its importance in locomotor performance. Boyer and Seiffert (2013) argue that fibular facet angle (FFa) is tied to relative support size based on the finding that smaller bodied stepsirrhines (e.g., *Microcebus*) have a significantly more "haplorhine-like" facet slope and are obligated to use relatively large supports compared with their larger-bodied relatives (Gebo, 1987b, 2004).

Because the described differences in talar form influence perceptions of early primate evolution to such a large degree, a strong quantitative framework verifying these descriptions is needed. The major goal of this study is to provide such a framework for the MTF. We aim to accurately quantify surface areas and other aspects of shape in a comprehensive sample of haplorhines, strepsirrhines, fossil primates, and outgroups, and to examine this variation in a context that is explicitly phylogenetic and functional.

Hypotheses and predictions

Due to the functional-adaptive interpretations applied to previous assessments of MTF variation (Gebo, 1986, 1993; Gebo et al., 2000; Yapuncich and Boyer, 2014), we frame our hypotheses in terms of functionally significant trade-offs.

H1. Strepsirrhines and tarsiers transmit relatively more weight through their MTF and relatively less weight through their lateral tibial and EF due to increased utilization of small diameter and inclined or vertical supports, leading to more habitually inverted and abducted foot postures.

P1a. Relative to body mass, anthropoids have smaller MTFs than strepsirrhines or tarsiers.

P1b. Relative to EF area, anthropoids have smaller MTFs than strepsirrhines or tarsiers.

P1c. Because variation in FFa might be explained by degree of habitual inversion of the foot (Boyer and Seiffert, 2013), relative MTF area will correlate with FFa.

P1d. Strepsirrhines and tarsiers will have a more plantarly extensive medial malleolus as inferred from the plantar extent of the MTF, as a longer malleolus will reduce the potential for joint dislocation due to more laterally directed forces.

P1e. If the dorsoplantar shallowness of the anthropoid MTF has been caused by migration of talotibial ligaments to a more distal position (Gebo, 1986), then anthropoids should have a less circular margin to their MTFs than strepsirrhines and tarsiers (Fig. 2).

H2. Adapiforms and omomyiforms emphasized the use of substrates that were similar in size and orientation to those used by living strepsirrhines, whereas early anthropoids utilized substrates similar to those employed by living anthropoids.

P2a. Adapiforms and omomyiforms will resemble strepsirrhines and tarsiers for variables representing MTF relative size, shape, and dorsoplantar depth (focal variables of H1).

P2b. Fossil anthropoids will resemble modern anthropoids for focal variables of H1.

H3. The strepsirrhine-like postural mode that has been inferred for early adapiforms and omomyiforms is a synapomorphy of euprimates that reflects a change in locomotor behavior and substrate use compared with more distal stem-primates during euprimate origins.

P3a. Stem primates exhibit patterns of MTF variation that are more similar to anthropoids than to strepsirrhines and non-anthropoid haplorhines.

P3b. Extant primate relatives (Scandentia and Dermoptera) exhibit patterns of MTF form that are more similar to anthropoids than to strepsirrhines and non-anthropoid haplorhines.

P3c. Ancestral state reconstructions (ASRs) will show substantial (if not significant) shifts from proximal stem primate nodes to the euprimate node so that values switch from more anthropoid-like to more "prosimian"-like. An oppositely directed shift in values will be seen along the anthropoid stem-lineage.

MATERIALS

Sample

The sample used here largely overlaps with that of Boyer and Seiffert (2013); however, it has been expanded to improve both taxonomic sampling and sampling density of previously included species, as well as to include subfossil lemurs. In total, we included 378 individuals representing 122 species (Tables 1–4; and Supporting Information tables).

Institutional abbreviations

AMNH, American Museum of Natural History, New York, NY, USA; CGM, Egyptian Geological Museum, Cairo, Egypt; DPC, Duke Lemur Center Division of Fossil Primates, Durham, NC, USA; CM, Carnegie Museum of Natural History, Pittsburgh, PA, USA; GU, H.N.B. Garhwal University, Srinagar, Uttarakhand, India; HTB, Cleveland Museum of Natural History, Hamann-Todd non-human primate osteological collection,

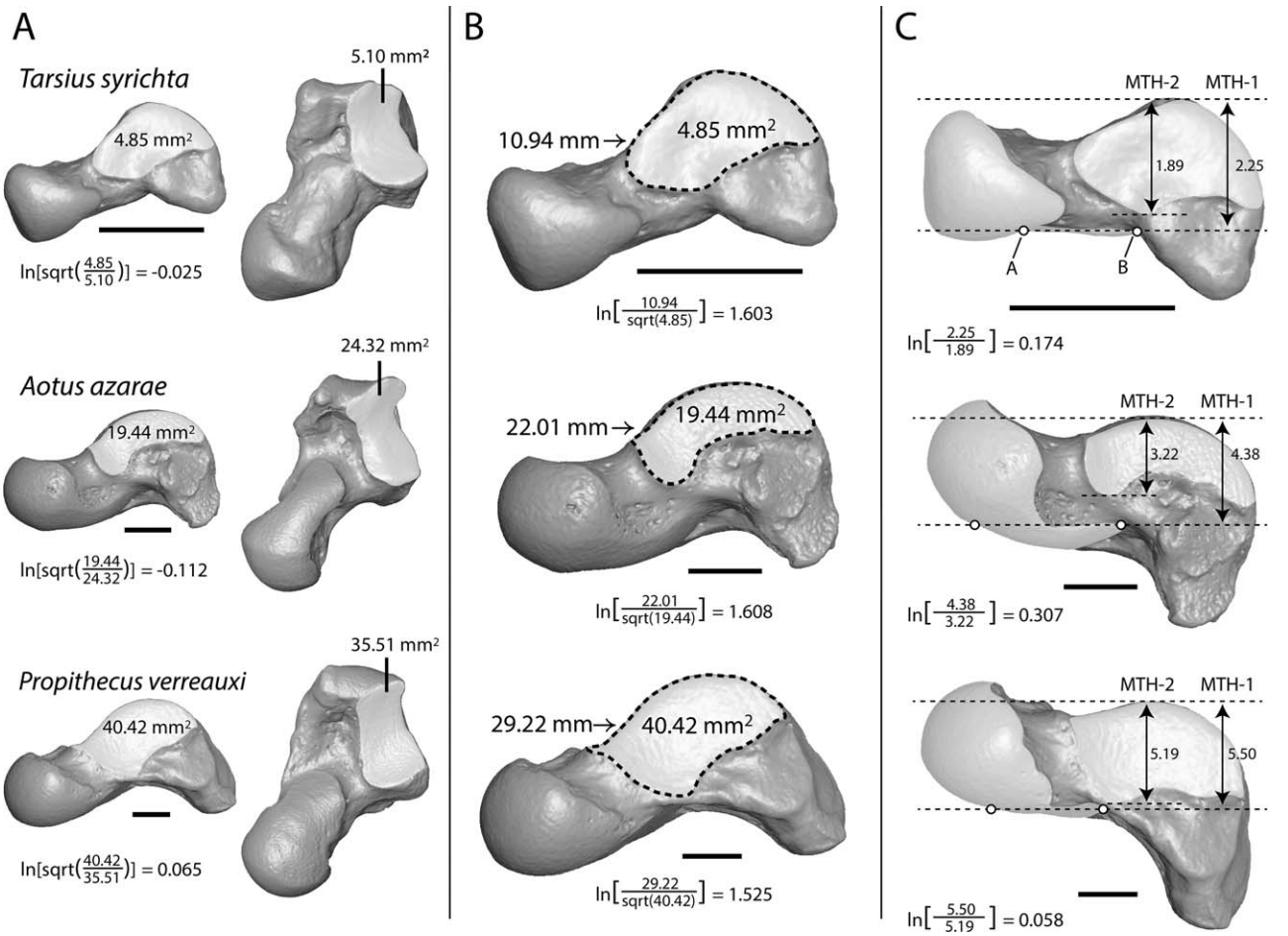

Fig. 2. Illustration of measurements taken using *Tarsius* (DPC 0127), *Aotus* (AMNH M 215056) and *Propithecus* (AMNH M 170474). (**A**) Two different facet areas were recorded using Avizo and Geomagic by highlighting the relevant surface and computing its area. Indices of MTF area were created relative to the EF area and body mass. (**B**) MTF area was used in calculation of a shape variable expressing how much MTF shape deviated from a circle. We did this by taking the ratio of the facet perimeter to the square root of facet area. The more elliptical or complex the facet margin, the higher the value. (**C**) Measuring the ratio of MTF depth to talar body depth was difficult to standardize. Ultimately, we took an approach that referenced the sustentacular facet and the axis of the trochlea as decribed in the methods. Anthropoids, with larger non-articular areas on the medial side of the talus, should have lower values than strepsirrhines, in which the facet may extend below the body.

Cleveland, Ohio; ISE-M, Institut des Sciences de l'Evolution de Montpellier, Montpellier, France; IRSNB, Institut Royal des Sciences Naturelles de Belgique, Brussels, Belgium; IVPP, Institute of Vertebrate Paleontology and Paleoanthropology, Chinese Academy of Sciences, Beijing, China; MCZ, Museum of Comparative Zoology, Harvard University, Cambridge, MA; MNHN, Muséum National d'Histoire Naturelle, Paris, France; NMB, Naturhistorisches Museum Basel, Basel, Switzerland; NYCEP, New York Consortium in Evolutionary Primatology, New York, NY; SBU, Stony Brook University, Stony Brook, NY; SDNHM, San Diego Natural History Museum, San Diego, California; UCM, University of Colorado Museum of Natural History, Boulder, CO; UF, University of Florida, Florida Museum of Natural History, Gainesville, FL, USA; UM, University of Michigan, Ann Arbor, Michigan; USGS, U.S. Geological Survey, Denver, Colorado; UNSM, University of Nebraska Science Museum, Lincoln, NB, USA; USNM, United States National Museum, Smithsonian Institute, Washington DC, USA.

METHODS

Generation of digital models

All measurements were taken on 3D digital surface models. These were created by various scanning modalities. Most specimens were scanned using one of four instruments: at SBU, two different ScancoMedical brand machines (VivaCT 75, μCT40) and a medical CT scanner were used; at the AMNH Microscopy and Imaging Facility, a Phoenix brand v/tome/x s240 was used; at Duke University, a Nikon XTH 225 CT model was used; at ISE, a SkyScan in-vivo 1076 was used; and for specimens of *Nasalis, Gorilla, Pan*, and *Pongo* a GE eXplore Locus SP machine was used at the Ohio University μCT Facility. A small subset of specimens was created with a Cyberware 3D scanner. These include the *Homo* sample (from the New York medical collection housed in the AMNH Department of Anthropology), the *Hoolock hoolock* sample, and AMNH 106581 and AMNH 106584 of the *Symphalangus* sample. Most specimens were scanned at a resolution of 39μm or less. The highest

TABLE 1. Measured quantities for extant taxa

Taxa	*n*	MTFa	min–max	EFa	min–max	Troch	min–max	MTFa*	min–max	Pmtr	min–max	MTH1	min–max	MTH2	min–max
Hominidae															
Gorilla gorilla	5	335.8(17.22)	317.7–359.1	620.6(152.3)	423.6–769.57	27.12(2.5)	24.1–29.6	362.8(15.41)	342.32–379.2	89.89(2.54)	87.46–93.13	21.7(3.69)	16.39–24.93	14.48(2.63)	11.23–17.22
Homo sapiens	5	217.9(31.95)	179.0–263.5	661.9(94.13)	527.7–764.0	30.12(1.87)	27.14–32.15	225.75(28.76)	185–258	78.1(7.83)	69–88.9	23.39(3.59)	18.44–27.01	12.61(0.91)	11.72–13.96
Pan troglodytes	5	172.4(29.36)	143.7–217.4	343.1(22.67)	321.0–380.8	18.93(1.27)	17.7–20.74	189.56(25.59)	168.94–230.02	70.32(5.93)	64.72–79.1	13.47(1.8)	11.12–15.12	9.88(2.15)	8.11–12.8
Pongo pygmaeus	5	122.8(14.21)	100.3–138.8	248.7(17.04)	223.6–271.5	18.82(1.25)	16.74–20.01	122.28(13.33)	107.4–140	65.72(8.2)	51.15–70.1	7.37(0.43)	6.93–7.92	5.92(0.91)	4.61–6.77
Hylobatidae															
Hoolock hoolock	7	44.85(5.82)	35.74–51.77	66.36(6.1)	58.8–74.6	9.64(0.5)	8.91–10.3	47.86(5.13)	40.8–55.77	35.29(1.37)	33.72–37.7	6.88(1.33)	5.95–9.74	5.27(0.29)	4.69–5.55
Hylobates lar	5	41.25(4.16)	35.66–46.72	62.3(8.59)	53.32–74.24	8.67(1.01)	7.35–9.81	42.55(6.08)	36.12–50.3	35.04(3.93)	28.09–37.2	6.55(1.19)	5.26–7.96	5(0.27)	4.63–5.3
Symphalangus syndactylus	3	63.61(7.38)	59.26–72.14	83.46(5.64)	79.47–87.44	11.76(0.55)	11.25–12.34	67.23(10.85)	59.9–79.69	41.09(1.43)	39.44–42.02	7.54(1.5)	5.87–8.78	6.02(0.81)	5.1–6.63
Cercopithecoidea															
Macaca fascicularis	3	37.05(0.83)	36.32–37.96	53.61(4.8)	48.13–57.1	9.11(0.41)	8.64–9.39	38.5(1.21)	37.15–39.46	31.96(1.49)	30.45–33.42	5.77(0.54)	5.15–6.13	5.1(0.11)	4.98–5.18
Macaca nemestrina	4	56.64(15.38)	44.65–79.06	74.62(17.86)	61.77–101.06	10.37(0.86)	9.57–11.58	60.12(13.73)	46.35–79.1	38.99(4.35)	33.26–43.82	5.73(0.65)	4.8–6.3	5.67(0.73)	4.8–6.3
Presbytis melalophos	1	62.71(–)	–	76.82(–)	–	10.85(–)	–	54.48(–)	–	38.66(–)	–	9.26(–)	–	6.28(–)	–
Semnopithecus entellus	1	67.57(–)	–	79.92(–)	–	11.58(–)	–	63.33(–)	–	40.86(–)	–	9.78(–)	–	6.95(–)	–
Trachypithecus cristatus	3	53.36(5.7)	48.66–59.7	69.03(7.02)	60.98–73.86	9.81(0.79)	9.32–10.72	56.34(7.05)	49.44–63.52	35.85(2.89)	32.99–38.78	8.87(0.62)	8.19–9.4	6.14(0.34)	5.86–6.52
Trachypithecus obscurus	1	39.28(–)	–	61.88(–)	–	10.46(–)	–	42.28(–)	–	36.36(–)	–	7.29(–)	–	4.99(–)	–
Nasalis larvatus	4	111.82(10.47)	98.15–123.35	173.33(12.34)	163.86–191.45	14.88(0.51)	14.18–15.31	121.92(10.09)	107.8–129.34	53.51(2.04)	51.53–56.15	12.06(0.98)	11–12.94	7.31(0.73)	6.73–8.37
Atelidae															
Alouatta caraya	6	30.75(5.43)	22.82–39.42	66.72(12.61)	51.23–78.86	9.75(0.86)	8.39–10.77	31.71(4.62)	25.49–37.65	27.82(2.62)	24.25–30.46	6.34(0.73)	5.12–7.04	4.72(0.39)	4.32–5.16
Ateles belzebuth	4	47.85(5.88)	38.72–55.15	90.04(19.62)	58.83–110.2	12.13(0.82)	10.93–12.9	49.98(9.24)	41.14–63.5	33.62(2.45)	31.53–37.83	7.43(1.01)	6.28–8.84	6.39(0.94)	5.5–7.84
Ateles fusciceps	1	49.14(–)	–	110.2(–)	–	12.9(–)	–	54.1(–)	–	32.58(–)	–	7.49(–)	–	6.76(–)	–
Ateles geoffroyi	1	46.7(–)	–	118(–)	–	13.19(–)	–	46.48(–)	–	36.2(–)	–	8.41(–)	–	5.45(–)	–
Lagothrix lagotricha	3	31.69(4.23)	28.17–36.38	57.49(5.77)	52.03–63.53	10.32(0.32)	10.01–10.65	31.22(2.75)	28.73–34.17	26.71(2.18)	24.69–29.02	5.31(0.19)	5.17–5.53	4.87(0.6)	4.29–5.48
Lagothrix lugens	1	46.05(–)	–	71.22(–)	–	10.58(–)	–	48.36(–)	–	34.2(–)	–	7.67(–)	–	5.71(–)	–
Callitrichinae															
Callimico goeldii	6	8.6(0.51)	7.71–9.05	11.62(0.62)	11.09–12.6	4.2(0.24)	3.93–4.5	8.85(0.52)	8.25–9.49	16.5(1.12)	14.71–17.7	3.38(0.22)	3.08–3.73	2.6(0.13)	2.44–2.76
Callithrix jacchus	5	4.27(0.84)	3–5.35	6.33(0.87)	5.48–7.56	3.3(0.22)	3.1–3.58	4.57(0.9)	3.37–5.8	11.11(0.9)	9.94–12.36	2.08(0.2)	1.78–2.31	1.53(0.24)	1.21–1.82
Callithrix pygmaea	5	1.9(0.21)	1.68–2.21	2.75(0.18)	2.45–2.9	2.26(0.08)	2.13–2.33	1.94(0.2)	1.68–2.19	8(0.78)	7.28–9.13	1.3(0.1)	1.19–1.39	1.01(0.17)	0.78–1.24
Leontopithecus rosalia	4	7.13(0.49)	6.61–7.65	10.38(0.73)	9.37–11.13	4.61(0.22)	4.4–4.86	7.44(0.42)	7.07–7.99	14.2(0.3)	13.9–14.51	3.05(0.2)	2.82–3.29	1.96(0.1)	1.86–2.08
Saguinus midas	3	7.49(0.78)	6.61–8.11	11.73(2.31)	9.84–14.3	4.26(0.38)	3.88–4.64	7.49(1.28)	6.28–8.83	14.17(1.01)	13.01–14.9	2.75(0.46)	2.22–3.08	2.02(0.16)	1.85–2.16
Saguinus mystax	3	5.1(0.57)	4.7–5.5	7.22(0.14)	7.12–7.32	3.56(0.04)	3.53–3.58	4.99(0.66)	4.52–5.46	12.37(0.39)	12.09–12.65	2.31(0.22)	2.15–2.46	1.58(0.13)	1.48–1.67
Saguinus oedipus	1	6.86(–)	–	9.65(–)	–	3.86(–)	–	7.17(–)	–	13.08(–)	–	2.58(–)	–	2.05(–)	–
Cebinae/Aotinae															
Aotus infulatus	1	10.67(–)	–	17.66(–)	–	4.84(–)	–	11.04(–)	–	18.09(–)	–	3.67(–)	–	2.84(–)	–
Aotus trivirgatus	2	12.95(3.81)	10.25–15.64	19(0.91)	18.35–19.64	5.14(0.05)	5.1–5.17	11.78(1.55)	10.68–12.88	18.79(0.91)	18.15–19.43	3.95(0.08)	3.89–4.01	3.02(0.28)	2.82–3.22
Aotus azarae	3	17.53(3.61)	13.37–19.78	23.14(2.97)	19.76–25.33	5.54(0.37)	5.28–5.97	15.93(2.99)	12.5–17.87	21.25(2.55)	18.41–23.32	4.1(0.53)	3.49–4.44	3.25(0.26)	3.01–3.52
Cebus apella	6	28.51(4.78)	23.97–35.6	37.17(6.15)	31.62–45.68	7.63(0.68)	7.04–8.86	27.74(7.01)	18.68–38.11	29.87(3.41)	25.63–33.58	5.39(0.58)	4.48–6.14	4.12(0.48)	3.42–4.81
Saimiri boliviensis	3	12.03(0.54)	11.41–12.37	17.54(2.88)	15.86–20.86	4.43(0.27)	4.2–4.73	10.99(0.23)	10.75–11.2	17.88(0.86)	16.92–18.6	3.36(0.23)	3.13–3.59	2.85(0.25)	2.65–3.13
Saimiri sciureus	2	13.14(0.55)	12.75–13.53	15.48(1.6)	14.35–16.61	4.47(0.04)	4.44–4.49	12.85(0.8)	12.28–13.42	20.51(0.07)	20.46–20.56	3.38(0.18)	3.25–3.51	2.68(0.04)	2.65–2.71
Pitheciidae															
Cacajao calvus	3	30.92(2.59)	27.93–32.45	40.43(0.76)	39.8–41.28	7.79(0.96)	6.83–8.75	29.06(3.37)	26–32.68	33.55(3.6)	29.54–36.5	5.62(0.49)	5.07–6.01	4.04(0.49)	3.49–4.42
Callicebus donacophilus	2	11.57(0.69)	11.09–12.06	17.85(2.08)	16.38–19.32	5.38(0.06)	5.33–5.42	11.4(0.81)	10.83–11.97	18.48(0.87)	17.86–19.1	3.44(0.03)	3.42–3.46	2.43(0.02)	2.41–2.44
Callicebus moloch	3	16.08(2.55)	13.57–18.67	19.97(2.48)	18.07–22.77	5.33(0.12)	5.2–5.43	16.9(3.9)	13.15–20.94	20.66(1.74)	18.81–22.26	4.05(0.39)	3.73–4.48	3.21(0.37)	2.96–3.64
Chiropotes sp.	2	28.26(4.03)	25.41–31.11	40.3(15.32)	29.46–51.13	7.86(1.14)	7.05–8.66	28.22(0.44)	27.91–28.53	31.87(4.43)	28.73–35	5.10(0.79)	4.54–5.66	4.05(0.47)	3.72–4.38
Pithecia pithecia	3	20.21(2.77)	17.2–22.66	32.85(5.97)	26.15–37.6	7.25(0.83)	6.33–7.95	20.28(2.91)	17.23–23.01	24.19(1.6)	22.38–25.41	5.13(0.2)	4.94–5.33	3.79(0.18)	3.62–3.98
Tarsiidae															
Tarsius bancanus	2	4.56(0.23)	4.39–4.72	4.89(0.01)	4.88–4.9	3.3(0.08)	3.24–3.36	4.83(0.3)	4.62–5.04	9.79(0.32)	9.57–10.02	2.47(0.01)	2.46–2.47	2.53(0.06)	2.49–2.57
Tarsius syrichta	2	4.08(1.09)	3.3–4.85	4.9(0.28)	4.7–5.1	3.2(0)	3.2–3.2	4.73(0.18)	4.61–4.85	10.49(0.64)	10.03–10.94	2.44(0.26)	2.25–2.62	2.09(0.28)	1.89–2.28
Tarsius tarsier	2	4.06 (0.01)	4.06–4.07	4.64 (0.16)	4.53–4.75	3.11 (0)	3.11–3.11	3.92 (0.19)	3.78–4.05	9.19 (0.57)	8.78–9.59	2.1 (0.03)	2.08–2.12	1.82 (0.01)	1.81–1.83

TABLE 1. Continued

Taxa	*n*	MTFa	min–max	EFa	min–max	Troch	min–max	MTFa*	min–max	Pmtr	min–max	MTH1	min–max	MTH2	min–max
Cheirogaleidae															
Cheirogaleus major	1	7.47 (–)	–	8.93 (–)	–	3.89 (–)	–	8.1 (–)	–	15.15 (–)	–	2.44 (–)	–	2.44 (–)	–
Cheirogaleus major	1	7.47 (–)	–	8.93 (–)	–	3.89 (–)	–	8.1 (–)	–	15.15 (–)	–	2.44 (–)	–	2.44 (–)	–
Cheirogaleus medius	3	3.99 (0.31)	3.64–4.21	4.14 (0.33)	3.88–4.51	2.79 (0.15)	2.61–2.89	3.78 (0.56)	3.15–4.19	9.7 (0.98)	8.61–10.52	1.85 (0.11)	1.72–1.93	1.63 (0.05)	1.6–1.68
Microcebus griseorufus	10	1.65 (0.17)	1.43–1.95	1.93 (0.19)	1.72–2.41	1.71 (0.09)	1.62–1.96	1.68 (0.17)	1.52–2.02	6.09 (0.33)	5.62–6.45	1.05 (0.06)	0.96–1.17	1.11 (0.08)	1.01–1.27
Mirza coquereli	2	4.69 (0)	4.69–4.69	6.1 (0.14)	6.01–6.2	3.18 (0.08)	3.12–3.23	4.81 (0.03)	4.79–4.83	10.1 (0.05)	10.06–10.13	2.11 (0.09)	2.04–2.17	1.92 (0.03)	1.9–1.94
Lepilemuridae															
Lepilemur mustelinus	6	11.38 (1.48)	8.78–12.67	11.88 (1.43)	9.7–14.03	4.38 (0.34)	3.84–4.74	10.36 (2.31)	6.39–13.65	15.19 (1.82)	11.72–16.37	3.02 (0.31)	2.66–3.45	3.2 (0.26)	2.75–3.45
Daubentoniidae															
Daubentonia madagascariensis	3	26.85 (4.18)	24.08–31.66	31.19 (1.8)	29.7–33.19	6.36 (0.24)	6.14–6.61	25.78 (2.44)	23.11–27.9	22.83 (2.66)	20.46–25.7	4.78 (0.33)	4.53–5.15	5.02 (0.19)	4.8–5.15
Indriidae															
Avahi laniger	4	23.1 (2.91)	20.48–26.24	20.22 (1.66)	17.94–21.78	5.31 (0.3)	5.03–5.66	23.88 (3.3)	19.94–27.33	21.56 (0.99)	20.74–22.8	4.14 (0.51)	3.46–4.58	4.45 (0.5)	3.87–4.96
Indri indri	2	85.48 (1.48)	84.43–86.53	60.08 (2.57)	58.26–61.9	9.55 (0.24)	9.38–9.72	92.54 (12.26)	83.87–101.21	44.56 (2.3)	42.94–46.19	8.54 (0.74)	8.02–9.06	8.54 (0.74)	8.02–9.06
Propithecus diadema	1	82.05 (–)	–	73.45 (–)	–	10.93 (–)	–	82.34 (–)	–	42.5 (–)	–	7.56 (–)	–	7.79 (–)	–
Propithecus verreauxi	6	42.81 (3.54)	37.79–47.21	34.09 (3.2)	28.67–37.76	7.83 (0.43)	7.1–8.3	38.28 (2.92)	33.35–42.03	28.91 (1.12)	27.55–30.3	5.36 (0.11)	5.23–5.5	5.39 (0.16)	5.19–5.67
Lemuridae															
Eulemur albifrons	3	29.07 (1.28)	27.6–29.95	25.42 (3.66)	21.79–29.1	5.66 (0.43)	5.38–6.15	29.36 (3.78)	26.22–33.55	23.86 (2.13)	22.45–26.31	4.73 (0.08)	4.64–4.78	4.95 (0.15)	4.78–5.05
Eulemur collaris	2	34.16 (0.8)	33.59–34.72	29.23 (0.01)	29.22–29.23	5.62 (0.16)	5.5–5.73	34.02 (0.43)	33.72–34.32	26.02 (0.43)	25.71–26.33	4.76 (0.05)	4.72–4.79	5.41 (0.15)	5.3–5.51
Eulemur fulvus	1	25.65 (–)	–	22.74 (–)	–	6.03 (–)	–	25.81 (–)	–	23.59 (–)	–	4.21 (–)	–	4.21 (–)	–
Eulemur mongoz	2	23.93 (2.44)	22.2–25.65	22.6 (0.2)	22.46–22.74	5.76 (0.38)	5.49–6.03	23.21 (3.69)	20.6–25.81	22.85 (1.06)	22.1–23.59	4.08 (0.18)	3.95–4.21	4.33 (0.16)	4.21–4.44
Hapalemur griseus	3	16.44 (1.96)	15.05–18.68	13.94 (2.34)	11.54–16.22	4.83 (0.17)	4.68–5.02	15.7 (2.62)	13.9–18.7	18.17 (1.5)	17.08–19.88	3.14 (0.18)	3–3.35	3.91 (0.19)	3.7–4.08
Lemur catta	4	30.57 (1.67)	28.4–32	25.57 (0.83)	24.92–26.76	6.59 (0.45)	6.33–7.26	29.89 (2.18)	27.08–32.02	24.39 (0.87)	23.26–25.16	4.23 (0.2)	4.01–4.49	5.25 (0.39)	4.9–5.59
Prolemur simus	4	29.07 (3.11)	25.94–32.16	29.61 (2.4)	26.84–31.11	6.96 (0.44)	6.59–7.6	31.54 (4.28)	27.12–35.58	26.26 (2.21)	24.21–29.17	4.62 (0.44)	4.23–5.23	4.88 (0.35)	4.41–5.23
Varecia variegata	4	41.5 (4.67)	35.15–46.27	39.76 (4.39)	36.41–46.2	7.88 (0.41)	7.55–8.44	42.33 (4.58)	37.35–48.44	28.39 (0.93)	27.79–29.75	5.14 (0.43)	4.61–5.59	6.31 (0.5)	5.62–6.78
Galagidae															
Euoticus elegantulus	2	10.45 (0.62)	10.01–10.89	7.48 (0.27)	7.29–7.67	3.56 (0.09)	3.49–3.62	10.32 (1.09)	9.55–11.09	14.12 (0.67)	13.65–14.6	2.5 (0.46)	2.17–2.82	3.1 (0.23)	2.94–3.26
Galago senegalensis	5	8.31 (0.83)	7.5–9.65	6.29 (0.37)	6.01–6.87	3.25 (0.14)	3.1–3.43	7.96 (0.68)	7.3–9.05	12.16 (0.53)	11.44–12.91	2.5 (0.23)	2.26–2.88	2.89 (0.16)	2.73–3.06
Galagoides demidoff	6	4.11 (0.34)	3.55–4.58	3.07 (0.2)	2.77–3.36	2.14 (0.09)	2–2.23	4.15 (0.35)	3.68–4.75	9.62 (0.58)	8.66–10.3	1.57 (0.08)	1.45–1.7	2.2 (0.12)	2.01–2.34
Otolemur crassicaudatus	5	24.31 (5.11)	18.3–31.02	17.31 (3.33)	13.8–21.38	4.79 (0.72)	4.23–5.76	25.59 (5.96)	19.44–33.6	23.69 (3.54)	19.39–27.5	4.12 (0.45)	3.71–4.76	5.3 (0.77)	4.56–6.4
Lorisidae															
Arctocebus calabarensis	2	5.91 (1.03)	5.18–6.64	3.71 (0.25)	3.53–3.88	2.84 (0.11)	2.76–2.91	5.45 (0.35)	5.2–5.7	11.35 (0.35)	11.1–11.59	1.27 (0.07)	1.22–1.32	2.43 (0.05)	2.39–2.46
Loris tardigradus	4	4.33 (2.01)	2.59–6.51	3.89 (1.26)	2.82–5.32	2.73 (0.54)	2.26–3.34	4.17 (1.96)	2.37–6.27	9.85 (2.52)	6.99–12.15	1.66 (0.39)	1.35–2.18	1.86 (0.52)	1.41–2.42
Nycticebus coucang	3	10.03 (1.1)	8.81–10.93	6.29 (0.41)	5.83–6.61	3.67 (0.27)	3.43–3.97	9.82 (1.31)	8.64–11.23	15.34 (1.77)	13.63–17.17	2.28 (0.12)	2.2–2.42	2.82 (0.26)	2.57–3.09
Perodicticus potto	6	10.96 (1.14)	9.13–12.4	10.57 (1.8)	8.61–13.51	4.44 (0.42)	3.77–5.04	10.5 (1.26)	8.72–12.16	16.7 (1.17)	15.66–18.86	2.74 (0.22)	2.45–3	2.46 (0.18)	2.24–2.78
Euarchonta															
Cynocephalus volans	3	7.9 (2.43)	6.03–10.64	10.6 (2.23)	8.53–12.97	4.49 (0.44)	4.22–5	8.43 (1.44)	7.4–10.07	15.67 (1.82)	13.98–17.6	2.94 (0.53)	2.33–3.31	2 (0.25)	1.85–2.29
Ptilocercus lowii	3	1.11 (0.17)	0.93–1.27	1.46 (0.01)	1.45–1.47	1.45 (0.02)	1.43–1.47	1.13 (0.15)	0.99–1.28	6.06 (0.42)	5.63–6.46	0.81 (0.01)	0.81–0.82	0.82 (0.02)	0.8–0.83
Tupaia glis	3	2.66 (0.38)	2.36–3.09	4.52 (0.35)	4.12–4.77	2.65 (0.08)	2.58–2.74	2.54 (0.4)	2.16–2.95	8.95 (0.56)	8.31–9.33	1.31 (0.11)	1.19–1.4	1.32 (0.11)	1.19–1.41

Standard deviation in parentheses.

TABLE 2. Measured quantities for fossil taxa

Higher taxon	Taxon	*n*	MTFa	min–max	EFa	min–max	Troch	min–max	MTFa*	min–max	Pmtr	min–max	MTH1	min–max	MTH2	min–max
Anthropoidea: *incertae sedis* and stem																
Eosimiidae	*Eosimias sinensis*	3	2.46(0.29)	2.25–2.79	3.61(0.2)	3.5–3.84	2.32(0.1)	2.2–2.38	2.51(0.37)	2.22–2.93	8.48(1.03)	7.7–9.64	1.77(0.06)	1.72–1.83	1.24(0.03)	1.21–1.26
incertae sedis	"Protoanthropoid" IVPP 12305	1	–(–)	–	–(–)	–	1.91(–)	–	–(–)	–	–(–)	–	1.3(–)	–	1.3(–)	–
incertae sedis	"Protoanthropoid" IVPP 12306	1	1.77(–)	–	2.42(–)	–	2.08(–)	–	2.05(–)	–	6.99(–)	–	1.15(–)	–	1.15(–)	–
incertae sedis	"Amphipithecidae" (?) NMMP 39	1	25.38(–)	–	34.51(–)	–	7.45(–)	–	26.27(–)	–	23.57(–)	–	5.38(–)	–	5.76(–)	–
Parapithecidae	Parapithecidae	6	18.84(6.57)	12.71–30.75	19.22(4.72)	15.15–26.64	5.19(0.46)	4.74–5.91	19.04(4.67)	14.06–26.94	22.73(2.69)	20.34–27.66	4.32(0.95)	3.28–5.73	3.47(0.63)	2.81–4.49
Proteopithecidae	*Proteopithecus sylviae*	1	8.13(–)	–	8.25(–)	–	3.69(–)	–	8.33(–)	–	14.66(–)	–	2.2(–)	–	2.03(–)	–
Catarrhini																
Hominidae	*Australopithecus afarensis*	1	115.56(–)	–	264(–)	–	17.6(–)	–	115.88(–)	–	60.9(–)	–	13.9(–)	–	8.8(–)	–
Hominidae	*Homo habilis* OH8	1	158.83(–)	–	212(–)	–	20.3(–)	–	174(–)	–	89.1(–)	–	16.38(–)	–	12.38(–)	–
Hominidae	*Homo* sp. KNM ER 1464	1	156.41(–)	–	473(–)	–	25.6(–)	–	166.4(–)	–	81.1(–)	–	18.84(–)	–	11.13(–)	–
Hominidae	*Homo* sp. KNM ER 813	1	139.67(–)	–	392(–)	–	23.4(–)	–	139(–)	–	75.8(–)	–	20.58(–)	–	10.38(–)	–
Propliopithecidae	*Aegyptopithecus zeuxis*	2	34.02(–)	–	53.8(0.92)	–	9.32(0.42)	–	37.14(–)	–	30.83(–)	–	6.15(–)	–	4.71(–)	–
Oligopithecidae	*Catopithecus browni*	1	10.18(–)	–	12.92(–)	–	4.27(–)	–	9.85(–)	–	15.28(–)	–	3.05(–)	–	2.71(–)	–
Platyrrhini																
Pitheciinae	*Cebupithecia sarmientoi*	1	16.72(–)	–	23.56(–)	–	5.87(–)	–	15.88(–)	–	25.5(–)	–	5.04(–)	–	3.42(–)	–
incertae sedis	*Dolichocebus gaimanensis*	1	20.74(–)	–	23.89(–)	–	6.1(–)	–	–(–)	–	–(–)	–	4.97(–)	–	4.21(–)	–
Pitheciinae	*Proteropithecia neuquenensis*	1	23.49(–)	–	25.95(–)	–	6.59(–)	–	25.33(–)	–	24.92(–)	–	4.83(–)	–	4.58(–)	–
Omomyiformes																
Omomyidae	*Necrolemur antiquus*	4	4.65(0.52)	4.1–5.26	5.99(0.96)	4.77–7.12	2.58(0.07)	2.48–2.66	4.4(0.6)	3.82–5.01	9.54(0.43)	9.01–10.03	2.07(0.1)	1.98–2.21	2.26(0.24)	2.06–2.61
Omomyidae	*Absarokius abbotti*	1	3.59(–)	–	3.83(–)	–	2.27(–)	–	3.45(–)	–	8.1(–)	–	1.56(–)	–	1.64(–)	–
Omomyidae	*Anemorhysis pearcei*	10	1.63(0.21)	1.37–2.03	1.84(0.28)	1.49–2.32	1.67(0.06)	1.62–1.79	1.68(0.15)	1.44–1.86	5.65(0.32)	5.03–6.09	1.15(0.11)	0.97–1.24	1.24(0.14)	1.06–1.4
Omomyidae	*Hemiacodon gracilis*	7	6.08(0.71)	5.29–7.56	6.2(0.87)	4.95–7.4	3.39(0.2)	3.13–3.64	5.9(0.83)	4.62–7.05	12.08(0.91)	10.7–13.13	2.37(0.25)	2.08–2.81	2.65(0.21)	2.35–2.86
Omomyidae	*Omomys carteri*	5	4.4(0.5)	3.88–5.08	4.73(0.47)	4.31–5.36	2.64(0.11)	2.51–2.75	4.31(0.5)	3.93–5.05	9.26(0.75)	8.21–10.05	1.84(0.21)	1.49–2.05	2.11(0.23)	1.72–2.27
Omomyidae	*Ourayia uintensis*	2	16.64(2.22)	15.07–18.21	20.01(4.96)	16.51–23.52	5.43(0.58)	5.02–5.84	16.77(2.73)	14.84–18.7	20.69(3.12)	18.49–22.9	3.43(–)	–	4.73(–)	–
Omomyidae	*Shoshonius cooperi*	3	2.56(0.54)	2.04–3.12	2.71(0.55)	2.14–3.23	1.95(0.13)	1.85–2.09	2.57(0.28)	2.28–2.83	7.56(0.52)	6.98–7.98	1.38(0.17)	1.2–1.54	1.51(0.07)	1.46–1.59
Omomyidae	*Steinius ?*	4	2.66(0.25)	2.33–2.93	2.88(0.4)	2.47–3.35	2.38(0.2)	2.16–2.64	2.72(0.3)	2.39–3.02	7.24(0.08)	7.15–7.34	1.46(0.19)	1.24–1.61	1.59(0.13)	1.5–1.74
Omomyidae	*Teilhardina belgica*	2	1.12(0.07)	1.07–1.18	1.41(0.06)	1.37–1.45	1.61(0.03)	1.59–1.63	1.21(0.27)	1.02–1.4	4.93(0.23)	4.77–5.09	1.09(0.01)	1.08–1.1	1.05(0.02)	1.03–1.06
Omomyidae	*Teilhardina brandti*	2	1.28(–)	–	1.42(0.08)	–	1.84(0.1)	–	1.22(–)	–	5.07(–)	–	1.05(–)	–	1.17(–)	–
Omomyidae	*Tetonius homunculus*	3	1.9(0.16)	1.74–2.05	2.22(0.28)	1.92–2.48	1.93(0.13)	1.85–2.08	1.69(0.28)	1.37–1.88	5.57(0.61)	4.92–6.14	1.19(0.02)	1.17–1.21	1.32(0.07)	1.26–1.39
Omomyidae	*Washakius insignis*	2	2.83(0.39)	2.55–3.11	3.29(0.08)	3.23–3.35	2.17(0.11)	2.09–2.24	2.97(0.53)	2.6–3.35	8.07(0.94)	7.4–8.74	1.63(0)	1.63–1.63	1.6(0.05)	1.56–1.63
Lemuriformes																
Megaladapidae	*Megaladapis* sp.	4	137.55(27.7)	104.72–162.67	158.16(24.33)	124.6–180	17.19(1.72)	15.55–19.49	141.03(26.31)	113–169	72.85(8.46)	66.7–84.8	11.52(0.78)	10.49–12.36	7.19(0.63)	6.54–7.9
Lemuridae	*Pachylemur insignis*	1	72.23(–)	–	–(–)	–	12.39(–)	–	78.97(–)	–	43.04(–)	–	9.01(–)	–	7.77(–)	–
Archaeolemuridae	*Archaeolemur edwardsi*	6	102.78(9.15)	89.44–114.22	110.17(18.19)	92.83–134.79	13.36(0.98)	11.53–14.35	106.25(9.62)	93.77–115.9	46.01(2.14)	43.37–48.79	8.71(0.56)	8.01–9.58	10.16(0.69)	8.92–10.94
Palaeopropithecidae	*Babakotia radofilai*	3	34.69(9.46)	27.93–48.41	50.07(6.27)	41.28–56.1	9.19(1.58)	6.83–10.09	36.83(12.77)	26–55.16	33.52(4.72)	28.29–38.39	5.13(0.27)	4.76–5.36	4.29(0.93)	3.49–5.63
Palaeopropithecidae	*Palaeopropithecus* sp.	4	112.46(5.88)	106.13–120.25	55.53(2.16)	53.34–57.66	10.48(0.46)	9.92–11.02	116.89(4.29)	111.2–121.21	44.73(2.56)	42.29–47.59	10.29(0.46)	9.78–10.67	14.98(0.81)	14.12–15.72
Adapiformes																
Adapinae	*Adapis* sp.	8	13.3(2.49)	10.54–17.34	15.54(2.37)	12.6–18.98	4.78(0.25)	4.46–5.17	14.63(2.76)	10.33–17.89	17.55(1.48)	15.58–19.56	2.68(0.24)	2.33–3.07	3.36(0.36)	2.98–4.01
Adapinae	*Leptadapis magnus*	3	60.07(10.67)	49.68–71	73.25(9.96)	62.53–82.23	9.76(0.99)	8.7–10.66	60.58(11.66)	47.93–70.9	34.8(3.75)	30.68–37.99	6.09(0.09)	5.98–6.16	6.93(0.66)	6.46–7.68
Asiadapinae	*Asiadapis cambayensis* GU 747	1	5.81(–)	–	6.33(–)	–	3.17(–)	–	5.74(–)	–	10.51(–)	–	2.38(–)	–	2.46(–)	–
Asiadapinae	*Marcgodinotius indicus*	3	2.99(0.33)	2.64–3.29	3.52(0.24)	3.25–3.71	2.04(0.07)	1.96–2.1	3.18(0.26)	3.02–3.48	8.31(0.02)	8.29–8.33	1.26(0.12)	1.15–1.38	1.49(0.13)	1.36–1.62
Caenopithecinae	*Afradapis longicristatus*	1	20.17(–)	–	18.96(–)	–	5.51(–)	–	19.93(–)	–	23.23(–)	–	2.88(–)	–	3.99(–)	–
Anchomomyini	*Anchomomys frontanyensis*	3	3.85(0.13)	3.73–3.99	4.34(0.24)	4.11–4.59	2.43(0.11)	2.34–2.55	3.75(0.13)	3.61–3.86	10.08(0.8)	9.18–10.7	1.72(0.08)	1.64–1.8	2.06(0.04)	2.03–2.11
Notharctidae	*Cantius abditus*	6	27.46(2.41)	25.44–31.55	31.84(1.06)	30.86–32.97	6.22(0.2)	6.03–6.49	25.77(2.66)	20.87–29.01	23.47(2.29)	20.17–26.16	4.49(0.14)	4.39–4.65	5.04(0.24)	4.9–5.32
Notharctidae	*Cantius frugivorous*	1	19.61(–)	–	na(–)	–	5.46(–)	–	20.04(–)	–	18.88(–)	–	3.56(–)	–	4.06(–)	–
Notharctidae	*Cantius mckennai*	2	18.16(–)	–	15.8(–)	–	4.85(0.03)	–	–(–)	–	–(–)	–	3.05(–)	–	3.49(–)	–
Notharctidae	*Cantius nuniensis*	1	35.43(–)	–	35.9(–)	–	7.07(–)	–	36.55(–)	–	26.37(–)	–	5.65(–)	–	6.37(–)	–
Notharctidae	*Cantius ralstoni*	4	11.42(1.27)	9.96–12.26	15.18(–)	15.18–15.18	4.08(0.46)	3.39–4.37	10.77(1.78)	8.82–12.29	14.03(1.33)	12.49–14.88	2.84(0.57)	2.44–3.24	2.94(0.24)	2.77–3.11
Notharctidae	*Cantius trigonodus*	6	18.82(2.24)	16.97–21.36	20.57(2.27)	18.21–22.74	5.37(0.38)	4.85–5.89	17.22(3.45)	11.18–20.85	18.56(1.4)	16.14–19.89	3.61(0.47)	3.18–4.48	4.16(0.19)	3.91–4.48
Djebelemuridae	*Djebelemur martinezi*	1	1.84(–)	–	2.23(–)	–	1.65(–)	–	1.89(–)	–	7.1(–)	–	1.41(–)	–	1.41(–)	–

TABLE 2. Continued

Higher taxon	Taxon	*n*	MTFa	min–max	EFa	min–max	Troch	min–max	MTFa*	min–max	Pmtr	min–max	MTH1	min–max	MTH2	min–max
Notharctidae	*Notharctus tenebrosus*	10	32.32(6.5)	23.92–43.75	34.38(7.23)	27.4–47.8	7.03(0.7)	6.12–8.4	33.86(8.59)	27.35–49.06	26.46(3.85)	23.07–33.83	4.95(0.58)	4.14–5.9	5.37(0.59)	4.56–6.28
Notharctidae	*Notharctus venticolus*	3	36.66(1.37)	35.08–37.52	40.29(4.63)	36.89–45.56	7.17(0.21)	6.94–7.35	33.19(4.19)	30.71–38.04	26(1.28)	24.54–26.92	4.57(0.14)	4.45–4.73	5.42(0.38)	5.18–5.85
Notharctidae	*Pelycodus jarrovii*	1	44.37(–)	–	na(–)	–	7.96(–)	–	45.63(–)	–	30.09(–)	–	5.29(–)	–	5.84(–)	–
Notharctidae	*Smilodectes gracilis*	2	30.25(2.95)	28.16–32.33	30.4(0)	30.4–30.4	6.91(0.28)	6.71–7.1	30.22(0.73)	29.7–30.74	26.18(0.59)	25.77–26.6	5(0.16)	4.89–5.11	5.64(0.04)	5.61–5.66
Plesiadapiformes																
Carpolestidae	*Carpolestes simpsoni*	1	0.99(–)	–	2.51(–)	–	2.08(–)	–	0.99(–)	–	6.28(–)	–	0.97(–)	–	0.55(–)	–
Paromomyidae	*Ignacius graybullianus*	1	1.37(–)	–	2.67(–)	–	2.07(–)	–	1.61(–)	–	6.77(–)	–	0.86(–)	–	0.55(–)	–
Plesiadapidae	*Plesiadapis cookei*	1	8.96(–)	–	17.3(–)	–	5.14(–)	–	9.87(–)	–	16.77(–)	–	2.34(–)	–	1.35(–)	–
Plesiadapidae	*Plesiadapis rex*	1	5.87(–)	–	9.25(–)	–	3.77(–)	–	5.57(–)	–	12.25(–)	–	1.53(–)	–	1.05(–)	–

Standard deviation in parentheses.

resolutions were 3–5μm for the smallest fossil specimens. The scanning resolution was usually high enough to result in an initial surface of 1–5 million faces (i.e., the surface resulting from creation of a "label field" representing the boundary between the bone and air in the image stack of raw microCT data using the software Avizo 6.0–8.0 [Visualization Sciences Group, 2009], followed by application of the "Surf-Gen" function with "no smoothing"). All specimens were subsequently downsampled using the "Simplify" function in Avizo to 200,000–700,000 faces. More details on resolution and scanner type used for the majority of this sample can be found in Boyer and Seiffert's (2013) appendix. Otherwise details on scans used in this study can be found by searching for specimen numbers in www.MorphoSource.org.

Measurements

A total of seven values were measured or computed for this study (Fig. 2, Tables 1 and 2). All were acquired from digital models using either Geomagic Studio (3D Systems Inc., 2013) or Avizo. For extant taxa, body mass was collected from published sources (Smith and Jungers, 1997; Rasoazanabary, 2010; Tacutu et al., 2013).

Facet areas. MTF area (MTFa) and EF area (EFa) were measured on each specimen (Fig. 2A, Tables 1 and 2) using Geomagic Studio (3D Systems Inc., 2013) or Avizo. EFa measurement protocol is identical to Boyer and Seiffert (2013, their Fig. 2). For the MTF, which often has more ambiguous boundaries than the EF, the mean value of three measurements taken independently was used. A fourth and final replicate of MTF measurements was recorded separately (Tables 1 and 2: MTFa*). This value is associated with the recorded MTF perimeter (see below) and used for computation of the variable (MTF-Perimeter)/($MTFa^{1/2}$) (see below).

Linear measures. Three linear measurements were collected. Trochlear width was measured according to the protocol of Boyer and Seiffert (2013, their Fig. 2), and two measures quantifying the plantar extent of the MTF were taken according to the following protocol: in Avizo, using an orthographic viewing mode, each talus was oriented roughly in medial view, then adjusted so the medial and lateral trochlear rims were parallel and overlapping (i.e., the axis of rotation of the trochlea was parallel to the viewing axis and perpendicular to the computer screen). The talus was then rotated around this axis, so that the neck and head pointed more upward or downward using the "camera trackball" tool (which allows rotations in a single plane). The goal of this rotation was to orient the sustentacular facet as close to horizontal as possible. We used three variably available reference features (measurement landmarks) for this task (notably, the same result is obtained using different subsets of these landmarks in taxa where all three are available). Landmarks included A) the point of contact between the navicular facet and sustentacular facet, expressed as a depression in the plantar outline of the bone (Fig. 2C), B) the proximodorsal termination of the sustentacular facet (Fig. 2C), and third, the dorsomedial margin of the sustentacular facet, which is not a landmark per se, but a linear feature (Fig. 2C). When A

TABLE 3. Analyzed variables for extant taxa

Taxon	*n*	FIB	min–max	MTFa/EFa	min–max	Pmtr/MTF	min–max	MTH–R	min–max
Hominidae									
Gorilla gorilla	5	82.8(3.85)	76.03–85.01	−0.339(0.09)	−0.42 to −0.2	1.552(0.03)	1.53–1.59	0.405(0.07)	0.37–0.51
Homo sapiens	5	96.5(3.16)	93.44–101.28	−0.555(0.04)	−0.6 to −0.5	1.648(0.04)	1.6–1.71	0.61(0.13)	0.42–0.72
Pan troglodytes	5	88.3(4.3)	82.16–94.16	−0.349(0.06)	−0.42 to −0.28	1.631(0.02)	1.59–1.65	0.32(0.13)	0.17–0.47
Pongo pygmaeus	5	81.9(5.85)	73.33–86.8	−0.355(0.08)	−0.5 to −0.3	1.778(0.12)	1.58–1.9	0.228(0.11)	0.12–0.41
Hylobatidae									
Hoolock hoolock	7	89.9(5.82)	84.05–102.07	−0.198(0.07)	−0.3 to −0.11	1.631(0.06)	1.55–1.7	0.254(0.16)	0.1–0.59
Hylobates lar	5	99.2(2.87)	94.33–101.7	−0.205(0.02)	−0.23 to −0.18	1.68(0.1)	1.54–1.81	0.258(0.13)	0.11–0.41
Symphalangus syndactylus	3	93.8(5.51)	87.8–98.66	−0.17(0.03)	−0.19 to −0.15	1.615(0.11)	1.49–1.69	0.217(0.07)	0.14–0.28
Cercopithecoidea									
Macaca fascicularis	3	81.7(4.46)	76.6–84.9	−0.183(0.04)	−0.21 to −0.14	1.639(0.03)	1.61–1.67	0.119(0.11)	0–0.21
Macaca nemestrina	4	83.8(1.51)	82.11–85.77	−0.141(0.02)	−0.16 to −0.12	1.62(0.04)	1.59–1.66	0.011(0.07)	−0.07 to 0.11
Presbytis melalophos	1	87.7(–)	–	−0.102(–)	–	1.656(–)	–	0.388(–)	–
Semnopithecus entellus	1	84.8(–)	–	−0.084(–)	–	1.636(–)	–	0.342(–)	–
Trachypithecus cristatus	3	87.7(2.88)	84.85–90.61	−0.129(0.03)	−0.17 to −0.11	1.564(0.02)	1.55–1.58	0.367(0.09)	0.3–0.47
Trachypithecus obscurus	1	84.3(–)	–	−0.227(–)	–	1.721(–)	–	0.379(–)	–
Nasalis larvatus	4	81.5(3.5)	78.59–86.14	−0.22(0.03)	−0.26 to −0.19	1.579(0.03)	1.54–1.62	0.501(0.08)	0.43–0.62
Atelidae									
Alouatta caraya	6	98(2.64)	95.14–102.63	−0.386(0.06)	−0.48 to −0.3	1.598(0.04)	1.55–1.63	0.292(0.15)	0.01–0.47
Ateles belzebuth	4	99(5.24)	94.25–107.7	−0.308(0.07)	−0.4 to −0.21	1.564(0.06)	1.49–1.64	0.152(0.14)	0.01–0.38
Ateles fusciceps	1	107.7(–)	–	−0.404(–)	–	1.488(–)	–	0.103(–)	–
Ateles geoffroyi	1	98.4(–)	–	−0.463(–)	–	1.67(–)	–	0.434(–)	–
Lagothrix lagotricha	3	102.7(1.53)	100.99–103.81	−0.299(0.05)	−0.35 to −0.27	1.564(0.04)	1.53–1.6	0.091(0.12)	−0.04 to 0.19
Lagothrix lugens	1	96.1(–)	–	−0.218(–)	–	1.593(–)	–	0.295(–)	–
Callitrichinae									
Callimico goeldii	6	90.1(6.07)	83.8–97.82	−0.15(0.03)	−0.2 to −0.12	1.712(0.07)	1.62–1.82	0.262(0.03)	0.23–0.3
Callithrix jacchus	5	89.5(1.38)	87.17–90.65	−0.202(0.06)	−0.3 to −0.13	1.654(0.03)	1.63–1.69	0.317(0.13)	0.24–0.56
Callithrix pygmaea	5	80.5(1.55)	78.82–82.87	−0.188(0.06)	−0.25 to −0.13	1.745(0.1)	1.63–1.91	0.259(0.19)	0.08–0.58
Leontopithecus rosalia	4	79.2(8)	70.19–88.43	−0.188(0.02)	−0.21 to −0.16	1.651(0.03)	1.62–1.68	0.441(0.03)	0.4–0.47
Saguinus midas	3	87.1(4.82)	81.92–91.49	−0.22(0.06)	−0.28 to −0.18	1.647(0.06)	1.59–1.7	0.302(0.1)	0.18–0.37
Saguinus mystax	3	85.4(6.12)	81.05–89.7	−0.176(0.05)	−0.21 to −0.14	1.713(0.03)	1.69–1.74	0.38(0.01)	0.37–0.39
Saguinus oedipus	1	85.8(–)	–	−0.171(–)	–	1.586(–)	–	0.23(–)	–
Cebinae/Aotinae									
Aotus infulatus	1	99.2(–)	–	−0.252(–)	–	1.694(–)	–	0.256(–)	–
Aotus trivirgatus	2	94.9(5.31)	91.15–98.66	−0.202(0.13)	−0.29 to −0.11	1.701(0.02)	1.69–1.71	0.271(0.07)	0.22–0.32
Aotus azarae	3	95(2.78)	91.99–97.46	−0.144(0.05)	−0.2 to −0.11	1.673(0.03)	1.65–1.71	0.229(0.08)	0.15–0.31
Cebus paella	6	90.5(3.02)	87.16–94.62	−0.133(0.01)	−0.14 to −0.12	1.743(0.06)	1.66–1.82	0.27(0.07)	0.18–0.38
Saimiri boliviensis	3	91.8(1.41)	90.19–92.9	−0.185(0.07)	−0.26 to −0.13	1.685(0.05)	1.63–1.74	0.166(0.15)	0–0.3
Saimiri sciureus	2	96.7(0.3)	96.48–96.91	−0.081(0.03)	−0.1 to −0.06	1.745(0.03)	1.73–1.76	0.231(0.04)	0.2–0.26
Pitheciinae									
Cacajao calvus	3	98.7(4.84)	94.42–103.97	−0.135(0.05)	−0.2 to −0.1	1.827(0.13)	1.71–1.97	0.334(0.03)	0.31–0.37
Callicebus donacophilus	2	98.4(2.49)	96.61–100.13	−0.215(0.03)	−0.24 to −0.2	1.7(0.01)	1.69–1.71	0.35(0)	0.35–0.35
Callicebus moloch	3	96.4(0.92)	95.87–97.46	−0.11(0.06)	−0.17 to −0.06	1.621(0.03)	1.58–1.65	0.234(0.15)	0.08–0.39
Chiropotes sp.	2	90.6(5.42)	86.77–94.43	−0.161(0.12)	−0.25 to −0.07	1.787(0.13)	1.69–1.88	0.225(0.05)	0.20–0.26
Pithecia pithecia	3	96.9(2.56)	94.9–99.77	−0.24(0.03)	−0.26 to −0.21	1.683(0.04)	1.64–1.72	0.302(0.07)	0.22–0.35
Tarsiidae									
Tarsius bancanus	2	93.5(0.5)	93.19–93.9	−0.036(0.02)	−0.05 to −0.02	1.495(0)	1.49–1.5	−0.026(0.02)	−0.04 to −0.01
Tarsius syrichta	2	98.1(1.45)	97.07–99.12	−0.101(0.11)	−0.18 to −0.03	1.572(0.04)	1.54–1.6	0.157(0.02)	0.14–0.17
Tarsius tarsier	2	91.1(2.18)	89.58–92.67	−0.066(0.02)	−0.08 to −0.06	1.534(0.04)	1.51–1.56	0.143(0.01)	0.14–0.15
Cheirogaleidae									
Cheirogaleus major	1	117(–)	–	−0.09(–)	–	1.672(–)	–	0(–)	–

TABLE 3. Continued

Taxon	*n*	FIB	min–max	MTFa/EFa	min–max	Pmtr/MTF	min–max	MTH–R	min–max
Cheirogaleus medius	3	110.3(4.66)	105.47–114.75	−0.018(0.03)	−0.03–0.01	1.608(0.04)	1.58–1.66	0.126(0.06)	0.07–0.19
Microcebus griseorufus	10	103.1(2.99)	97.2–106.25	−0.08(0.04)	−0.14 to −0.02	1.549(0.05)	1.49–1.63	−0.053(0.07)	−0.2 to 0
Mirza coquereli	2	108.3(1.98)	106.9–109.7	−0.131(0.01)	−0.14 to −0.12	1.527(0)	1.53–1.53	0.092(0.06)	0.05–0.13
Lepilemuridae									
Lepilemur mustelinus	6	113.8(3.2)	108.74–117.58	−0.022(0.05)	−0.08–0.04	1.556(0.06)	1.47–1.62	−0.058(0.08)	−0.18 to 0
Daubentoniidae									
Daubentonia madagascariensis	3	111.3(2)	109.88–113.62	−0.078(0.05)	−0.11 to −0.02	1.5(0.07)	1.45–1.58	−0.05(0.06)	−0.12 to 0
Indriidae									
Avahi laniger	4	120.7(6.61)	110.87–125.01	0.065(0.04)	0.01–0.11	1.487(0.03)	1.46–1.54	−0.075(0.03)	−0.11 to −0.05
Indri indri	2	112.8(3.06)	110.64–114.97	0.177(0.03)	0.16–0.2	1.535(0.01)	1.52–1.55	0(0)	0–0
Propithecus diadema	1	117.4(–)	–	0.055(–)	–	1.544(–)	–	−0.03(–)	–
Propithecus verreauxi	6	112.4(2.81)	109.57–116.72	0.114(0.03)	0.06–0.14	1.542(0.03)	1.5–1.58	−0.006(0.04)	−0.04 to 0.06
Lemuridae									
Eulemur albifrons	3	112.4(0.97)	111.33–113.26	0.07(0.06)	0.01–0.12	1.482(0.03)	1.46–1.51	−0.045(0.04)	−0.08 to 0
Eulemur collaris	2	116.5(0.04)	116.51–116.57	0.078(0.01)	0.07–0.09	1.495(0.01)	1.49–1.5	−0.128(0.04)	−0.15 to −0.1
Eulemur fulvus	1	116.2(–)	–	0.06(–)	–	1.536(–)	–	0(–)	–
Eulemur mongoz	2	115.6(0.91)	114.95–116.24	0.027(0.05)	−0.01–0.06	1.559(0.03)	1.54–1.58	−0.059(0.08)	−0.12 to 0
Hapalemur griseus	3	113(2.15)	110.83–115.13	0.085(0.06)	0.03–0.15	1.525(0)	1.52–1.53	−0.219(0.05)	−0.28 to −0.18
Lemur catta	4	111.9(3.45)	108.21–115.21	0.089(0.04)	0.03–0.13	1.496(0.01)	1.48–1.51	−0.213(0.08)	−0.33 to −0.14
Prolemur simus	4	107.9(3.58)	103.81–112.41	0.002(0.02)	−0.02–0.02	1.543(0.05)	1.5–1.6	−0.056(0.08)	−0.18 to 0
Varecia variegata	4	111.3(1.57)	109.96–113.59	0.021(0.03)	−0.02–0.05	1.475(0.04)	1.45–1.53	−0.207(0.02)	−0.24 to −0.19
Galagidae									
Euoticus elegantulus	2	103.8(2.54)	102.01–105.6	0.167(0.01)	0.16–0.18	1.482(0.01)	1.48–1.49	−0.224(0.11)	−0.3 to −0.14
Galago senegalensis	5	109.8(3.34)	104.96–113.19	0.138(0.02)	0.11–0.17	1.462(0.04)	1.42–1.52	−0.148(0.07)	−0.22 to −0.06
Galagoides demidoff	6	113.1(3.04)	110.72–118.42	0.146(0.06)	0.07–0.22	1.553(0.07)	1.45–1.63	−0.339(0.06)	−0.42 to −0.28
Otolemur crassicaudatus	5	108.9(1.79)	107.22–111.92	0.168(0.02)	0.14–0.19	1.546(0.07)	1.47–1.65	−0.247(0.12)	−0.38 to −0.13
Lorisidae									
Arctocebus calabarensis	2	112.6(2.47)	110.81–114.31	0.23(0.05)	0.19–0.27	1.581(0)	1.58–1.58	−0.647(0.04)	−0.67 to −0.62
Loris tardigradus	4	108.7(1.51)	107.66–110.98	0.031(0.08)	−0.04–0.1	1.592(0.06)	1.51–1.65	−0.103(0.08)	−0.22 to −0.04
Nycticebus coucang	3	111.8(2.83)	108.52–113.54	0.232(0.02)	0.21–0.25	1.587(0.05)	1.53–1.63	−0.209(0.11)	−0.33 to −0.14
Perodicticus potto	6	112.2(3.49)	108.47–116.74	0.022(0.07)	−0.05–0.13	1.64(0.06)	1.57–1.73	0.109(0.15)	−0.13 to 0.25
Euarchonta									
Cynocephalus volans	3	108(1.15)	107.21–109.35	−0.155(0.05)	−0.19 to −0.1	1.686(0.04)	1.64–1.71	0.379(0.15)	0.23–0.54
Ptilocercus lowii	3	96(1.96)	93.84–97.69	−0.14(0.08)	−0.22 to −0.07	1.744(0.02)	1.73–1.76	−0.004(0.01)	−0.01 to 0.01
Tupaia glis	3	74(0.26)	73.73–74.24	−0.267(0.05)	−0.31 to −0.22	1.728(0.03)	1.69–1.76	−0.003(0)	−0.01–0

Standard deviation in parentheses.

TABLE 4. Analyzed variables for fossil taxa

Higher taxon	Taxon	n	FIB	min–max	MTFa/EFa	min–max	Pmtr/MTF	min–max	MTH-R	min–max
Anthropoidea: *incertae sedis* and stem										
Eosimiidae	*Eosimias sinensis*	3	95.3(2.23)	92.88–97.24	−0.194(0.03)	−0.22 to −0.16	1.676(0.06)	1.61–1.73	0.358(0.04)	0.31–0.39
incertae sedis	"Protoanthropoid" IVPP 12305	1	–	–	—	–	–	–	−0.001(–)	–
incertae sedis	"Protoanthropoid" IVPP 12306	1	94.5(–)	–	−0.156(–)	–	1.587(–)	–	−0.001(–)	–
incertae sedis	"Amphipithecidae" (?) NMMP 39	1	93(–)	–	−0.154(–)	–	1.526(–)	–	−0.068(–)	–
Parapithecidae	Parapithecidae	6	82.6(5.64)	77.21–93.12	−0.026(0.06)	−0.1–0.07	1.657(0.04)	1.61–1.72	0.215(0.05)	0.15–0.27
Proteopithecidae	*Proteopithecus sylviae*	1	95.1(–)	–	−0.007(–)	–	1.625(–)	–	0.08(–)	–
Catarrhini										
Hominoidea	*Australopithecus afarensis*	1	110.3(–)	–	−0.413(–)	–	1.733(–)	–	0.457(–)	–
Hominoidea	*Homo* sp. KNM ER 1464	1	86.7(–)	–	−0.553(–)	–	1.838(–)	–	0.526(–)	–
Hominoidea	*Homo* sp. KNMER 813	1	92.8(–)	–	−0.516(–)	–	1.861(–)	–	0.684(–)	–
Hominoidea	*Homo habilis*	1	92.6(–)	–	−0.144(–)	–	1.91(–)	–	0.28(–)	–
Propliopithecidae	*Aegyptopithecus zeuxis*	2	91.5(7.31)	–	−0.235(–)	–	1.621(–)	–	0.267(–)	–
Oligopithecidae	*Catopithecus browni*	1	96(–)	–	−0.119(–)	–	1.583(–)	–	0.118(–)	–
Platyrrhini										
Pitheciinae	*Cebupithecia sarmientoi*	1	101(–)	–	−0.172(–)	–	1.856(–)	–	0.388(–)	–
incertae sedis	*Dolichocebus gaimanensis*	1	94.4(–)	–	−0.071(–)	–	–	–	0.166(–)	–
Pitheciinae	*Proteropithecia neuquenensis*	1	104.9(–)	–	−0.05(–)	–	1.6(–)	–	0.053(–)	–
Omomyiformes										
Omomyidae	*Necrolemur antiquus*	4	89.6(5.72)	84.34–96.51	−0.123(0.04)	−0.16 to −0.08	1.517(0.03)	1.48–1.56	−0.083(0.07)	−0.17 to 0
Omomyidae	*Absarokius abbotti*	1	103.6(–)	–	−0.032(–)	–	1.472(–)	–	−0.05(–)	–
Omomyidae	*Anemorhysis pearcei*	10	96.3(2.63)	92.8–101.6	−0.055(0.06)	−0.18 to −0.01	1.474(0.03)	1.41–1.5	−0.079(0.09)	−0.15 to 0.06
Omomyidae	*Hemiacodon gracilis*	7	99.6(3.41)	93.64–102.82	−0.007(0.03)	−0.04 to 0.03	1.606(0.06)	1.51–1.69	−0.113(0.06)	−0.17 to 0
Omomyidae	*Omomys carteri*	5	101.4(4.27)	96.32–106.34	−0.037(0.04)	−0.08 to 0.02	1.494(0.06)	1.41–1.55	−0.138(0.08)	−0.18 to 0
Omomyidae	*Ourayia uintensis*	2	93.6(4.94)	90.06–97.05	−0.087(0.06)	−0.13 to −0.05	1.618(0.07)	1.57–1.67	−0.321(–)	−0.32 to −0.32
Omomyidae	*Shoshonius cooperi*	3	98.2(3.46)	95.77–102.2	−0.03(0.02)	−0.05 to −0.02	1.55(0.02)	1.53–1.56	−0.092(0.09)	−0.2 to −0.03
Omomyidae	*Steinius ?*	4	97.9(2.58)	94.52–100.77	−0.038(0.03)	−0.07 to 0.01	1.482(0.05)	1.44–1.53	−0.089(0.13)	−0.19 to 0.05
Omomyidae	*Teilhardina belgica*	2	102.9(0.45)	102.6–103.23	−0.113(0.05)	−0.15 to −0.07	1.505(0.07)	1.46–1.55	0.042(0.01)	0.04–0.05
Omomyidae	*Teilhardina brandti*	2	102(2.49)	–	−0.029(–)	–	1.524(–)	–	−0.108(–)	–
Omomyidae	*Tetonius homunculus*	3	98.8(3.08)	95.5–101.63	−0.076(0.06)	−0.13 to 0	1.456(0.04)	1.43–1.5	−0.105(0.04)	−0.14 to −0.06
Omomyidae	*Washakius insignis*	2	96.9(0.07)	96.8–96.9	−0.077(0.06)	−0.12 to −0.04	1.544(0.03)	1.53–1.56	0.022(0.03)	0–0.04
Lemuriformes										
Megaladapidae	*Megaladapis* sp.	4	133.9(3.26)	129.14–136.37	−0.073(0.03)	−0.11 to −0.04	1.816(0.05)	1.76–1.88	0.473(0.11)	0.33–0.58
Lemuridae	*Pachylemur insignis*	1	104.5(–)	–	–	–	1.578(–)	–	0.148(–)	–
Archaeolemuridae	*Archaeolemur edwardsi*	6	103.1(2.67)	99.99–107.15	−0.031(0.06)	−0.11 to 0.06	1.497(0.02)	1.47–1.52	−0.155(0.12)	−0.26 to 0.07
Palaeopropithecidae	*Babakotia radofilai*	3	114.9(12.32)	97.84–124.59	−0.193(0.11)	−0.28 to −0.04	1.722(0.16)	1.62–1.97	0.194(0.19)	−0.06 to 0.37
Palaeopropithecidae	*Palaeopropithecus* sp.	4	137.3(4.04)	132.28–141.79	0.355(0.05)	0.32–0.41	1.419(0.06)	1.36–1.48	−0.376(0.03)	−0.41 to −0.35
Adapiformes										
Adapinae	*Adapis* sp.	8	109(2.69)	105.53–113.98	−0.075(0.04)	−0.12 to −0.02	1.529(0.02)	1.5–1.58	−0.225(0.16)	−0.54 to 0
Adapinae	*Leptadapis magnus*	3	106.3(2.16)	104.32–108.61	−0.101(0.02)	−0.12 to −0.07	1.5(0.01)	1.49–1.51	−0.126(0.09)	−0.23 to −0.08
Asiadapinae	*Asiadapis cambayensis*	1	100.4(–)	–	−0.043(–)	–	1.478(–)	–	−0.033(–)	–
Asiadapinae	*Marcgodinotius indicus*	3	107.4(2.11)	105.57–109.71	−0.084(0.02)	−0.1 to −0.06	1.54(0.04)	1.49–1.57	−0.165(0.15)	−0.34 to −0.08
Caenopithecinae	*Afradapis longicristatus*	1	116.4(–)	–	0.031(–)	–	1.649(–)	–	−0.326(–)	–
Cercamoniidae	*Anchomomys frontanyensis*	3	108.5(3.05)	105.02–110.86	−0.06(0.01)	−0.07 to −0.05	1.648(0.07)	1.58–1.71	−0.181(0.04)	−0.21 to −0.13
Notharctidae	*Cantius abditus*	6	101.8(5.07)	92.73–106.96	−0.102(0.04)	−0.13 to −0.07	1.529(0.07)	1.44–1.63	−0.146(0.06)	−0.19 to −0.1
Notharctidae	*Cantius frugivorous*	1	110.4(–)	–	–	–	1.439(–)	–	−0.131(–)	–
Notharctidae	*Cantius mckennai*	2	96.4(3.82)	–	0.07(–)	–	–	–	−0.135(–)	–
Notharctidae	*Cantius nuniensis*	1	117.7(–)	–	−0.007(–)	–	1.473(–)	–	−0.12(–)	–
Notharctidae	*Cantius ralstoni*	4	99.8(3.7)	94.68–103.18	−0.116(–)	–	1.454(0.02)	1.44–1.48	−0.043(0.12)	−0.13 to 0.04
Notharctidae	*Cantius trigonodus*	6	98.3(3.72)	92.5–103.12	−0.049(0.03)	−0.08 to −0.03	1.505(0.04)	1.45–1.57	−0.148(0.1)	−0.26 to 0
Djebelemuridae	*Djebelemur martinezi*	1	112.8(–)	–	−0.096(–)	–	1.642(–)	–	−0.001(–)	–

TABLE 4. Continued

Higher taxon	Taxon	n	FIB	min–max	MTFa/EFa	min–max	Pmtr/MTF	min–max	MTH-R	min–max
Notharctidae	*Notharctus tenebrosus*	10	107.8(3.7)	101.43–116	−0.06(0.05)	−0.12 to 0.02	1.519(0.04)	1.46–1.59	−0.082(0.07)	−0.19 to 0.04
Notharctidae	*Notharctus venticolus*	3	102.3(6.22)	95.6–107.9	−0.045(0.05)	−0.1 to 0.01	1.509(0.05)	1.47–1.56	−0.169(0.04)	−0.21 to −0.14
Notharctidae	*Pelycodus jarrovii*	1	99.1(–)	–	–	–	1.494(–)	–	−0.099(–)	–
Notharctidae	*Smilodectes gracilis*	2	108.8(1.34)	107.8–109.7	−0.004(0.05)	−0.04 to 0.03	1.561(0.03)	1.54–1.59	−0.12(0.04)	−0.15 to −0.09
Plesiadapiformes										
Carpolestidae	*Carpolestes simpsoni*	1	98.2(–)	–	−0.465(–)	–	1.842(–)	–	0.567(–)	–
Paromomyidae	*Ignacius graybullianus*	1	90.6(–)	–	−0.335(–)	–	1.675(–)	–	0.447(–)	–
Plesiadapidae	*Plesiadapis cookei*	1	100.4(–)	–	−0.329(–)	–	1.675(–)	–	0.55(–)	–
Plesiadapidae	*Plesiadapis rex*	1	102.7(–)	–	−0.228(–)	–	1.647(–)	–	0.376(–)	–

Standard deviation in parentheses.

and B were both available, they were the landmarks of choice. A line was drawn through these landmarks in Avizo. The additional two linear measures of this study were then taken perpendicular to the line through these landmarks. The first measure, "MTF height 1" (MTH1) was taken from the dorsal-most point on the medial trochlear rim to the line. The second measure (MTH2) was taken from this same point, down to the plantar-most extent of the MTF. Taxa with a dorsoplantarly narrow facet should have MTH1 > MTH2. In some taxa point A is not directly visible. In this case, a line intersecting point B is oriented so that it is parallel to the third reference feature, the dorsomedial margin of the sustentacular facet. In others, point B was not visible because it is obscured behind elements of the body. In this case, point B was approximated with reference to the dorsomedial margin of the sustentacular facet: specifically, where a line through it intersects the obscuring structures of the body (Fig. 2C, *Propithecus*).

MTF-perimeter. If the whole talar body is compressed dorsoplantarly, the comparison of linear measures above may not sufficiently describe narrow facets. Therefore, we collected facet perimeter measures to help quantify facet shape (Fig. 2B). In Geomagic, all surface material except the MTF was deleted from the digital file, and any holes in the facet surface were filled (since internal holes, if present, are included in Geomagic's computation of perimeter length). A curve was generated using the "Create from boundary" function, and the "Maximum Boundary Length" was recorded. To test whether scan resolution and the number of vertices/triangles in the surface mesh affected perimeter length, we used the "Decimate" tool in Geomagic to generate coarser versions of each facet surface mesh. For the six surfaces we tested, surface resolution had to be decreased by more than 85% (e.g., from ~43,000 faces to 5,000 faces) before maximum boundary length changed by more than 5%. Because the majority of included specimens have similar surface resolution, we used no down sampling or resolution standardization. The use of this measure for assessing facet shape is described below.

Fibular facet angle. Hypothesis 1 generates predictions about how MTF variation relates to variation in FFa, so we included these data as well. Most FFa values come directly from Boyer and Seiffert (2013, their tables 1 and 2, and their appendix). For specimens in our expanded sample, FFa was computed using the method illustrated in Boyer and Seiffert's (2013, their figure 2) (reported in Tables 3 and 4 of this article, as well as in Supporting Information tables).

Computed variables

Since our goal is to assess the distinctiveness of anthropoid and "prosimian" MTFs irrespective of absolute size, the following potentially "size free" variables were distilled from our measurements (Tables 3 and 4).

ln[(MTFa$^{1/2}$)/(BM$^{1/3}$)] and ln[(EFa$^{1/2}$)/(BM$^{1/3}$)]. The natural logarithm of the ratio of the square root of species mean MTFa or EFa to the cube root of species mean body mass. These can only be assessed in extant taxa for which body mass is reliably reported. Taxa with a larger MTFa for their body sizes have a higher value;

"prosimians" are expected to have higher values than anthropoids.

ln[(MTFa$^{1/2}$)/(EFa$^{1/2}$)]. The natural logarithm of the ratio of the square root of individual MTFa to the square root of EFa. It can be assessed in all specimens for which both facets are complete. Taxa with a larger MTFa relative to their EFa have a higher value; "prosimians" are expected to have higher values than anthropoids.

ln[(MTF-perimeter)/(MTFa$^{1/2}$)]. The natural logarithm of the ratio of length of the MTF perimeter to the square root of the MTFa. It can be assessed in all specimens that have a complete MTF. Taxa with a narrower facet should have a greater perimeter relative to facet area; anthropoids are expected to have higher values than "prosimians."

ln[(MTH1)/(MTH2)]. The natural logarithm of the ratio of the "MTF height 1" to "MTF height 2." It can be measured in all specimens that have intact trochlear rims, the plantar-most margin of the MTF, and some amount of the talar neck. Taxa with a more dorsally restricted MTF will have a higher ratio; anthropoids are expected to have higher values than "prosimians."

Analyses

Measurement error. To evaluate the degree to which measurement error influences patterns in our data, we selected a 30 specimen subsample encompassing the diversity of talar morphs in the complete dataset. On each specimen, we repeated the same measurement on separate days or with sufficient time intervening to ensure little memory of previous measurement events. Error on FFa has been previously reported (Boyer and Seiffert, 2013) and the methods have not changed for that variable. All other variables were checked for error rates. To quantify error, we computed percentage error of the three replicates (White and Folkens, 2010). We did this by subtracting each replicate from the mean of all three and taking the absolute value. We then took the average of these deviations, divided them by the mean, and multiplied the result by 100.

Regression of shape variables against body mass. Though shape ratios are dimensionless and thus potentially "size free," if there is a strong biomechanical basis for variation in MTF shape, then it is possible that some of these variables will exhibit allometry. If allometric effects are uniform and strong, they can potentially be subtracted by using residuals (Kay, 1975; Fleagle, 1985; Demes and Günther, 1989; Boyer et al., 2013a; but see Freckleton, 2009). On the other hand, if allometric effects are weaker or restricted to certain clades, the variables may remain diagnostic without accounting for size in general. In that case, any particular instances of clade specific size correlations can be used as further tests of functional explanations for differences between taxa (Boyer and Seiffert, 2013).

To check for allometric trends, we regressed all computed shape variables against body mass. Species mean values for all shape variables were computed for all extant taxa in our analyses (Supporting Information Table S1) and regressed against weighted species mean body masses (body mass was analyzed as the natural logarithm of the cube root) using phylogenetic generalized least squares (PGLS). Weighting of a species mean body mass was accomplished by: 1) taking sex specific body mass from the literature (see references above) and applying it to each specimen of a known sex. Individuals of unknown sex were assigned a body mass representing the average of male and female values for species with less than 10% sexual dimorphism (n = 35). A few extant specimens (n = 25) were of unknown sex and represented species with greater than 10% sexual dimorphism; data from these individuals were not incorporated into means for PGLS regressions. 2) A species mean was computed by averaging all specimens with assigned body masses; the species mean is therefore weighted by the number of males and females in our dataset. Analyses were conducted using *caper* (Orme et al., 2011) in R. The phylogenetic tree used for this analysis was downloaded from the 10 K trees website, version 3.0 (Arnold et al., 2010) and edited in Mesquite (Maddison and Maddison, 2011) to include non-primate euarchontans. Branch lengths for scandentians and dermopterans came from Roberts et al. (2011) and Janečka et al. (2007), respectively. The tree is provided in the Supporting Information documents (Tree1.nex). We employed ordinary least squares (OLS) regressions whenever 1) Pagel's lambda (λ), the measure of phylogenetic signal, had a maximum likelihood value equal to zero, 2) the confidence limits of λ included zero, or 3) the relationship was non-significant (i.e., no allometry detected).

ANCOVA of facet area (dependent) on body mass (covariate). Another method for dealing with allometry (instead of using shape indices and/or residuals) is to use body mass as a covariate in analyses of covariance (ANCOVA) (Yapuncich and Boyer, 2014) with other measures reflecting absolute dimensions. A slightly modified dataset (Supporting Information Table S2) is used for these regressions. Instead of using species mean (as required in PGLS approaches), we attempted to account for high levels of sexual dimorphism in some species. If the difference between male and female body masses was less than 10% of average body mass (low sexual dimorphism), species-mean body mass was used. If the difference between male and female body masses was greater than 10% of average body mass (high sexual dimorphism), then sex-specific body masses were used (Supporting Information Table S2). As above, individuals of unknown sex were only included in body mass regressions if they were from species of low sexual dimorphism. The groupings are presented in Supporting Information Table S4.

We test whether "prosimians" have a larger natural logarithm of square root MTFa (dependent) than anthropoids for a given natural logarithm of cube root body mass (covariate). We also test whether "prosimians" have a smaller natural logarithm square root EFa (dependent) than anthropoids for a given natural logarithm cube root body mass (covariate). ANCOVAs were conducted in JMP 11.0.0 (SAS Institute Inc., 1989-2013). In order for ANCOVAs to meaningfully address these questions, two preliminary tests must be passed: the samples must exhibit equal variance (homoscedasticity) and have non-significantly different slopes: heterogeneous slopes render ANCOVAs inappropriate (Engqvist,

2005). Because we were wary of Type II error in these preliminary analyses, we also ran OLS regressions of MTFa and EFa on body mass for the groups of interest (Supporting Information Table S2). While phylogenetic ANCOVA (PhyANCOVA) methods are available (BayesTraits) we feel that purposefully dividing the sample along clade lines (as we needed to do given our questions) reduces the effectiveness of this approach.

ANOVA of MTF variables using clade groups. To assess the major predictions of our hypotheses, we used one-way analysis of variance (ANOVA) in PAST (Hammer et al., 2006). We considered this more appropriate than PhyANOVA. Results of a PhyANOVA run using PGLS can be expected to diverge from standard ANOVA when there are consistent differences (offsets) between major clades represented by taxa in the sample, or based on interactions between clade offsets and interclade diversity differences. One of the primary reasons one might consider applying PhyANOVA is to assess categorical effects in which taxa come from broadly different clades and phylogenetic signal is suspected (Winchester et al., 2014). This, however, is not the data structure for our questions since they are focused on clade-level comparisons. To control for different species sample sizes we use species mean values in our analyses (Tables 3 and 4), though individual data points used in the calculations can be found in Supporting Information Table S3.

Regression of MTF variables against FFa. If both FFa and relative MTFa are related to foot inversion as a habitual locomotor and postural behavior, then a correlation should exist between FFa and relative MTFa. Therefore, we used PGLS to assess the correlation between FFa and each of the focal variables. These were performed on species mean data in Tables 3 and 4, except for regressions of FFa and $\ln[(MTFa^{1/2})/(BM^{1/3})]$ which were run on data in Supporting Information Table S1. Supporting Information Table S1 also gives the taxonomic inclusion for the eight different subsamples used. The tree associated with it was already referred to (Tree1.nex). However, the tree for species lists of Tables 1–4 (Tree2a.nex) was constructed using a more involved procedure described below (and Supporting Information Table S4 gives the taxonomic inclusion for sub-clades associated with this tree and Tables (1–4)). We also computed one additional MTF variable to regress against FFa: the first principal component score resulting from a principal components analysis using a correlation matrix based on all MTF variables except $\ln[(MTFa^{1/2})/(BM^{1/3})]$, as taken from the species mean dataset of Tables 3 and 4 (PC1 score is given in Supporting Information Table S4). PAST was used to execute this analysis and output PC scores. PC1 has an eigenvalue of 2.15 and represents 72% of the variance. All variables loaded roughly equally (-0.5812 for $\ln[(MTFa^{1/2})/(EFa^{1/2})]$, 0.5237 for ln[(MTF-Perimeter)/$(MTFa^{1/2})$], and 0.6228 for ln[(MTH1)/(MTH2)]). While any one of our MTF variables conceivably represents an incomplete description of the functionally and phylogenetically significant information perceived qualitatively by previous authors (e.g., Gebo, 1986; Dagosto, 1990), the principal axis of all three may more closely approximate a complete description.

Phylogenetic comparative analyses: modeling character evolution and ASR

Construction of phylogenetic trees for studies of character evolution. Reconstructing broad-scale patterns of evolution in the shape and relative size of the MTF over the course of primate evolution requires a taxonomically broad phylogeny of living and extinct primates. No single phylogenetic analysis of morphological data has sampled the gamut of taxonomic diversity in our dataset, and so we use Matrix Representation with Parsimony (MRP), a method that allowed us to combine the phylogenetic results of several independent analyses that densely sampled various primate clades (e.g., platyrrhines, hominins). The character matrix of Marigó et al. (in review) provided the "core evidence" for relationships among early primates, onto which the results of other smaller-scale analyses were incorporated to form a new composite "supertree"; that "core" matrix now includes 391 morphological characters and 108 taxa, of which 87 are fossil, and 84 are Paleogene in age (see Supporting Information document). Earlier versions of this matrix have also been employed in the phylogenetic analyses of Kirk and Williams (2011), Marigó et al. (2013), and as the "core matrix" of Boyer et al. (2013a). Parsimony analysis of the matrix was undertaken using PAUP 4.0b10, with 10,000 random addition-sequence replicates and a molecular "scaffold" (*sensu* Springer et al., 2001) enforced, based on the results of Springer et al. (2012). Some of the multistate characters in that matrix were treated as ordered, and steps between polymorphisms and adjacent "fixed" states were weighted as one half-step, so that all transitions between "fixed" states in the analysis were equal to one step.

Two additional analyses were run and constrained in ways similar to those used in Boyer et al. (2013a): one constrained *Tarsius* and extant anthropoids to be more closely related to each other than to any fossil "omomyiform" (cf. Kay et al., 1997)—that is, a constraint that enforced the monophyly of the so-called "strict tarsier-anthropoid clade." The other constrained adapiforms to be more closely related to *Tarsius* and extant anthropoids than to extant strepsirrhines (cf. Franzen et al., 2009). MRP analyses (run in PAUP) were then used to combine the results of these analyses with those of Springer et al. (2012) and Janečka et al. (2007) for extant euarchontans, Bloch et al. (2007) for basal fossil euarchontans, Tornow (2008) and Rose et al. (2011) for omomyiforms, Gunnell (2002) for notharctine adapiforms, Kay (2015) for living and extinct platyrrhines, and Strait and Grine (2004) for early hominins. The details of this approach closely followed Boyer and Seiffert (2013) and Boyer et al. (2013a). In order to timescale the phylogenetic tree, we again closely followed Boyer et al. (2013a), who used the divergence dates recovered by Springer et al.'s (2012) analysis with independent rates and soft bounds to date splits among extant taxa, and placed extinct clades along stem lineages at 1 Ma intervals, working down from crown nodes (terminal branches for extinct taxa were at least 1 Ma in length, or longer if sister taxa were geologically older; see Boyer et al. [2013a] for additional details). In addition, two isolated hominin tali of early Pleistocene age and uncertain specific attribution (KNM-ER 1464 and KNM-ER 813; see Gebo and Schwartz [2006]) were grafted onto the tree as terminal branches between *Homo habilis* and *Homo sapiens*. See Figure 3 for the

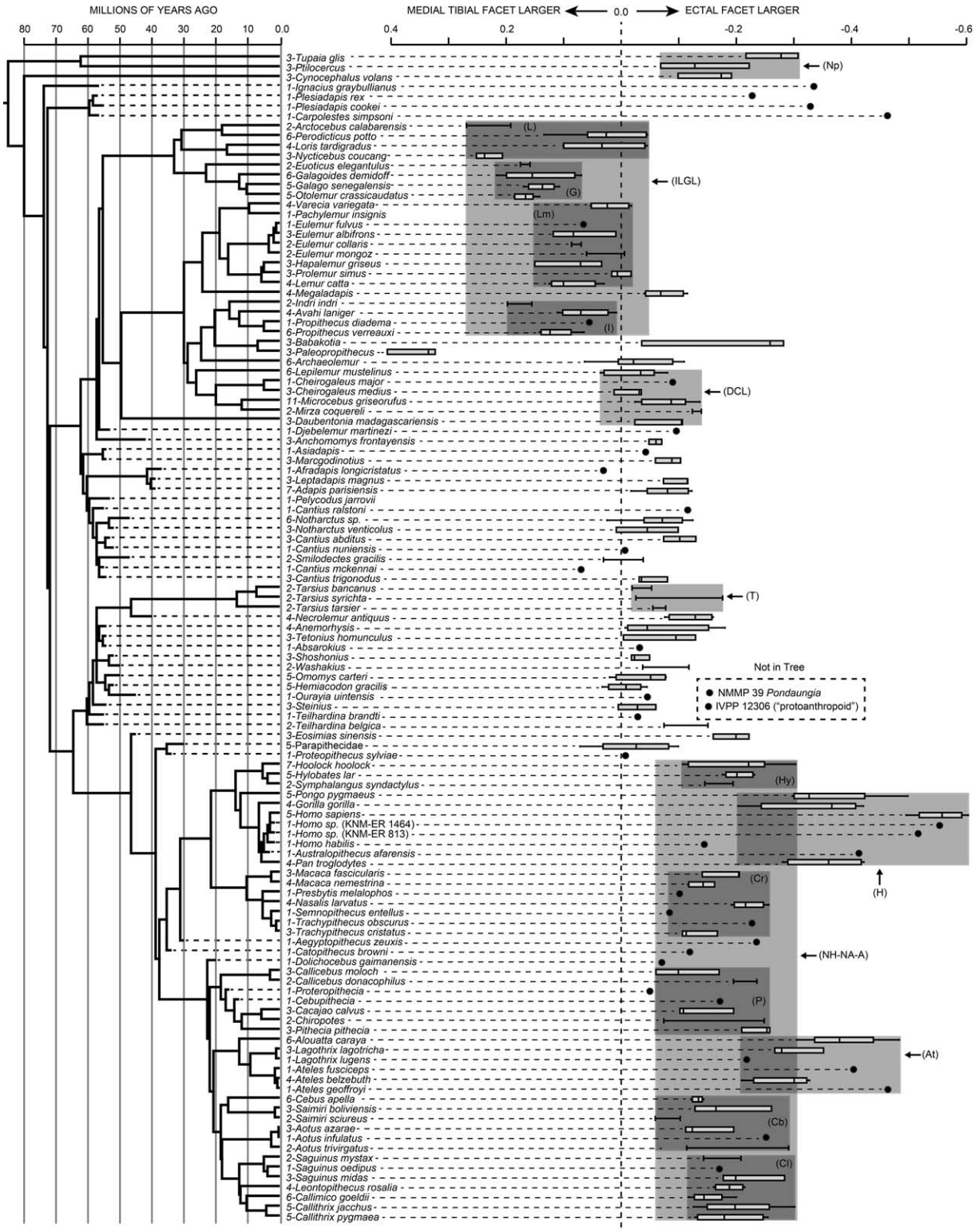

Fig. 3. Phylogenetic tree showing all included taxa. This tree also represents the operational taxonomic units, connectivity and branch lengths used for some phylogenetic comparative analyses (i.e., tree 2a in Supporting Information text). Species box and whisker plots to left display variance in MTFa/EFa ratios. Boxes represent 25%–75% quartiles. Horizontal line represents median. Whiskers extend at most to 1.5 times the interquartile range beyond the boxes. Points more distant are shown as outliers. The light gray boxes encompassing groups of species represent taxonomic groups used in within-strepsirrhine and within-anthropoid ANOVAs (Fig. 4, Table 10), while the gray boxes encompassing these represent groups for all-Euarchonta ANOVAs (Fig. 4, Table 10). Abbreviations for taxonomic groups given in Figure 4 caption.

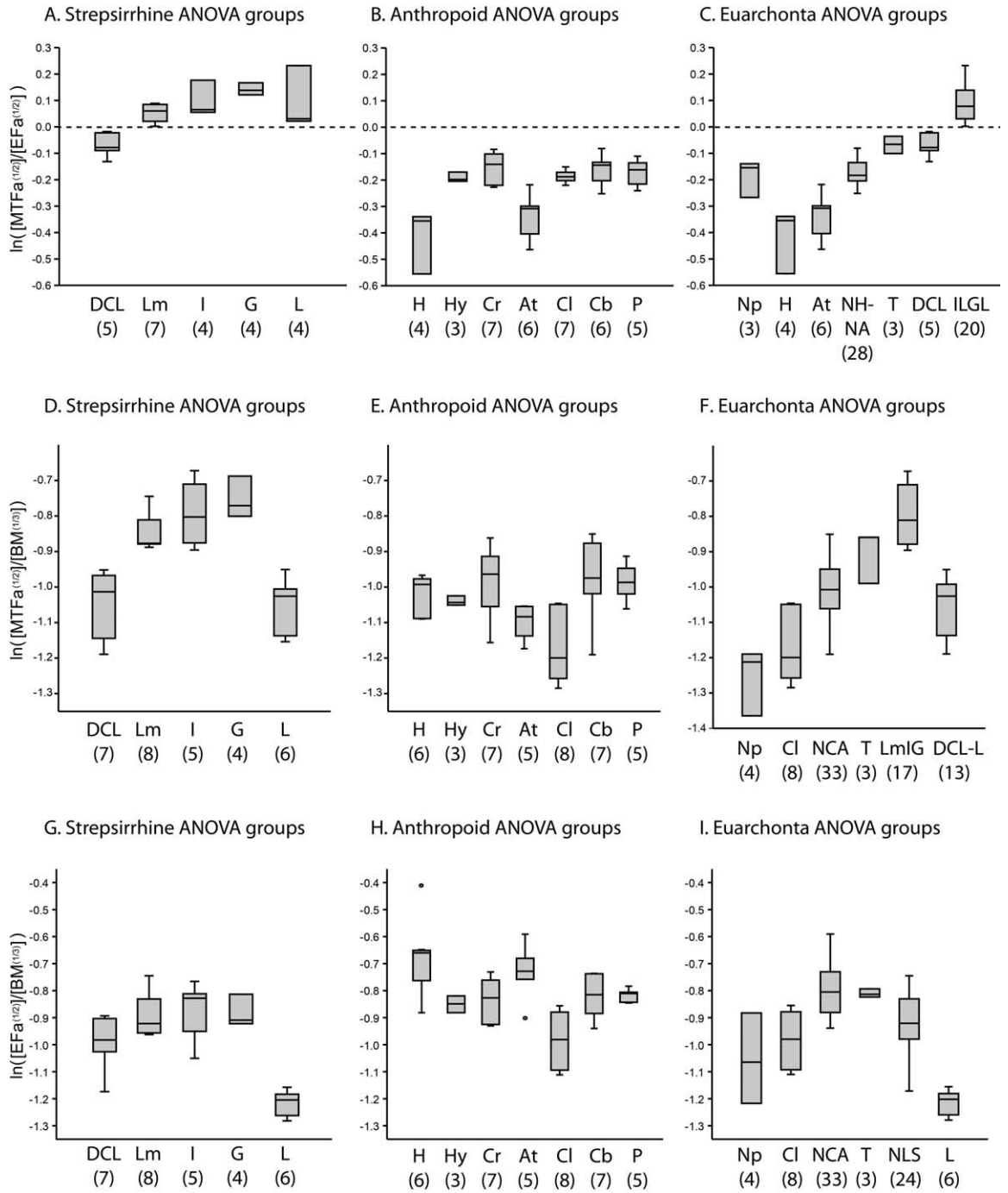

Fig. 4. (**A–C**) Plots of group means for MTFa/EFa that were compared with ANOVAs and reported in Table 10. (**D–F**) Plots of group means for MTFa/BM compared with ANOVAs and reported in Table 11. (**G–I**) Plots of group means for EFa/BM reported in Table 11. Abbreviations below box plots indicate included taxa. Number in parentheses below abbreviations are number of species per group. In A–C, *dashed line* represents value where a taxon's MTFa = EFa. Abbreviations in A, D, G: DCL, *Daubentonia*, Cheirogaleidae, Lepilemuridae. Abbreviations in B, E, F: H, Hominidae; Hy, Hylobatidae; Cr, Cercopithecoidea; At, Atelidae; Cl, Callitrichidae; Cb, Cebinae/Aotinae; P, Pitheciidae. Remaining abbreviations: Np, Non-primates; NHNA, Non-hominid, non-atelid anthropoids; T, tarsiers; ILGL, Indriidae, Lemuridae, Galagidae, Lorisidae; NCA, Non-callitrichine anthropoids; LmIG, Lemuridae, Indriidae, Galagidae; DCL-L, "DCL" + Lorisidae; NLS, Non-lorisid strepsirrhines.

primary time-scaled topology, and Supporting Information Figures S2 and S3 for alternative constraints (i.e., strict *Tarsius*-Anthropoidea clade, and adapiform-haplorhine clade, respectively). See Supporting Information documentation for nexus files of these trees.

Modeling character evolution and ASR. The methods employed for reconstruction of ancestral values closely followed those described by Boyer and Seiffert (2013) and Boyer et al. (2013a), and will only be briefly discussed. We used BayesTraits version 2 (Pagel and Meade, 2013) to

*TABLE 5. Error tests showing average percentage error (**x**%) documented by three replicates per specimen for 30 specimens and the standard deviation (**σ**%) in percentage error over those thirty specimens*

Variable	*N*	Rep/case	*x*% error	*σ*% error
MTH1	30	3	2.32	1.82
MTH2	30	3	1.68	1.11
TrochW	30	3	1.80	0.94
MTFa	30	3	2.44	1.40
EFa	29	3	1.70	1.11
MTFpmtr	30	3	1.81	1.10
MTH1/MTH2	30	3	2.30	1.61
$(MTFa/EFa)^{1/2}$	29	3	1.49	0.74
$MTFpmtr/(MTFa)^{1/2}$	30	3	1.97	1.44

determine which model (random walk or directional) and phylogenetic scaling parameters (delta, kappa, lambda, or none) best fit the distribution of the MTF-related traits evolving across each of the alternative trees described above. The maximum likelihood values for the trees, given each model/scaling parameter combination, were calculated in BayesTraits, and the combination that provided the highest log likelihood was then used in a Markov Chain Monte Carlo (MCMC) sampling run in order to create model files that would be used for ASRs. For each MCMC analysis, the rate deviation parameter was automatically tuned by BayesTraits to give acceptance rates of about 30%. MCMC analyses that were undertaken to create model files were run for 10,050,000 generations, with a burn-in period of 50,000 generations. Those model files were then employed in longer MCMC sampling runs (20,050,000 generations) to develop distributions for trait values at various nodes in the primate tree. The means and 95% highest posterior density intervals for each node were calculated in Tracer v1.5 (Rambaut and Drummond, 2009), and reported in Table 15 and Supporting Information Tables S7 and S8. Ancestral values were calculated at nodes of interest for FFa, $ln[(MTFa^{1/2})/(EFa^{1/2})]$, ln[(MTF-Perimeter)/$(MTFa^{1/2})$], and ln[(MTH1)/(MTH2)], but not $ln[(MTFa^{1/2})/(BM^{1/3})]$, because reliable fossil body mass values were unavailable.

RESULTS

Measurement error

We found low percentage error rates in all variables. On average, no variables showed error rates that would cause concern (Table 5). The highest average values for any measurement were less than 3%, with standard deviations lower than the average in most cases. Supporting Information Tables 5 and 6 provide more details. Tables 1 and 2 present another opportunity for estimating error in MTFa. The species means of MTFa (average of three replicated measures for each individual) can be compared with species means of MTFa* (a fourth replicate associated with reported perimeter values). The average species mean percent error between MTFa and MTFa* over the whole sample is 2.35% with a standard deviation of 1.74% and range of 0.1%–8% for the entire sample.

Regression of shape variables against body mass

Using PGLS, we checked four shape variables for correlations with the natural log of the cube root of body mass. Regressions were performed on several subclades. Because shape variables should be "size free," no significant correlation with body mass or a particular slope coefficient was expected. Results are presented in Table 6. In general, shape variables were not found to be correlated with body mass; however, FFa is correlated within the strepsirrhine, lemuriform, and platyrrhine subclades. These results are similar to those recovered by Boyer and Seiffert (2013) who regressed FFa on EFa (a facet highly correlated with body mass: Yapuncich and Boyer, 2014). However, Boyer and Seiffert (2013) found a significant relationship within lemuriforms but not within strepsirrhines. The major differences between their approach and ours are: 1) species means are slightly different due to inclusion of additional individuals; 2) we included two additional *Eulemur* species; 3) this study uses body mass rather than a body mass proxy. For $ln[(MTFa^{1/2})/(BM^{1/3})]$ we found significant correlations with body mass for the lemuriform group. For $ln[(MTFa^{1/2})/(EFa^{1/2})]$, significant correlations with body mass were found for haplorhines, anthropoids, and platyrrhines. For ln[(MTH1)/(MTH2)], a significant correlation with body mass was found only for haplorhines. Finally, for ln[(MTF-Perimeter)/$(MTFa^{1/2})$], no significant correlations with body mass were found.

ANCOVA of facet areas (dependent) on body mass (covariate)

Predictions 1a and 1b relate MTFa to body mass and EFa size respectively. These predictions produce the corollary that differences in EFa relative to body mass should also exist. ANCOVA results (Tables 7–9) comparing "prosimians" and anthropoids for MTFa versus body mass show equal variance and no treatment interaction (equal slopes). Additionally, anthropoids have a significantly lower intercept for MTFa than prosimians, as predicted (Tables 7–9). In contrast, comparisons between these same two groups for EFa returned violations of assumptions required for intercept comparison, due to a positively allometric slope in anthropoids and a significantly different isometric slope in "prosimians." Regrouping taxa as haplorhines and strepsirrhines returns equal slopes and significantly different intercepts for EFa vs. body mass, with haplorhines exhibiting a higher intercept than strepsirrhines (Tables 7–9). In contrast, using haplorhine/strepsirrhine groupings for MTFa returns unequal slopes (Tables 7–9). In this case, strepsirrhines exhibit positive allometry, while the haplorhine slope is isometric. Finally, using a strepsirrhine/anthropoid dataset (leaving tarsiers out) reveals equal variance and slopes for the two groups using either MTFa or EFa against body mass. For both of these analyses, the intercepts are unequal, with strepsirrhines having a higher MTFa intercept, but a lower EFa intercept than anthropoids. Comparisons of MTFa (dependent) to EFa (covariate) result in different slopes among all sets of groups compared, prohibiting comment on whether the intercepts differ in the predicted directions.

ANOVA of MTF variables using clade groups

Though our hypotheses refer to a comparison of anthropoids and "prosimians" as discrete groups, we began this assessment by plotting all values for all individuals by species, and then visually assessing the number of behaviorally and phylogenetically cohesive groups. We chose this approach to avoid missing meaningful inter-specific variation (Fig. 3), as overlap in values of

TABLE 6. Tests for correlations between body mass and computed shape ratios

Sample	Dependent	Independent	Method	n	Slope	Slope 95% CI	Intercept	Inter 95% CI	r_2	P	Lambda	Lambda 95% CI
Euarchontans	Fibular Facet Angle	ln[cbrtBM]	PGLS	74	2.459	(−2.061, 6.978)	92.631	(80.108, 105.153)	0.016	0.282	0.923	(0.821, 0.975)
Primates	Fibular Facet Angle	ln[cbrtBM]	PGLS	70	1.951	(−2.465, 6.367)	96.983	(84.728, 109.237)	0.011	0.381	0.886	(0.744, 0.961)
Haplorhines	Fibular Facet Angle	ln[cbrtBM]	PGLS	44	2.658	(−3.372, 8.687)	85.338	(68.400, 102.275)	0.018	0.379	0.844	(0.542, 0.965)
Strepsirrhines	Fibular Facet Angle	ln[cbrtBM]	PGLS	26	4.409	(1.199, 7.618)	101.926	(94.584, 109.268)	0.251	**	0.000	(NA, 0.499)
Anthropoids	Fibular Facet Angle	ln[cbrtBM]	PGLS	41	3.706	(−3.074, 10.486)	79.655	(59.094, 100.215)	0.030	0.276	0.801	(0.451, 0.959)
Prosimians	Fibular Facet Angle	ln[cbrtBM]	PGLS	29	3.353	(−1.536, 8.242)	99.444	(88.001, 110.886)	0.068	0.171	0.514	(NA, 0.883)
Platyrrhines	Fibular Facet Angle	ln[cbrtBM]	PGLS	25	12.319	(6.046, 18.593)	63.947	(48.566, 79.327)	0.418	***	0.325	(NA, 0.857)
Lemuriforms	Fibular Facet Angle	ln[cbrtBM]	PGLS	16	5.296	(0.832, 9.760)	99.954	(89.045, 110.863)	0.316	*	0.000	(NA, 0.923)
Euarchontans	ln[MTF Pmtr/sqrt(MTFa)]	ln[cbrtBM]	PGLS	74	−0.022	(−0.065, 0.022)	1.680	(1.567, 1.793)	0.014	0.320	0.712	(0.450, 0.875)
Primates	ln[MTF Pmtr/sqrt(MTFa)]	ln[cbrtBM]	PGLS	70	−0.012	(−0.056, 0.031)	1.607	(1.492, 1.721)	0.005	0.581	0.629	(0.325, 0.842)
Haplorhines	ln[MTF Pmtr/sqrt(MTFa)]	ln[cbrtBM]	PGLS	44	−0.014	(−0.075, 0.047)	1.645	(1.477, 1.812)	0.005	0.647	0.606	(0.099, 0.882)
Strepsirrhines	ln[MTF Pmtr/sqrt(MTFa)]	ln[cbrtBM]	PGLS	26	−0.012	(−0.067, 0.043)	1.569	(1.440, 1.699)	0.008	0.657	0.528	(NA, 0.892)
Anthropoids	ln[MTF Pmtr/sqrt(MTFa)]	ln[cbrtBM]	PGLS	41	−0.034	(−0.072, 0.004)	1.751	(1.645, 1.857)	0.076	0.080	0.000	(NA, 0.700)
Prosimians	ln[MTF Pmtr/sqrt(MTFa)]	ln[cbrtBM]	PGLS	29	−0.008	(−0.057, 0.041)	1.555	(1.446, 1.664)	0.005	0.729	0.514	(NA, 0.883)
Platyrrhines	ln[MTF Pmtr/sqrt(MTFa)]	ln[cbrtBM]	PGLS	25	−0.049	(−0.140, 0.041)	1.792	(1.570, 2.014)	0.052	0.271	0.362	(NA, 0.823)
Lemuriforms	ln[MTF Pmtr/sqrt(MTFa)]	ln[cbrtBM]	PGLS	16	−0.031	(−0.074, 0.012)	1.603	(1.498, 1.708)	0.145	0.145	0.000	(NA, 0.780)
Euarchontans	ln(MTH1/MTH2)	ln[cbrtBM]	PGLS	74	0.072	(−0.027, 0.172)	−0.074	(0.337, 0.190)	0.028	0.151	0.786	(0.531, 0.921)
Primates	ln(MTH1/MTH2)	ln[cbrtBM]	PGLS	70	0.068	(−0.036, 0.172)	−0.115	(−0.396, 0.165)	0.024	0.197	0.759	(0.484, 0.913)
Haplorhines	ln(MTH1/MTH2)	ln[cbrtBM]	PGLS	44	0.063	(0.002, 0.125)	0.100	(0.067, 0.267)	0.093	*	0.000	(NA, 0.759)
Strepsirrhines	ln(MTH1/MTH2)	ln[cbrtBM]	PGLS	26	0.066	(−0.103, 0.234)	−0.275	(0.665, 0.115)	0.026	0.430	0.286	(NA, 0.999)
Anthropoids	ln(MTH1/MTH2)	ln[cbrtBM]	PGLS	41	0.034	(−0.035, 0.102)	0.188	(−0.002, 0.378)	0.025	0.326	0.000	(NA, 0.649)
Prosimians	ln(MTH1/MTH2)	ln[cbrtBM]	PGLS	29	0.030	(−0.140, 0.200)	−0.131	(−0.513, 0.251)	0.005	0.717	0.593	(0.001, 1.000)
Platyrrhines	ln(MTH1/MTH2)	ln[cbrtBM]	PGLS	25	−0.074	(0.178, 0.030)	0.438	(0.187, 0.689)	0.086	0.155	0.000	(NA, 0.260)
Lemuriforms	ln(MTH1/MTH2)	ln[cbrtBM]	PGLS	16	−0.006	(0.162, 0.151)	−0.038	(−0.444, 0.369)	0.000	0.940	0.856	(NA, 1.000)
Euarchontans	ln[sqrt(MTFa/EFa)]	ln[cbrtBM]	PGLS	74	−0.043	(−0.113, 0.027)	−0.024	(−0.217, 0.169)	0.020	0.228	0.906	(0.775, 0.969)
Primates	ln[sqrt(MTFa/EFa)]	ln[cbrtBM]	PGLS	70	−0.050	(−0.123, 0.023)	0.058	(−0.144, 0.260)	0.027	0.174	0.889	(0.730, 0.965)
Haplorhines	ln[sqrt(MTFa/EFa)]	ln[cbrtBM]	PGLS	44	−0.133	(−0.208, −0.059)	0.142	(−0.063, 0.347)	0.236	***	0.630	(0.165, 0.895)
Strepsirrhines	ln[sqrt(MTFa/EFa)]	ln[cbrtBM]	PGLS	26	0.051	(−0.045, 0.148)	−0.060	(−0.307, 0.187)	0.048	0.280	1.000	(0.854, NA)
Anthropoids	ln[sqrt(MTFa/EFa)]	ln[cbrtBM]	PGLS	41	−0.139	(−0.225, −0.052)	0.169	(0.090, 0.428)	0.211	**	0.582	(0.171, 0.878)
Prosimians	ln[sqrt(MTFa/EFa)]	ln[cbrtBM]	PGLS	29	0.060	(−0.034, 0.154)	−0.111	(−0.343, 0.122)	0.059	0.204	1.000	(0.858, NA)
Platyrrhines	ln[sqrt(MTFa/EFa)]	ln[cbrtBM]	PGLS	25	−0.121	(−0.233, −0.009)	0.080	(−0.195, 0.355)	0.178	*	0.332	(NA, 0.802)
Lemuriforms	ln[sqrt(MTFa/EFa)]	ln[cbrtBM]	PGLS	16	0.097	(−0.004, 0.198)	−0.245	(−0.511, 0.022)	0.232	0.059	1.000	(NA, NA)
Euarchontans	ln[sqrt(MTFa)/cbrt(BM)]	ln[cbrtBM]	PGLS	74	0.049	(−0.035, 0.133)	−1.191	(−1.418, −0.965)	0.019	0.246	0.858	(0.680, 0.942)
Primates	ln[sqrt(MTFa)/cbrt(BM)]	ln[cbrtBM]	PGLS	70	0.046	(−0.038, 0.130)	−1.069	(−1.299, −0.839)	0.017	0.281	0.816	(0.579, 0.926)
Haplorhines	ln[sqrt(MTFa)/cbrt(BM)]	ln[cbrtBM]	PGLS	44	0.022	(−0.068, 0.112)	−1.040	(−1.286, −0.794)	0.006	0.623	0.612	(0.077, 0.874)
Strepsirrhines	ln[sqrt(MTFa)/cbrt(BM)]	ln[cbrtBM]	PGLS	26	0.059	(−0.095, 0.214)	−1.080	(−1.471, −0.689)	0.026	0.435	0.955	(0.673, NA)
Anthropoids	ln[sqrt(MTFa)/cbrt(BM)]	ln[cbrtBM]	PGLS	41	0.053	(−0.040, 0.147)	−1.183	(−1.460, −0.907)	0.033	0.256	0.427	(NA, 0.817)
Prosimians	ln[sqrt(MTFa)/cbrt(BM)]	ln[cbrtBM]	PGLS	29	0.055	(−0.089, 0.198)	−1.044	(−1.392, −0.696)	0.022	0.440	0.954	(0.680, NA)
Platyrrhines	ln[sqrt(MTFa)/cbrt(BM)]	ln[cbrtBM]	PGLS	25	0.070	(−0.094, 0.233)	−1.224	(−1.625, −0.823)	0.033	0.387	0.423	(NA, 0.809)
Lemuriforms	ln[sqrt(MTFa)/cbrt(BM)]	ln[cbrtBM]	PGLS	16	0.256	(0.126, 0.385)	−1.535	(−1.851, −1.218)	0.562	***	0.000	(NA, 0.979)

Datasets of species means used. See Supporting Information Table S1 for raw data, Supporting Information Table S4a for details on taxonomic inclusion. Nexus file Tree #1 in Supporting Information documents was used for phylogenetic comparative methods. *$P < 0.05$, **$P < 0.01$, ***$P < 0.001$.

TABLE 7. ANCOVA summary results

Clades compared (N)	Sample	Dependent	Covariate	Equal variance	Homogeneity of slopes	P	F(df)	r^2	Homogeneity of intercepts	P	Regression Parameter
Haplorhines (n = 55)	Dimorphic	**ln[sqrtMTFA]**	**ln[cbrtBM]**	**Y**	**N**	*	**15.705 (1,82)**	**0.957**	**N**	***	**Slope**
& strepsirrhines (30)	means	ln[sqrtEFA]	ln[cbrtBM]	Y	Y	0.732	19.992 (1,82)	0.971	N	***	Intercept
		lnTROCH	ln[cbrtBM]	Y	Y	0.659	16.440 (1,82)	0.968	N	***	Intercept
		ln[sqrtMTFA]	**ln[sqrtEFA]**	**Y**	**N**	**	**88.254 (1,82)**	**0.973**	**N**	***	**Slope**
Haplorhines (120) &	Individuals	lnMTFA	lnBM	**N**	**Y**	**–**	**13.237 (1,202)**	**0.934**	**N**	***	**Intercept**
strepsirrhines (85)		lnEFA	lnBM	**N**	**Y**	**–**	**58.321 (1,202)**	**0.970**	**N**	***	**Intercept**
[Y&B2014]											
Anthropoids (52)	Dimorphic	ln[sqrtMTFA]	ln[cbrtBM]	Y	Y	0.232	24.655 (1,82)	0.961	N	***	Intercept
& prosimians (33)	means	**ln[sqrtEFA]**	**ln[cbrtBM]**	**Y**	**N**	*	**9.380 (1,82)**	**0.967**	**N**	**	**Slope**
		lnTROCH	**ln[cbrtBM]**	**Y**	**N**	*	**4.030 (1,82)**	**0.964**	**N**	*	**Slope**
		ln[sqrtMTFA]	**ln[sqrtEFA]**	**Y**	**N**	***	**71.333 (1,82)**	**0.970**	**N**	***	**Slope**
Anthropoids (111)	Individuals	lnMTFA	lnBM	**N**	**Y**	**–**	**23.504 (1,193)**	**0.934**	**N**	***	**Intercept**
&strepsirrhines		lnEFA	lnBM	**N**	**N**	**–**	**35.883 (1,193)**	**0.970**	**N**	***	**Slope**
(85) [Y&B2014]											
Anthropoids (52) &	Dimorphic	ln[sqrtMTFA]	ln[cbrtBM]	Y	Y	0.096	22.8486 (1,82)	0.959	N	***	Intercept
strepsirrhines (30)	means	ln[sqrtEFA]	ln[cbrtBM]	Y	Y	0.370	13.5731 (1,82)	0.971	N	***	Intercept
		lnTROCH	ln[cbrtBM]	Y	Y	0.593	8.9412 (1,82)	0.973	N	**	Intercept
		ln[sqrtMTF]	**ln[sqrtEFA]**	**Y**	**N**	**	**84.2568**	**0.972**	**N**	***	**Slope**

Bold text indicates violation of ANCOVA assumptions.
Raw data found in Supporting Information Table S2 when "sample" column indicates "Dimorphic Means." Supporting Information Table S4a gives taxonomic inclusion for noted groups. $^{*}P < 0.05$, $^{**}P < 0.01$, $^{***}P < 0.001$.

any strepsirrhine taxa with any anthropoid taxa could imply corresponding functional and behavioral overlap. We were unable to begin by comparing all pairs of extant species with *t*-test or ANOVA as post hoc error rate correction becomes over-conservative. Therefore, upon observing the individual variation at the species level in $\ln[(MTFa^{1/2})/(EFa^{1/2})]$ (Fig. 3), we recognized five strepsirrhine groups (1: *Daubentonia*, Cheirogaleidae, and *Lepilemur* "DCL" [n = 6 species]; 2: Lemuridae [n = 7 species]; 3: Indriidae [n = 4]; 4: Galagidae [n = 4]; 5: Lorisidae [n = 4]), one tarsier group (n = 3), and seven anthropoid groups (1: Hominidae [n = 4]; 2: Hylobatidae [n = 3]; 3: Cercopithecoidea [n = 7]; 4: Atelidae [n = 6]; 5: Callitrichinae [n = 7]; 6: Cebinae/Aotinae [n = 6]; 7: Pitheciidae [n = 5]). These groups were used as the initial ANOVA groups for all variables.

ln[(MTFa$^{1/2}$)/(EFa$^{1/2}$)]. ANOVA (followed by *post hoc* comparisons using Tukey's Q in PAST) of the five identified strepsirrhine groups shows significant differences between the DCL group and all other strepsirrhine groups, while none of the other strepsirrhine groups are differentiated (Table 10). All species in the DCL group have a negative value for $\ln[(MTFa^{1/2})/(EFa^{1/2})]$ (Table 3; Fig. 4A), indicating that EFa is larger than MTFa. The remaining strepsirrhine species mean values are positive (indicating a larger MTFa). Going back to the individual data (Fig. 3; Supporting Information Table S3B), two individuals of *Loris* and *Perodicticus*, one *Varecia*, and one *Eulemur* have negative values, but again the mean values for these species are positive (Figs. 3, 4A; Table 3). Galagidae has values that are higher than and non-overlapping with those of Lemuridae despite the fact that they are not distinguished in *post hoc* comparisons; however, individual data (Fig. 3; Supporting Information Table S3) reveal substantially more overlap between these two groups. As a group, lorisids span a large range of values with some genera (*Arctocebus* and *Nycticebus*) being more galagid-like and other genera (*Perodicticus* and *Loris*) looking more lemurid-like. Based on these patterns, strepsirrhines are distilled into two groups for further analyses: 1) the DCL group (Figs. 3, 4AC), and 2) Indriidae, Lemuridae, Galagidae and Lorisidae as the "ILGL" group (Figs. 3, 4A; 4C).

ANOVA of anthropoid groups shows that hominids and atelids are indistinguishable, while both are significantly different from the remaining groups, which in turn are indistinguishable from each other (Table 10). While the similarities shared by non-hominid, non-atelid anthropoids are plausibly due to primitive retention of the ancestral anthropoid pattern, the hominid and atelid patterns are most likely convergent. Therefore, we created three groups of anthropoids: 1) hominids (Figs. 3, 4B; 4C); 2) atelids (Figs. 3, 4B; 4C); and 3) hylobatids, cercopithecoids, and non-atelid platyrrhines as a single group (non-hominid, non-atelid anthropoids, abbreviated "NH-NA-A") (Figs. 3, 4B; 4C).

The final ANOVA for $\ln[(MTFa^{1/2})/(EFa^{1/2})]$ included six groups of primates and one group of non-primates (NP). The analysis returned significant among-group variance in which Tukey's Q *post hoc* comparisons distinguish DCL from all groups except tarsiers and NH-NA-A (Table 10). Remaining strepsirrhines ("ILGL") are distinguished from all anthropoids and tarsiers, while tarsiers are distinguished from all remaining groups except NH-NA-A. NH-NA-A are significantly different from all

TABLE 8. Regression values for groups included in ANCOVAs (Table 7)

Sample	Variate	Covariate	Violates?	*n*	Slope	Slope SE	Slope 95% CI	Intcpt	Intcpt SE	Inter 95% CI	*P*
Anthropoids	ln[sqrtMTFa]	ln[cbrtBM]	N	52	1.078	0.026	(1.027, 1.130)	−1.249	0.079	(−1.407, −1.091)	***
Prosimians	ln[sqrtMTFa]	ln[cbrtBM]	N	33	1.078	0.026	(1.027, 1.130)	−1.173	0.064	(−1.302, −1.044)	***
Haplorhines	ln[sqrtMTFa]	ln[cbrtBM]	Y	55	1.055	0.025	(1.003, 1.107)	−1.173	0.079	(−1.335, −1.012)	***
Strepsirrhines	ln[sqrtMTFa]	ln[cbrtBM]	Y	30	1.055	0.025	(1.003, 1.106)	−1.113	0.064	(−1.242, −0.983)	***
Anthropoids	ln[sqrtMTFa]	ln[cbrtBM]	N	52	1.085	0.026	(1.032, 1.138)	−1.266	0.082	(−1.432, −1.101)	***
Strepsirrhines	ln[sqrtMTFa]	ln[cbrtBM]	N	30	1.085	0.026	(1.031, 1.139)	−1.192	0.067	(−1.329, −1.055)	***
Anthropoids	ln[sqrtEFa]	ln[cbrtBM]	Y	52	2.266	0.054	(2.158, 2.374)	−2.340	0.166	(−2.673, −2.007)	***
Prosimians	ln[sqrtEFa]	ln[cbrtBM]	Y	33	2.266	0.054	(2.156, 2.375)	−2.438	0.134	(−2.712, −2.164)	***
Haplorhines	ln[sqrtEFa]	ln[cbrtBM]	N	55	1.133	0.024	(1.085, 1.181)	−1.161	0.075	(−1.311, −1.011)	***
Strepsirrhines	ln[sqrtEFa]	ln[cbrtBM]	N	30	1.133	0.024	(1.084, 1.182)	−1.226	0.060	(−1.349, −1.102)	***
Anthropoids	ln[sqrtEFa]	ln[cbrtBM]	N	52	1.156	0.026	(1.104, 1.207)	−1.231	0.080	(−1.392, −1.070)	***
Strepsirrhines	ln[sqrtEFa]	ln[cbrtBM]	N	30	1.156	0.026	(1.103, 1.208)	−1.286	0.065	(−1.420, −1.153)	***
Anthropoids	ln[TrochL]	ln[cbrtBM]	Y	52	1.071	0.026	(1.018, 1.124)	−0.805	0.224	(−1.255, −0.355)	*
Prosimians	ln[TrochL]	ln[cbrtBM]	Y	33	1.071	0.026	(1.017, 1.125)	−0.837	0.066	(−0.972, −0.701)	***
Haplorhines	ln[TrochL]	ln[cbrtBM]	N	55	1.061	0.023	(1.014, 1.108)	−0.764	0.201	(−1.167, −0.361)	***
Strepsirrhines	ln[TrochL]	ln[cbrtBM]	N	30	1.061	0.023	(1.013, 1.109)	−0.822	0.059	(−0.942, −0.702)	***
Anthropoids	ln[TrochL]	ln[cbrtBM]	N	52	1.101	0.023	(1.054, 1.148)	−0.887	0.072	(−1.032, −0.741)	**
Strepsirrhines	ln[TrochL]	ln[cbrtBM]	N	30	1.101	0.023	(1.053, 1.148)	−0.927	0.059	(−1.048, −0.807)	***
Anthropoids	ln[sqrtMTFa]	ln[sqrtEFa]	Y	52	0.935	0.019	(0.897, 0.974)	−0.104	0.046	(−0.196, −0.012)	***
Prosimians	ln[sqrtMTFa]	ln[sqrtEFa]	Y	33	0.935	0.019	(0.896, 0.975)	0.012	0.032	(−0.054, 0.078)	***
Haplorhines	ln[sqrtMTFa]	ln[sqrtEFa]	Y	55	0.922	0.017	(0.887, 0.957)	−0.077	0.042	(−0.161, 0.007)	***
Strepsirrhines	ln[sqrtMTFa]	ln[sqrtEFa]	Y	30	0.922	0.017	(0.887, 0.958)	0.042	0.029	(−0.018, 0.102)	***
Anthropoids	ln[sqrtMTFa]	ln[sqrtEFa]	Y	52	0.928	0.019	(0.890, 0.965)	−0.089	0.045	(−0.179, 0.001)	***
Strepsirrhines	ln[sqrtMTFa]	ln[sqrtEFa]	Y	30	0.928	0.019	(0.889, 0.966)	0.033	0.032	(−0.032, 0.097)	***

Raw data found in Supporting Information Table S2 (dimorphic means). Supporting Information Table S4a gives taxonomic inclusion for noted groups. *$P < 0.05$, **$P < 0.01$, ***$P < 0.001$.

TABLE 9. OLS regressions for cases violating ANCOVA assumptions

Sample	Variate	Covariate	n	Slope	Slope SE	Slope 95% CI	Intcpt	Intcpt SE	Inter 95% CI	r	P
Haplorhines	ln[sqrtMTFa]	ln[cbrtBM]	55	1.023	0.025	(0.973, 1.073)	−1.089	0.069	(−1.227, −0.951)	0.984	***
Strepsirrhines	ln[sqrtMTFa]	ln[cbrtBM]	30	1.159	0.061	(1.035, 1.283)	−1.283	0.138	(−1.565, −1.001)	0.962	***
Haplorhines	ln[sqrtMTFa]	ln[sqrtEFa]	55	0.893	0.018	(0.856, 0.930)	−0.022	0.036	(−0.095, 0.051)	0.989	***
Strepsirrhines	ln[sqrtMTFa]	ln[sqrtEFa]	30	1.016	0.037	(0.940, 1.092)	0.045	0.049	(−0.056, 0.147)	0.981	***
Anthropoids	ln[sqrtEFa]	ln[cbrtBM]	52	1.169	0.026	(1.117, 1.221)	−1.267	0.072	(−1.412, −1.122)	0.988	***
Prosimians	ln[sqrtEFa]	ln[cbrtBM]	33	1.053	0.058	(0.934, 1.172)	−1.094	0.129	(−1.357, −0.831)	0.954	***
Anthropoids	ln[TrochL]	ln[cbrtBM]	52	1.109	0.028	(1.052, 1.165)	−0.909	0.078	(−1.066, −0.752)	0.984	***
Prosimians	ln[TrochL]	ln[cbrtBM]	33	0.988	0.053	(0.881, 1.095)	−0.688	0.116	(−0.925, −0.451)	0.958	***
Anthropoids	ln[sqrtMTFa]	ln[sqrtEFa]	52	0.896	0.020	(0.855, 0.936)	−0.028	0.041	(−0.110, 0.055)	0.987	***
Prosimians	ln[sqrtMTFa]	ln[sqrtEFa]	33	1.038	0.038	(0.961, 1.115)	0.006	0.049	(−0.094, 0.105)	0.979	***

Raw data found in Supporting Information Table S2 (dimorphic means). Supporting Information Table S4a gives taxonomic inclusion for noted groups. $^{*}P < 0.05$, $^{**}P < 0.01$, $^{***}P < 0.001$.

remaining groups except non-primates, which in turn are different from all other groups. In terms of size differences, atelids and hominids have the smallest MTFa relative to EFa. Taxa in the NP and NH-NA-A groups have significantly larger MTFa relative to EFa. *Daubentonia*, cheirogaleids, *Lepilemur*, and tarsiers have even larger MTFa, though on an individual level MTFa is rarely ever larger than EFa in these groups. Finally, galagids, lorisids, lemurids, and indriids exhibit the largest MTFa relative to EFa, with the former facet nearly always outsizing the latter.

ln[(MTFa$^{1/2}$)/(BM$^{1/3}$)] and ln[(EFa$^{1/2}$)/(BM$^{1/3}$)]. For ln[(MTFa$^{1/2}$)/(BM$^{1/3}$)], using the initial five strepsirrhine groups described above[1] results in lorisids and the DCL group being significantly different from indriid, lemurid and galagid groups (Fig. 4D, Table 11). Therefore we used a group composed of *Daubentonia*, cheirogaleids, lorisids, and *Lepilemur* (DCL-L), and a group composed of lemurids, indriids, and galagids (LmIG) for the combined ANOVA. The anthropoid ANOVA shows differences between callitrichines as compared with cercopithecoids, cebines/aotines, and pitheciids, but no other significant differences (Fig. 4E, Table 11). Therefore, we recognized a callitrichine group (Cl) and a non-callitrichine anthropoid group (NClA). ANOVA of the two strepsirrhine, two anthropoid, tarsier, and non-primate euarchontan groups reveals significant differences between most groups (Fig. 4F, Table 11). However, the DCL-L group is not distinguishable from either anthropoid group, tarsiers are not distinguishable from non-callitrichines or the LmIG group, and callitrichines and non-primates are not distinguishable from one another.

For ln[(EFa$^{1/2}$)/(BM$^{1/3}$)], using the same initial five strepsirrhine groups for ANOVA results in lorisids being distinguished from all other groups (Fig. 4G; Table 11). *Cheirogaleus medius* has an exceptionally small ln[(EFa$^{1/2}$)/(BM$^{1/3}$)] ratio as well and plots in the lorisid range, but otherwise *Daubentonia*, cheirogaleids, lepilemurids, lemurids, indriids, and galagids broadly overlap with each other. We thus recognized two groups of strepsirrhines for further analyses: a lorisid (L) group and a non-lorisid strepsirrhine (NLS) group.

Among anthropoids, initial plots show *Homo sapiens* to be an extreme outlier to the rest of the distribution (Fig. 4H). We therefore excluded it from the analyses as this difference is likely functionally related to bipedalism (see discussion). Running the analysis on the remaining anthropoid taxa using the initial groups described at the beginning of the ANOVA section, we find that only callitrichines differ from other groups including hominids, atelids, cebines, aotines, and pitheciids (Table 11). Therefore we recognized two anthropoid groups: a callitrichine (Cl) group and a non-callitrichine anthropoid (NClA) group. For the combined analysis (Fig. 4I, Table 11), lorisids are differentiated from all other taxa, while callitrichines and non-primates are additionally differentiated from non-callitrichine anthropoids and tarsiers. The comparison between non-lorisid strepsirrhines and

[1]We could not determine ANOVA groups using individual variation as was done for ln[(MTFa$^{1/2}$)/(EFa$^{1/2}$)] due to the fact that these ratios can only be computed for species means when incorporating body mass.

TABLE 10. ANOVA and post hoc comparison tests for ln[(MTFa/EFa)$^{1/2}$]

ANOVA	Strepsirrhine	Anthropoid	Combined	Combined (w Np)
df (B, W)	4, 21	6, 31	5, 61	6, 63
MSE (B,W)	0.039, 0.003	0.049, 0.004	0.329, 0.004	0.277, 0.004
F	11.7	12.27	88.57	73.91
P (same)	<<0.0001	<<0.0001	<<0.0001	<<0.0001
Tukey's Q	DCL/Lm	H/Hy	H/At	H/Np
	*	***	0.6613	***
	DCL/I	H/Cr	H/NH-NA-A	H/At
	**	***	***	0.7982
	DCL/G	H/At	H/T	H/NH-NA-A
	***	0.8345	***	***
	DCL/L	H/Cl	H/DCL	H/T
	***	***	***	***
	Lm/I	H/Cb	H/ILGL	H/DCL
	0.6849	***	***	***
	Lm/G	H/P	At/NH-NA-A	H/ILGL
	0.1667	***	***	***
	Lm/L	Hy/Cr	At/T	At/Np
	0.2932	0.9714	***	**
	I/G	Hy/At	At/DCL	At/NH-NA-A
	0.8335	**	***	***
	I/L	Hy/Cl	At/ILGL	At/T
	0.9544	1.0000	***	***
	G/L	Hy/Cb	NH-NA-A/T	At/DCL
	0.9969	0.9958	*	***
		Hy/P	NH-NA-A/DCL	At/ILGL
		0.9992	0.0566	***
		Cr/At	NH-NA-A/ILGL	NH-NA-A/Np
		***	***	0.9996
		Cr/Cl	T/DCL	NH-NA-A/T
		0.9884	1.0000	0.1013
		Cr/Cb	T/ILGL	NH-NA-A/DCL
		1.0000	***	0.1168
		Cr/P	DCL/ILGL	NH-NA-A/ILGL
		0.9994	***	***
		At/Cl		T/Np
		**		*
		At/Cb		T/DCL
		**		1.0000
		At/P		T/ILGL
		**		**
		Cl/Cb		DCL/Np
		0.9991		*
		Cl/P		DCL/ILGL
		0.9999		***
		Cb/P		ILGL/Np
		1.0000		***

*$P < 0.05$, **$P < 0.01$, ***$P < 0.001$. Abbreviations for treatment groups are given in Figure 4 caption and main text.

non-callitrichine anthropoids approaches, but does not reach, significance.

ln[(MTF-Perimeter)/(MTFa$^{1/2}$)]. Both ANOVAs of initial strepsirrhine and anthropoid groups returned significant results (Figs. 5 and 6; Table 12). *Post hoc* comparisons showed that lorisids are significantly different from lemurids and galagids. Among anthropoids, atelids are significantly different from cebines/aotines and pitheciids. Based on these results we consolidated the strepsirrhine sample into two groups: a non-lorisid strepsirrhine (NLS) group and lorisids. The anthropoid sample was consolidated into a catarrhine group (Ct), an atelid group (At), and a non-atelid platyrrhine group (NAP). ANOVA including these five groups, the non-primate euarchontan group, and the tarsier group returned significant results. Non-primates differ from all "prosimians" and atelids. Non-lorisid strepsirrhines differ from all haplorhines except tarsiers and atelids. NLS differ from atelids and all "prosimians." Catarrhines differ only from non-lorisid strepsirrhines (as implied above) and tarsiers (Table 12).

ln[(MTH1)/(MTH2)]. Neither ANOVA of initial strepsirrhine or anthropoid groups returned significance (Figs. 7 and 8; Table 13). Therefore, we consolidated all initial strepsirrhine groups into a single subgroup (Str), did the same for all anthropoid subgroups (An), and included these groups along with a tarsier group and a non-primate euarchontan group in a final ANOVA with four groups. This resulted in significant differences between strepsirrhines and non-primates, as well as between strepsirrhines and anthropoids. Tarsiers were not differentiated from any other group, probably due to power limitations in the case of their comparison to non-primates.

Regression of MTF variables and FFa

The ln[(MTFa$^{1/2}$)/(EFa$^{1/2}$)] was found to be significantly correlated with FFa for the total sample, for the primate-only sample, and for all "prosimian" sub-groups checked. However, the correlation is not significant when the sample is limited to haplorhines, anthropoids, or platyrrhines (Table 14). ln[(MTFa$^{1/2}$)/(BM$^{1/3}$)] is also generally correlated with FFa. However, the correlation breaks down in different places. Strepsirrhine and "prosimian" subgroups do not show significant correlations, while the haplorhine subsample *is* correlated. Platyrrhine ln[(MTFa$^{1/2}$)/(BM$^{1/3}$)] is not correlated with FFa. In contrast, the other two MTF variables, ln[(MTH1)/(MTH2)] and ln[(MTF-Perimeter)/(MTFa$^{1/2}$)], show no significant correlation with FFa, nor does the MTF PC1 variable. Nonetheless, ln[(MTFa$^{1/2}$)/(EFa$^{1/2}$)] is strongly correlated with ln[(MTH1)/(MTH2)] and shows limited correlation with ln[(MTF-Perimeter)/(MTFa$^{1/2}$)] (Table 14).

Position of fossil taxa

Figure 9 illustrates variation among extant and fossil taxa.

ln[(MTFa$^{1/2}$)/(EFa$^{1/2}$)]. Separation of fossil taxa into groups for statistical comparison is not straightforward, since many taxa are represented by fewer than three individuals and their phylogenetic positions are often tenuous. Therefore this section takes a mainly descriptive approach. For ln[(MTFa$^{1/2}$)/(EFa$^{1/2}$)], plesiadapiforms have a relatively small facet and are restricted to the low end of the range of extant taxa. Adapiforms and omomyiforms are characterized by values that overlap with both extant strepsirrhines and anthropoids (Table 4; Fig. 3), though their range is relatively narrow: no adapiform or omomyiform obtains values as high as certain members of Indriidae, Lemuridae, Lorisidae, or Galagidae. Most extant anthropoid groups include individuals with values lower than exhibited by any fossil "prosimian". As a group, ln[(MTFa$^{1/2}$)/(EFa$^{1/2}$)] values for adapiforms and omomyiforms most closely approximate living *Daubentonia*, cheirogaleids, lepilemurids, and tarsiers. There is nothing unusual or unexpected about MTF proportions of the oldest euprimates *Teilhardina* and *Cantius*, in contrast to the

TABLE 11. ANOVA and post hoc *comparison tests for ratios between facet area and body mass*

	$Ln[(MTFa)^{1/2}/(BM)^{1/3}]$ ANOVA			$Ln[(EFa)^{1/2}/(BM)^{1/3}]$ ANOVA		
ANOVA	Strep.	Anth.	Combined	Strep.	Anth.	Combined
df (B, W)	4, 25	6, 34	5, 72	4, 25	6, 34	5, 72
MSE (B,W)	0.125, 0.006	0.036,0.007	0.239, 0.007	0.125, 0.006	0.036,0.007	0.231, 0.008
F	20.8700	5.1340	34.3000	20.8700	5.1340	27.5400
P (same)	<<0.0001	0.0008	<<0.0001	<<0.0001	0.0008	<<0.0001
Tukey's Q	DCL/Lm	H/Hy	Np/Cl	DCL/Lm	H/Hy	Np/Cl
	***	0.9997	0.5929	0.2389	0.1926	0.9135
	DCL/I	H/Cr	Np/NCA	DCL/I	H/Cr	Np/NCA
	***	0.9951	***	0.1515	0.3233	***
	DCL/G	H/At	Np/T	DCL/G	H/At	Np/T
	***	0.6915	***	0.1308	1.0000	***
	DCL/L	H/Cl	Np/LmIG	DCL/L	H/Cl	Np/NLS
	1.0000	0.0827	***	***	***	0.2300
	Lm/I	H/Cb	Np/DCL-L	Lm/I	H/Cb	Np/L
	0.8219	0.9781	***	0.9990	0.5739	**
	Lm/G	H/P	Cl/NCA	Lm/G	H/P	Cl/NCA
	0.2129	0.9941	*	0.9971	0.5114	**
	Lm/L	Hy/Cr	Cl/T	Lm/L	Hy/Cr	Cl/T
	***	0.9419	***	***	0.9999	*
	I/G	Hy/At	Cl/LmIG	I/G	Hy/At	Cl/NLS
	0.7878	0.8941	***	1.0000	0.2817	0.8171
	I/L	Hy/Cl	Cl/DCL-L	I/L	Hy/Cl	CL/L
	***	0.1874	0.1352	***	0.1715	***
	G/L	Hy/Cb	NCA/T	G/L	Hy/Cb	NCA/T
	***	0.8715	0.1649	***	0.9902	0.9992
		Hy/P	NCA/LmIG		Hy/P	NCA/NLS
		0.9360	***		0.9956	0.1551
		Cr/At	NCA/DCL-L		Cr/At	NCA/L
		0.3105	0.9346		0.4431	***
		Cr/Cl	T/LmIG		Cr/Cl	T/NLS
		*	0.2402		0.0931	0.3083
		Cr/Cb	T/DCL-L		Cr/Cb	T/L
		1.0000	*		0.9995	***
		Cr/P	LmIG/DCL-L		Cr/P	NLS/L
		1.0000	***		0.9999	***
		At/Cl			At/Cl	
		0.8362			***	
		At/Cb			At/Cb	
		0.2169			0.7078	
		At/P			At/P	
		0.2994			0.6470	
		Cl/Cb			Cl/Cb	
		*			*	
		Cl/P			Cl/P	
		*			*	
		Cb/P			Cb/P	
		1.0000			1.0000	

*$P < 0.05$, **$P < 0.01$, ***$P < 0.001$. Abbreviations for treatment groups are given in Figures 4 and 6 captions and main text.

latter's unexpectedly low FFa values (Boyer and Seiffert, 2013).

Eosimias has MTF proportions outside the range of any fossil or living "prosimian" (with the exception of *Megaladapis*) and overlaps only extant anthropoids and non-primate euarchontans. NMMP 39, attributed to *Pondaungia* or *Amphipithecus* (e.g., Marivaux et al., 2003), has values higher than, but close to, *Eosimias*. The Shanghuang "protoanthropoid" talus IVPP 12306 is similar to NMMP 39 in this regard.

Surprisingly, other early anthropoids (including Parapithecidae, *Proteopithecus*, and some fossil platyrrhines) have unusually high values compared with living anthropoids and appear more characteristic of "prosimians" in the sample. On the other hand, basal catarrhines *Aegyptopithecus* and *Catopithecus* plot within the range of extant anthropoids.

Among fossil hominins, KNM-ER 1464 and KNM-ER 813 plot with modern *Homo sapiens*, while AL 288-1 (*Australopithecus afarensis*) has a much larger $ln[(MTFa^{1/2})/(EFa^{1/2})]$ value in the range of chimpanzees. The value for *Homo habilis* (OH8) is unusually high, but this is likely due to a severely abraded EF.

ln[(MTF-perimeter)/(MTFa$^{1/2}$)]. This variable exhibits substantial intraspecific variability and a large amount of overlap among extant strepsirrhines, tarsiers, and anthropoids. Still, the former group tends to have lower values indicating more circular facets, while anthropoids have higher values indicating more elliptical ones. Plesiadapiforms again match extant non-primate euarchontans and anthropoids, though they also overlap with some extant strepsirrhines (Fig. 5). Adapiforms and

omomyiforms are characterized by values that overlap with both extant strepsirrhines and anthropoids (Table 4; Fig. 5), but they are in no way distinguished from extant "prosimians" as a group. There is nothing unusual about MTF shape of *Teilhardina* or *Cantius*.

Mirroring the pattern of ln[(MTFa$^{1/2}$)/(EFa$^{1/2}$)] values, *Eosimias* has a MTF shape that extends outside the range of any fossil or living "prosimian" (with the exception of *Megaladapis*) into values that include only extant anthropoids and non-primates. Nonetheless, *Eosimias* is almost completely overlapping with the stem strepsirrhine *Anchomomys frontanyensis*. NMMP 39 has a value in the range of *Eosimias*, while IVPP 12306 has lower values. These two probable haplorhines also broadly overlap "prosimians."

Though Parapithecidae, *Proteopithecus* and some fossil platyrrhines exhibit "prosimian"-like ln[(MTFa$^{1/2}$)/(EFa$^{1/2}$)] values, their MTF shape overlaps with Eosimiidae and most anthropoid groups. The basal catarrhines *Aegyptopithecus* and *Catopithecus* again plot within the range of extant anthropoids.

Turning to fossil hominins, KNM-ER 1464, KNM-ER 813, and OH8 are fairly similar to each other and have relatively dorsoplantarly narrow MTFs that plot well outside the range of extant African apes and *Homo sapiens*, but among extant orangutans. AL 288-1 (*Australopithecus afarensis*) has a more circular MTF and comes close to the range of *Homo sapiens*.

ln[(MTH1)/(MTH2)]. This variable tends to separate anthropoids and strepsirrhines cleanly. Overlapping exceptions include *Cheirogaleus medius, Mirza*, some *Perodicticus*, and many of the subfossil lemurs, which exhibit a dorsoplantarly shallower MTF with more non-articular area exposed on the medial aspect of the body. Likewise, our sample (albeit small) of *Tarsius tarsier* and *Tarsius syrichta* show these taxa to have modest non-articular exposure in contrast to *Tarsius bancanus* and the general strepsirrhine condition. Some individuals of *Lagothrix, Ateles, Saimiri*, and *Macaca* have MTFs that extend plantad to the sustentacular facet (Fig. 7). Plesiadapiforms again look like extant non-primate euarchontans, particularly dermopterans, and they do not overlap with any "prosimians" except *Megaladapis*. Adapiforms and omomyiforms (including *Teilhardina* and *Cantius*) exhibit values well within the range of extant "prosimians" (Table 4, Fig. 7).

Eosimias, Parapithecidae, *Proteopithecus*, fossil platyrrhines, *Aegyptopithecus* and *Catopithecus* all plot in the middle of the anthropoid range. NMMP 39 and "protoanthropoids" IVPP 12306 and IVPP 12305 exhibit values that are more "prosimian"-like.

Fossil hominins AL 288-1, KNM-ER 1464, and KNM-ER 813 are fairly similar to one another and in the range of *Homo sapiens*, while OH8 has a more dorsoventrally extensive MTF.

Modeling character evolution and ASR

The favored models for ancestral reconstructions were the same for each variable across all three trees (the "unconstrained" parsimony tree, as well as trees constrained to recover a tarsier-anthropoid clade to the exclusion of omomyiforms, or an adapiform-haplorhine clade to the exclusion of extant strepsirrhines). FFa was the only variable for which the random walk model (model "A" in BayesTraits) best fit the data given the tree, with the phylogenetic scaling parameter Pagel's lambda (λ). Analysis of all other variables employed the directional model (model "B" in BayesTraits), with the phylogenetic scaling parameter kappa for ln[(MTFa$^{1/2}$)/(EFa$^{1/2}$)], and the phylogenetic scaling parameter lambda for ln[(MTF-Perimeter)/(MTFa$^{1/2}$)] and ln[(MTH1)/(MTH2)]. Means and upper and lower 95% HPDs are presented in Table 15 and Supporting Information Tables S7 and S8, and plots of nodal reconstructions through time on the "unconstrained" tree are provided in Figure 10.

The ancestral reconstructions for FFa (Fig. 10A) closely match those recovered by Boyer and Seiffert (2013), with a clear divide between haplorhines and strepsirrhines and no large shifts in any of the major clades considered. We recovered an ancestral mean value of 99.8° for crown Primates, very close to the value of 99.5° recovered by Boyer and Seiffert (2013).

Ancestral reconstructions for ln[(MTFa$^{1/2}$)/(EFa$^{1/2}$)] (Fig. 10B) indicate there were independent early shifts in haplorhines and strepsirrhines away from the ancestral primate condition toward higher values (i.e., toward relatively larger MTFa). These trends continue in tarsiiforms and strepsirrhines, and are further exaggerated in lorisiforms, whereas anthropoids show no further increase along the stem lineage leading to the node shared with *Eosimias*. There is an increase between the node shared with *Eosimias* and that shared with parapithecoids, followed by parallel decreases in platyrrhines and catarrhines (particularly hominoids). The only strepsirrhine group to show a slight reduction of MTFa relative to EFa is the *Microcebus-Mirza* clade ("mouse lemurs" in Fig. 10), which also shows a slight shift toward a more haplorhine-like fibular facet orientation.

Our data suggest that the evolution of ln[(MTF-Perimeter)/(MTFa$^{1/2}$)] (Fig. 10C) was characterized by independent shifts toward lower values (i.e., more circular facets) in stem strepsirrhines and stem haplorhines, followed by a strong reversal of those trends along the anthropoid stem lineage, with less circular facets being acquired through the Eocene. Oddly, the ancestral crown Strepsirrhini node shows a strong positive shift and subsequent gradual decrease; this might be due largely to the inclusion of high (anthropoid-like) values for the *Djebelemur* (Table 4).

Finally, the evolution of ln[(MTH1)/(MTH2)] on the unconstrained tree (Fig. 10D) once again shows convergent evolution of lower values (i.e., dorsoventrally deeper facets relative to medial talar body height) in tarsiiforms and strepsirrhines, and a reversal toward higher values (dorsoventrally shallow facets) in anthropoids; this trend continues gradually in stem catarrhines and stem and crown hominoids. Lemuriforms deviate very little from the ancestral condition that was established very early in the Paleogene, whereas lorisiforms and adapids gradually evolve even deeper facets.

DISCUSSION AND CONCLUSIONS

We begin this section by revisiting our initial hypotheses and predictions. We follow with a discussion of factors considered while interpreting results of the various analyses performed. We conclude with a synthetic discussion of the implications of our results for hypotheses bearing on adaptive scenarios for primate origins.

TABLE 12. ANOVA and post hoc comparison tests for ln[(MTF Pmtr)/(MTFa)$^{1/2}$]

Pmtr/MTFa			
ANOVA	Strepsirrhine	Anthropoid	Combined
***df* (B, W)**	4, 21	6, 31	6,63
MSE (B,W)	0.0072,0.0017	0.013,0.004	0.058,0.003
F	4.172	3.73	20.97
P (**same**)	0.012	0.007	<<0.0001
Tukey's *Q*	DCL/Lm	H/Hy	Np/NLS
	0.29	0.9900	***
	DCL/I	H/Cr	Np/L
	0.55	0.99	**
	DCL/G	H/At	Np/T
	0.23	0.49	***
	DCL/L	H/Cl	Np/Ct
	0.77	0.99	0.17
	Lm/I	H/Cb	Np/At
	0.99	0.77	***
	Lm/G	H/P	Np/NAP
	0.99	0.51	0.99
	Lm/L	Hy/Cr	NLS/L
	*	0.9419	0.31
	I/G	Hy/At	NLS/T
	0.97	0.65	0.99
	I/L	Hy/Cl	NLS/Ct
	0.084	0.98	*
	G/L	Hy/Cb	NLS/At
	*	0.62	0.72
		Hy/P	NLS/NAP
		0.35	***
		Cr/At	L/T
		0.82	0.36
		Cr/Cl	L/Ct
		0.92	0.88
		Cr/Cb	L/At
		0.43	0.99
		Cr/P	L/NAP
		0.21	*
		At/Cl	T/Ct
		0.21	*
		At/Cb	T/At
		*	0.78
		At/P	T/NAP
		*	***
		Cl/Cb	Ct/At
		0.97	0.49
		Cl/P	Ct/NAP
		0.83	0.51
		Cb/P	At/NAP
		0.99	**

*$P < 0.05$, **$P < 0.01$, ***$P < 0.001$. Abbreviations for treatment groups are given in Figures 4 and 6 captions and main text.

TABLE 13. ANOVA and post hoc comparison tests for ln(MTH1/MTH2)

MTH1/2			
ANOVA	Strepsirrhine	Anthropoid	Combined
***df* (B, W)**	4, 21	6, 31	3, 66
MSE (B,W)	0.055, 0.020	0.016, 0.015	0.77, 0.020
F	2.819	1.08	38.96
P (**same**)	0.051 (ns)	0.40 (ns)	<<0.0001
Tukey's *Q*	–	–	Np/Str
			*
			Np/T
			0.98
			Np/An
			0.27
			Str/T
			0.1
			Str/An
			***
			T/An
			0.13

*$P < 0.05$, **$P < 0.01$, ***$P < 0.001$. Abbreviations for treatment groups are given in Figures 4 and 8 captions and main text.

Hypotheses and predictions

H1. The hypothesis that strepsirrhines and tarsiers transmit proportionally more weight through their MTFs than anthropoids is largely supported due to the fact that most of its predictions were borne out by our data.

P1a. *Relative to body mass, anthropoids have a smaller MTFa than strepsirrhines and tarsiers*. ANCOVA of MTFa on body mass shows a significantly higher intercept in both strepsirrhines and "prosimians" compared with anthropoids (Tables 7–9). Furthermore, most strepsirrhines also have a higher MTFa to BM ratio than any extant anthropoids. Strepsirrhines having relative facet sizes that broadly overlap those of anthropoids include *Daubentonia*, cheirogaleids, *Lepilemur*, and lorisids.

P1b. *Relative to EFa, anthropoids have a smaller MTFa than strepsirrhines and tarsiers*. ANCOVA of EFa on body mass shows a lower intercept for strepsirrhines than anthropoids (Tables 7–9), which—if considered together with the ANCOVA results for MTFa—suggests a smaller EFa relative to MTFa in strepsirrhines. Furthermore, the comparison between ln[(MTFa$^{1/2}$)/(EFa$^{1/2}$)] shows substantial differences between all strepsirrhines (except lorisids) and anthropoids (Fig. 4). Though tarsiers and the DCL group are not significantly different from NH-NA-A group, this likely reflects insufficient power rather than real similarity.

P1c. *If variation in FFa can be explained by degree of habitual inversion of the foot (Boyer and Seiffert*, 2013), *relative MTFa will correlate with FFa*. This prediction was borne out for the total sample and "prosimian" groups that were previously shown to have significant correlations between FFa and body size (Table 14), which Boyer and Seiffert (2013) (among others) suggest should correlate with support size and inversion requirements.

P1d. *Strepsirrhines and tarsiers will have a more plantarly extensive medial malleolus as inferred from the plantar extent of the MTF, as a longer malleolus will reduce the potential for joint dislocation due to laterally directed forces*. This prediction was borne out by ANOVA comparing strepsirrhine and anthropoid groups for ln(MTH1/MTH2) (Fig. 8). Tarsiers appear intermediate, but their range does not overlap extensively with that of anthropoids.

P1e. *If the dorsoplantar shallowness of the anthropoid MTF has been caused by migration of talotibial ligaments to a more distal position (Gebo*, 1986), *then this should result in a less*

TABLE 14. Tests for correlations

Sample	Dependent	Independent	Method	*n*	Slope	Slope 95% CI	Intercept	Inter 95% CI	*r*	*P*	Lambda	Lambda 95% CI
Euarchontans	ln[sqrt(MTFa/EFa)]	ln[MTF Pmtr/sqrt(MTFa)]	PGLS	115	−0.395	(−0.61, −0.18)	0.460	(0.09,0.83)	0.312	***	0.787	(0.620, 0.894)
Primates	ln[sqrt(MTFa/EFa)]	ln[MTF Pmtr/sqrt(MTFa)]	PGLS	108	−0.215	(−0.44,0.01)	0.262	(−0.09,0.61)	0.155	0.059	0.704	(0.490, 0.852)
Haplorhines	ln[sqrt(MTFa/EFa)]	ln[MTF Pmtr/sqrt(MTFa)]	PGLS	65	−0.066	(−0.35,0.22)	0.018	(−0.43,0.47)	0.113	0.648	0.758	(0.507, 0.899)
Strepsirrhines	ln[sqrt(MTFa/EFa)]	ln[MTF Pmtr/sqrt(MTFa)]	PGLS	30	−0.818	(−1.25, −0.38)	1.326	(0.64,2.01)	0.568	***	0.588	(0.009, NA)
Anthropoids	ln[sqrt(MTFa/EFa)]	ln[MTF Pmtr/sqrt(MTFa)]	PGLS	49	−0.052	(−0.64,0.54)	−0.078	(−0.43,0.27)	0.223	0.658	0.775	(0.510, 0.920)
Prosimians	ln[sqrt(MTFa/EFa)]	ln[MTF Pmtr/sqrt(MTFa)]	PGLS	59	−0.290	(−0.58,0)	0.387	(−0.06,0.83)	0.050	*	0.546	(0.237, 0.821)
Platyrrhines	ln[sqrt(MTFa/EFa)]	ln[MTF Pmtr/sqrt(MTFa)]	PGLS	26	−0.188	(−0.57,0.19)	0.145	(−0.49,0.79)	0.035	0.320	0.718	(0.264, 0.923)
Lemuriforms	ln[sqrt(MTFa/EFa)]	ln[MTF Pmtr/sqrt(MTFa)]	PGLS	22	−0.845	(−1.31, −0.38)	1.304	(0.58,2.03)	0.622	**	0.48	(NA, NA)
Euarchontans	Fibular Facet Angle	ln[sqrt(MTFa/EFa)]	PGLS	115	15.367	(3.51,27.23)	100.471	(92.52,108.42)	0.216	*	0.78	(0.576, 0.900)
Primates	Fibular Facet Angle	ln[sqrt(MTFa/EFa)]	PGLS	108	13.696	(0.03,27.36)	103.528	(98.12,108.93)	0.164	*	0.71	(0.453, 0.877)
Haplorhines	Fibular Facet Angle	ln[sqrt(MTFa/EFa)]	PGLS	65	0.965	(−15.592, 17.522)	98.961	(94.097, 103.284)	0.126	0.908	0.702	(0.367, 0.891)
Strepsirrhines	Fibular Facet Angle	ln[sqrt(MTFa/EFa)]	PGLS	30	27.930	(9.09,46.77)	110.907	(101.02,120.8)	0.469	**	0.944	(NA, NA)
Anthropoids	Fibular Facet Angle	ln[sqrt(MTFa/EFa)]	PGLS	49	−3.509	(−21.374, 14.356)	94.327	(90.181, 98.473)	0.134	0.695	0.619	(0.190, 0.888)
Prosimians	Fibular Facet Angle	ln[sqrt(MTFa/EFa)]	PGLS	59	32.457	(11.85,53.06)	105.213	(100.6,109.83)	0.365	**	0.551	(0.221, 0.891)
Platyrrhines	Fibular Facet Angle	ln[sqrt(MTFa/EFa)]	PGLS	26	5.319	(−22.409, 33.047)	98.428	(91.608, 105.248)	0.187	0.697	0.771	(0.366, 0.968)
Lemuriforms	Fibular Facet Angle	ln[sqrt(MTFa/EFa)]	PGLS	22	32.070	(9.632, 54.508)	114.568	(101.090, 128.046)	0.520	**	0.967	(NA, NA)
Euarchontans	ln[sqrt(MTFa/EFa)]	ln(MTH1/MTH2)	PGLS	115	−0.409	(−0.5, −0.32)	−0.121	(−0.21, −0.03)	0.627	***	0.763	(0.555, 0.887)
Primates	ln[sqrt(MTFa/EFa)]	ln(MTH1/MTH2)	PGLS	108	−0.361	(−0.47, −0.26)	−0.087	(−0.15, −0.02)	0.544	***	0.732	(0.512, 0.871)
Haplorhines	ln[sqrt(MTFa/EFa)]	ln(MTH1/MTH2)	PGLS	65	−0.345	(−0.493, −0.197)	−0.077	(−0.145, −0.009)	0.496	***	0.778	(0.510, 0.912)
Strepsirrhines	ln[sqrt(MTFa/EFa)]	ln(MTH1/MTH2)	PGLS	30	−0.421	(−0.59, −0.25)	0.017	(−0.02,0.05)	0.685	***	0.000	(NA, 0.739)
Anthropoids	ln[sqrt(MTFa/EFa)]	ln(MTH1/MTH2)	PGLS	49	−0.428	(−0.607, −0.249)	−0.039	(−0.111, 0.032)	0.562	***	0.777	(0.508, 0.917)
Prosimians	ln[sqrt(MTFa/EFa)]	ln(MTH1/MTH2)	PGLS	59	−0.316	(−0.45, −0.18)	−0.084	(−0.13, −0.03)	0.521	***	0.557	(0.258, 0.816)
Platyrrhines	ln[sqrt(MTFa/EFa)]	ln(MTH1/MTH2)	PGLS	26	−0.252	(−0.475, −0.029)	−0.114	(−0.193, −0.034)	0.388	*	0.663	(0.279, 0.896)
Lemuriforms	ln[sqrt(MTFa/EFa)]	ln(MTH1/MTH2)	PGLS	22	−0.422	(−0.673, −0.171)	0.006	(−0.037, 0.048)	0.589	**	0.000	(NA, NA)
Euarchontans	Fibular Facet Angle	ln[MTF Pmtr/sqrt(MTFa)]	PGLS	115	−2.498	(−17.33,12.34)	101.734	(76.22,127.25)	0.089	0.739	0.766	(0.562, 0.895)
Primates	Fibular Facet Angle	ln[MTF Pmtr/sqrt(MTFa)]	PGLS	108	3.668	(−12.75,20.08)	96.909	(71.11,122.71)	0.087	0.659	0.671	(0.432, 0.854)
Haplorhines	Fibular Facet Angle	ln[MTF Pmtr/sqrt(MTFa)]	PGLS	65	−9.699	(−28.38,8.98)	113.809	(84.65,142.97)	0.034	0.305	0.69	(0.328, 0.889)
Strepsirrhines	Fibular Facet Angle	ln[MTF Pmtr/sqrt(MTFa)]	PGLS	30	20.824	(−12.96,54.6)	80.879	(28.39,133.37)	0.141	0.218	0.037	(NA, 0.842)
Anthropoids	Fibular Facet Angle	ln[MTF Pmtr/sqrt(MTFa)]	PGLS	49	−7.606	(−29.98,14.77)	107.697	(70.24,145.16)	0.106	0.498	0.66	(0.262, 0.903)
Prosimians	Fibular Facet Angle	ln[MTF Pmtr/sqrt(MTFa)]	PGLS	59	20.848	(−3.81,45.51)	71.639	(33.78,109.5)	0.176	0.096	0.474	(0.210, 0.780)
Platyrrhines	Fibular Facet Angle	ln[MTF Pmtr/sqrt(MTFa)]	PGLS	26	−19.244	(−43.38,4.89)	129.697	(89.18,170.21)	0.251	0.114	0.811	(0.413, 0.973)
Lemuriforms	Fibular Facet Angle	ln[MTF Pmtr/sqrt(MTFa)]	PGLS	22	20.464	(−20.79,61.72)	82.891	(18.88,146.9)	0.053	0.316	0	(NA, NA)
Euarchontans	ln[MTF Pmtr/sqrt(MTFa)]	ln(MTH1/MTH2)	PGLS	115	0.235	(0.15,0.32)	1.594	(1.54,1.65)	0.470	***	0.461	(NA, 0.773)
Primates	ln[MTF Pmtr/sqrt(MTFa)]	ln(MTH1/MTH2)	PGLS	108	0.177	(0.08,0.28)	1.550	(1.5,1.6)	0.308	***	0.544	(0.146, 0.806)
Haplorhines	ln[MTF Pmtr/sqrt(MTFa)]	ln(MTH1/MTH2)	PGLS	65	0.173	(0.03,0.32)	1.539	(1.48,1.6)	0.263	*	0.687	(0.294, 0.887)
Strepsirrhines	ln[MTF Pmtr/sqrt(MTFa)]	ln(MTH1/MTH2)	PGLS	30	0.278	(0.15,0.4)	1.583	(1.54,1.63)	0.635	***	0.239	(NA, 0.925)
Anthropoids	ln[MTF Pmtr/sqrt(MTFa)]	ln(MTH1/MTH2)	PGLS	49	0.222	(0.07,0.37)	1.602	(1.55,1.65)	0.377	**	0	(NA, 0.777)
Prosimians	ln[MTF Pmtr/sqrt(MTFa)]	ln(MTH1/MTH2)	PGLS	59	0.091	(−0.04,0.23)	1.538	(1.51,1.56)	0.118	0.183	0.044	(NA, 0.827)
Platyrrhines	ln[MTF Pmtr/sqrt(MTFa)]	ln(MTH1/MTH2)	PGLS	26	0.422	(0.3,0.55)	1.572	(1.49,1.65)	0.805	***	1	(0.497, NA)
Lemuriforms	ln[MTF Pmtr/sqrt(MTFa)]	ln(MTH1/MTH2)	PGLS	22	0.455	(0.34,0.58)	1.567	(1.55,1.59)	0.805	***	0.000	(NA, 0.664)
Euarchontans	Fibular Facet Angle	ln(MTH1/MTH2)	PGLS	115	−4.727	(−12.570, 3.117)	98.388	(90.638, 106.137)	0.061	0.235	0.767	(0.553, 0.898)
Primates	Fibular Facet Angle	ln(MTH1/MTH2)	PGLS	108	−3.380	(−12.490, 5.730)	102.399	(97.206, 107.591)	0.066	0.464	0.678	(0.422, 0.865)
Haplorhines	Fibular Facet Angle	ln(MTH1/MTH2)	PGLS	65	−1.631	(−12.852, 9.589)	98.899	(94.260, 103.537)	0.121	0.773	0.698	(0.343, 0.890)
Strepsirrhines	Fibular Facet Angle	ln(MTH1/MTH2)	PGLS	30	6.652	(−7.400, 20.704)	113.989	(110.996, 116.982)	0.048	0.342	0.000	(NA, 0.994)
Anthropoids	Fibular Facet Angle	ln(MTH1/MTH2)	PGLS	49	−4.747	(−18.340, 8.847)	96.586	(91.326, 101.845)	0.103	0.486	0.660	(0.262, 0.898)
Prosimians	Fibular Facet Angle	ln(MTH1/MTH2)	PGLS	59	0.565	(−12.699, 13.829)	103.484	(98.691, 108.276)	0.132	0.932	0.514	(0.234, 0.825)
Platyrrhines	Fibular Facet Angle	ln(MTH1/MTH2)	PGLS	26	−12.626	(−27.461, 2.209)	100.319	(94.561, 106.077)	0.276	0.093	0.775	(0.317, 0.972)
Lemuriforms	Fibular Facet Angle	ln(MTH1/MTH2)	PGLS	22	5.711	(−16.296, 27.719)	114.815	(111.099, 118.531)	0.187	0.596	0.000	(NA, NA)
Euarchontans	Fibular Facet Angle	ln[sqrt(MTFa)/cbrt(BM)]	PGLS	75	13.702	(2.575, 24.829)	112.765	(98.110, 127.420)	0.076	*	0.930	(0.834, 0.977)
Primates	Fibular Facet Angle	ln[sqrt(MTFa)/cbrt(BM)]	PGLS	71	14.083	(2.881, 25.284)	115.066	(102.324, 127.807)	0.084	*	0.893	(0.755, 0.964)

TABLE 14. Continued

Sample	Dependent	Independent	Method	n	Slope	Slope 95% CI	Intercept	Inter 95% CI	r	P Lambda	Lambda	95% CI
Haplorhines	Fibular Facet Angle	ln[sqrt(MTFa)/cbrt(BM)]	PGLS	44	15.888	(0.039, 31.737)	107.189	(89.286, 125.091)	0.089	* 0.844	(0.536, 0.963)	
Strepsirrhines	Fibular Facet Angle	ln[sqrt(MTFa)/cbrt(BM)]	PGLS	27	7.189	(−3.319, 17.697)	118.394	(108.239, 128.549)	0.074	0.171	0.330	(NA, 0.938)
Anthropoids	Fibular Facet Angle	ln[sqrt(MTFa)/cbrt(BM)]	PGLS	41	17.068	(0.685, 33.451)	107.687	(89.231, 126.053)	0.102	*	0.806	(0.475, 0.955)
Prosimians	Fibular Facet Angle	ln[sqrt(MTFa)/cbrt(BM)]	PGLS	30	7.914	(−8.294, 24.122)	113.647	(98.815, 128.480)	0.044	0.267	0.906	(0.627, 0.993)
Platyrrhines	Fibular Facet Angle	ln[sqrt(MTFa)/cbrt(BM)]	PGLS	25	16.333	(−3.076, 35.743)	111.017	(90.138, 131.897)	0.117	0.095	0.672	(0.223, 0.939)
Lemuriforms	Fibular Facet Angle	ln[sqrt(MTFa)/cbrt(BM)]	PGLS	17	15.755	(2.916, 28.593)	127.490	(115.539, 139.441)	0.313	*	0.000	(NA, 0.969)
Euarchontans	Fibular Facet Angle	MTF PC1	PGLS	115	−1.066	(−2.37,0.24)	98.247	(90.51,105.98)	0.119	0.108	0.774	(0.561, 0.903)
Primates	Fibular Facet Angle	MTF PC1	PGLS	108	−0.708	(−2.29,0.87)	101.960	(96.54,107.38)	0.045	0.377	0.689	(0.432, 0.873)
Haplorhines	Fibular Facet Angle	MTF PC1	PGLS	65	−0.710	(−2.66,1.24)	98.426	(93.61,103.24)	0.087	0.469	0.703	(0.349, 0.893)
Strepsirrhines	Fibular Facet Angle	MTF PC1	PGLS	30	0.516	(−1.95,2.98)	114.092	(109.79,118.4)	0.170	0.672	0.000	(NA, NA)
Anthropoids	Fibular Facet Angle	MTF PC1	PGLS	49	−0.551	(−2.76,1.66)	95.643	(91.95,99.34)	0.126	0.619	0.668	(0.256, 0.904)
Prosimians	Fibular Facet Angle	MTF PC1	PGLS	59	−0.348	(−2.79,2.1)	103.050	(97.66,108.44)	0.127	0.777	0.522	(0.235, 0.841)
Platyrrhines	Fibular Facet Angle	MTF PC1	PGLS	26	−1.919	(−4.32,0.48)	99.100	(93.95,104.25)	0.253	0.113	0.772	(0.364, 0.961)
Lemuriforms	Fibular Facet Angle	MTF PC1	PGLS	22	−2.166	(−4.76,0.43)	111.831	(96.28,127.39)	0.295	0.099	0.975	(NA, NA)

Uses Tables 3 and 4, Supporting Information Table S4b, and nexus file Tree 2a in Supporting Information. $^{*}P < 0.05$, $^{**}P < 0.01$, $^{***}P < 0.001$.

circular outline for the anthropoid medial talotibial facet. Though our measure of this feature exhibits substantial scatter at the level of individuals (Fig. 5), species-level analyses showed general support for this assessment, with the exception of lorises which likely have a less circular facet due to a dorsoplantarly shallow body.

H2. The hypothesis that adapiforms and omomyiforms were "prosimian"-like in locomotor and postural behavior (while early anthropoids were not) is supported since all of its predictions were borne out by our data.

P2a. *Adapiforms and omomyiforms will resemble strepsirrhines and tarsiers for variables representing MTF relative size, shape and dorsoplantar depth*. Though we could not test the pattern of MTFa size relative to body mass for the fossils, other measures generally revealed the fossils to resemble "prosimians" more than anthropoids. Exceptions include *Afradapis, Djebelemur, Anchomomys, Ourayia* and *Hemiacodon*, which have values indicating a more anthropoid-like facet shape (Fig. 5). It is also worth noting that for $\ln[(MTFa^{1/2})/(EFa^{1/2})]$, the fossil taxa overlapped most extensively with the extant "prosimians" least distinct from anthropoids (*Daubentonia*, cheirogaleids, *Lepilemur*, and *Tarsius*).

P2b. *Fossil anthropoids will resemble modern anthropoids for focal features of H1*. This was generally true with the exception of parapithecids, *Proteopithecus*, and *Proteropithecia* for $\ln[(MTFa^{1/2})/(EFa^{1/2})]$. Furthermore, NMMP 39 (cf. Amphipithecidae) and Shanghuang "protoanthropoids" had a more "prosimian"-like dorsoplantar extent of the MTF.

H3. Though both P3a and P3b are supported by our data, P3c is not, so the hypothesis that a "prosimian"-like postural mode is a homologous synapomorphy of euprimates is not supported. ASRs suggest a basal anthropoid-like postural mode is primitive for euprimates (see further discussion below).

P3c. *ASRs will show substantial (if not significant) shifts from proximal stem primate nodes to the euprimate node so that values become less anthropoid-like and more "prosimian"-like. Another shift in values will be seen along the anthropoid stem-lineage*. In contrast to this prediction, only very minor shifts occurred between the last stem primate and ancestral euprimate nodes. Thus our reconstruction of the ancestral euprimate posits a distinctly non-"prosimian"-like morphology (either treeshrew-like, anthropoid-like, or plesiadapiform-like) for this taxon (Fig. 10, Table 15 and Supporting Information Tables S7 and S8). Interestingly, both haplorhine and strepsirrhine descendent lineages show parallel trends toward more "prosimian"-like values, so a certain degree of reversal along the stem-anthropoid lineage is still implied. This scenario is more complex than previously envisioned. Positing a monophyletic "prosimian" clade as a sister to an anthropoid clade would reduce the complexity of morphological transitions by avoiding reversals within the anthropoid lineage. However, this topology is not justified by current cladistic evidence.

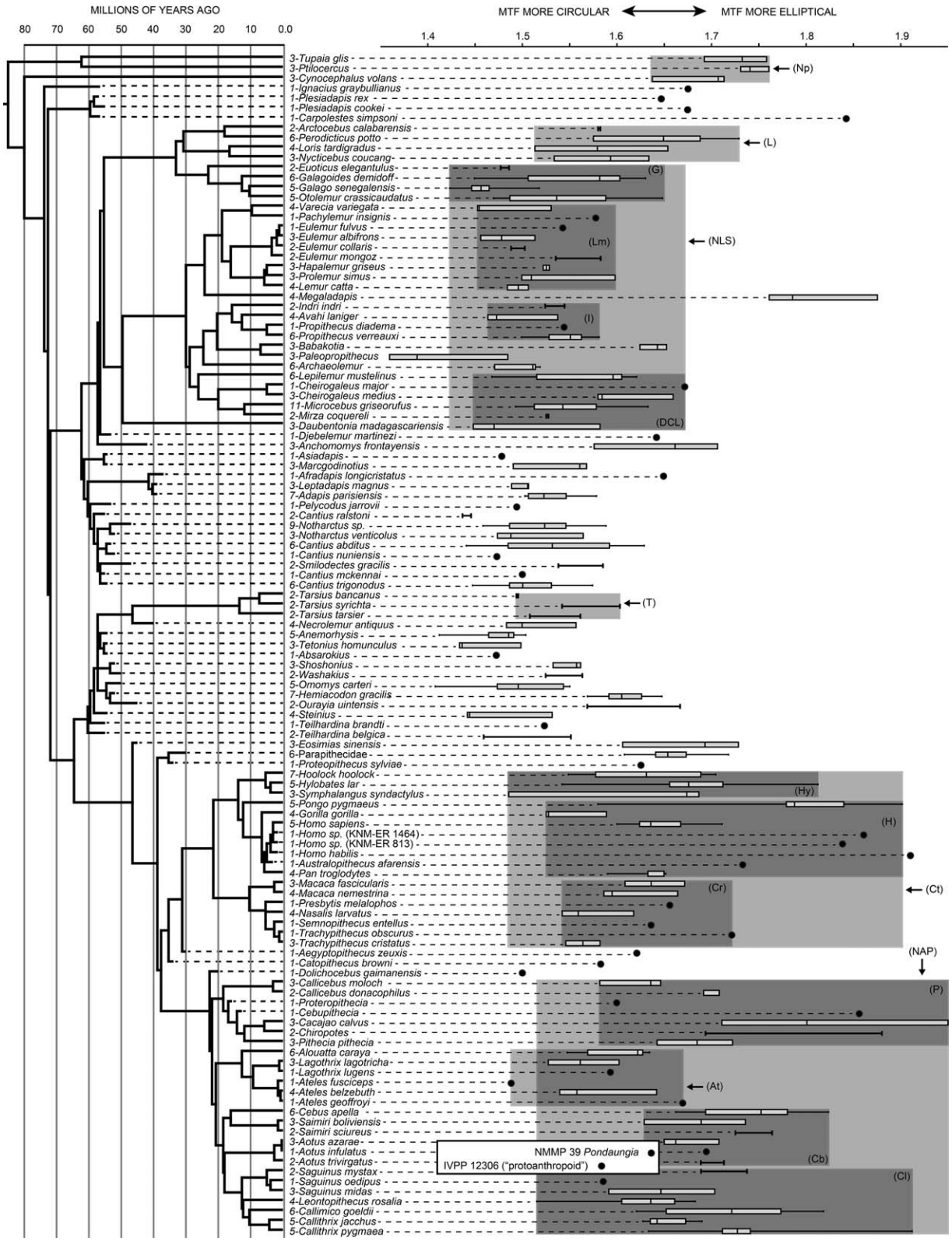

Fig. 5. Phylogenetic tree with Pmtr/MTFa species boxplots (see Fig. 2b). Detailed explanations of tree, boxplot representation and other components from Figure 3 are applicable here. Abbreviations for taxonomic groups can be found in captions of Figures 4 and 6.

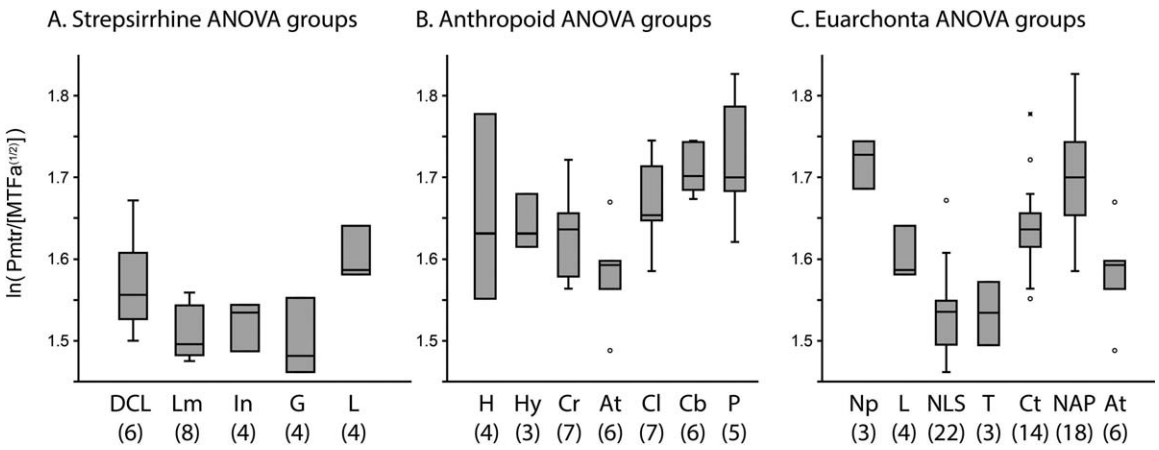

Fig. 6. Plots of group means for Pmtr/MTFa that were compared with ANOVAs and reported in Table 12. Figure symbology explanations and most abbreviations can be found in Figure 4 caption. New abbreviations include: Ct, Catarrhines; NAP, Non-atelid platyrrhines.

Regression of shape variables against body mass

This analysis revealed that there is generally little variation driven by body size alone. Exceptions to this generality provide insight on functional contingencies. For $\ln[(MTFa^{1/2})/(BM^{1/3})]$, lemuriforms show a significant positively allometric relationship, with larger-bodied taxa having higher values. This result is consistent with previous work (and ANCOVA results in Tables 7–9) suggesting differences in facet scaling between strepsirrhines and haplorhines: Yapuncich and Boyer (2014) argued that facets receiving a greater proportion of body mass during positional behaviors should exhibit stronger positive allometry in area (within groups of species exhibiting sufficient variation in body mass) than facets receiving a smaller or more interspecifically variable proportion of body mass. If use of inverted foot postures in lemuriforms results in a greater proportion of weight being transmitted through the MTF than it does in anthropoids, then the functional demands on this facet should be impacted more significantly by absolute body mass in lemuriforms than in anthropoids.

One might expect $\ln[(MTFa^{1/2})/(EFa^{1/2})]$ to show similar correlations with size. In this case at least two causal factors can be envisioned: 1) lemuriforms might be expected to exhibit reduced allometry in EFa scaling compared with haplorhines due to force transmission tradeoffs with the MTF (described above); this relationship would accentuate the $\ln[(MTFa^{1/2})/(EFa^{1/2})]$ ratio in larger-bodied animals compared with smaller ones; 2) all groups in which degree of inversion varies with body size might be expected to show a correlation between $\ln[(MTFa^{1/2})/(EFa^{1/2})]$ and body mass. Boyer and Seiffert (2013) reasoned that larger-bodied members of a relatively behaviorally uniform clade should exhibit greater degrees of inversion due to reduced availability of large supports. Their FFa data support this idea by showing a shallower angle with increasing body mass in lemuriforms and platyrrhines. If this reasoning is correct, larger taxa should have greater MTFa relative to EFa than smaller taxa. However, the only correlations we found are among haplorhines, anthropoids, and platyrrhines, in which the sign of the relationship is opposite of the prediction. That is, in these groups, larger members have a proportionally smaller MTFa relative to EFa. This suggests degree of inversion is not the cause of body mass correlated variation in $\ln[(MTFa^{1/2})/(EFa^{1/2})]$ for the significant groups. We suggest that anthropoids exhibit this "reverse from expected" pattern due to increased force distribution on the lateral margin of the talus during locomotion (Yapuncich and Boyer, 2014). For these haplorhine groups, the demands for a proportionally hypertrophied EFa among larger-bodied taxa may overwhelm any shift in weight distribution toward the medial side due to use of inverted postures that are more pronounced or more frequent in larger taxa. It could be argued that increased inversion requirements would not hold with increasing body size in catarrhines because many species are terrestrial while others use bridging or suspensory behavior in the trees [though suspensory postures often involve highly inverted ankle configurations, only inversion during pronogrady is expected to influence FFa - see Boyer and Seiffert (2013) for more explanation]. The same argument could be made for platyrrhines, for which the largest members (atelids) utilize more bridging and suspensory behaviors; however, Boyer and Seiffert's (2013) data show these taxa to have the most strepsirrhine-like talofibular facet angles, suggesting increased importance of inversion during pronograde quadrupedalism. For ln[(MTH1)/(MTH2)], a significant correlation with body mass is found only for haplorhines, but any trend found in haplorhines (but not anthropoids) must be driven by tarsiers, a taxon that presents a coincidence of small body size and low MTH1/MTH2 values.

ANCOVA of facet areas (dependent) on body mass (covariate)

After running a number of analyses our results support the hypothesis that strepsirrhines load their MTFs with a greater proportion of body mass than anthropoids, while anthropoids load EFs more than strepsirrhines. This was borne out by intercept and slope differences between the clades when comparing the scaling of facet size to body mass. The functional affinities of tarsiers appear somewhat ambiguous since results of some analyses were more intuitive when tarsiers were included in the haplorhine group, while in other analyses a "prosimian" group remained distinct from anthropoids. Specifically, finding that "prosimians" have larger MTFa for body mass (greater intercept) and that

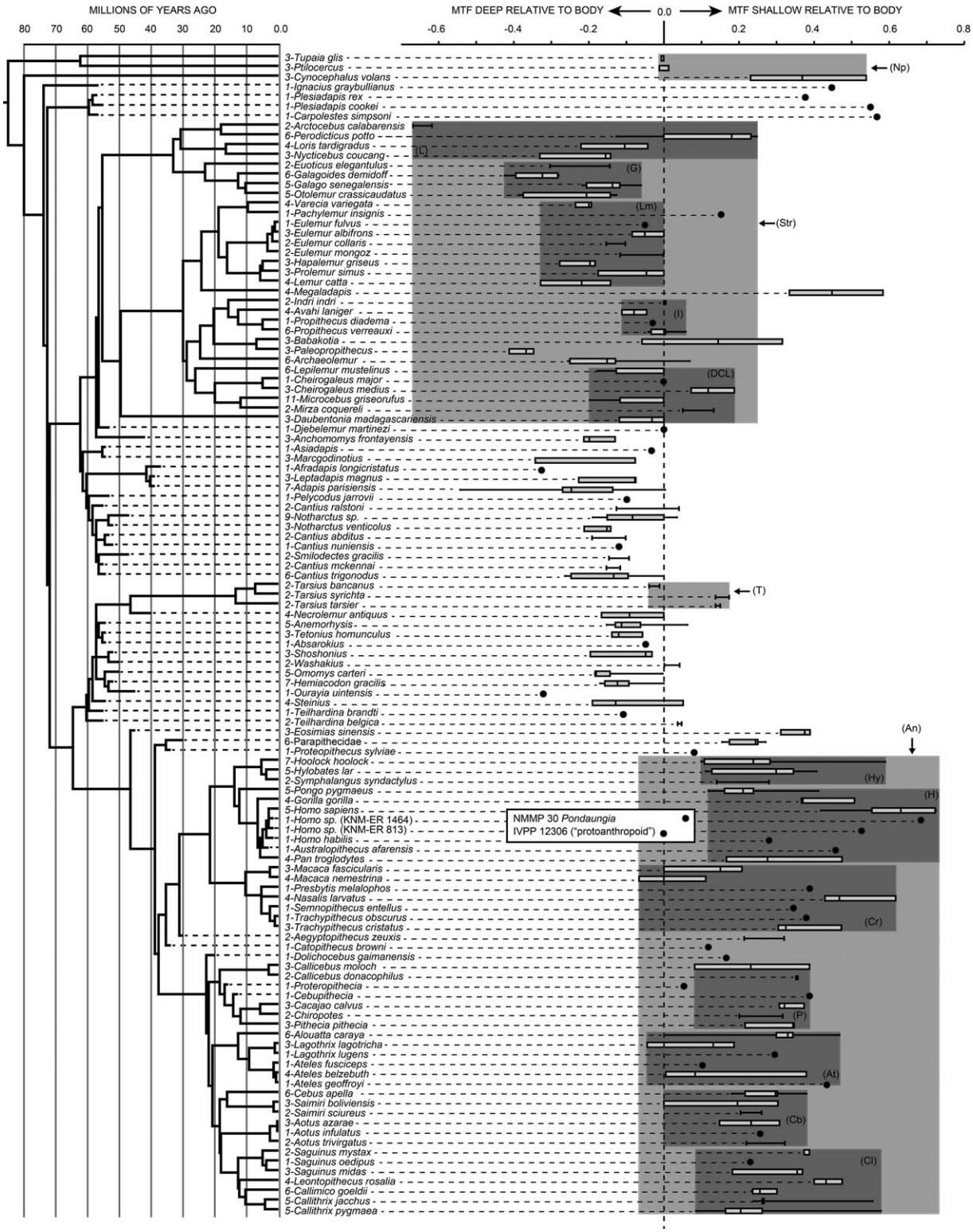

Fig. 7. Phylogenetic tree with MTH1/MTH2 species boxplots (see Fig. 2c). Detailed explanations of tree, boxplot representation, and other components from Figure 3 are applicable here. Abbreviations for taxonomic groups can be found in Figures 4 and 8.

strepsirrhines exhibit a higher slope of MTFa to body mass suggests relatively higher force transmission through MTF. As a corollary, the finding that strepsirrhines have smaller EFa for their body mass and that "prosimians" exhibit lower slope of EFa to body mass suggests less weight transmission through the lateral part of the talus. Ignoring tarsiers and comparing anthropoids and strepsirrhines directly for MTFa scaling returns equivalent slopes and a higher intercept for strepsirrhines, which supports the hypothesis that

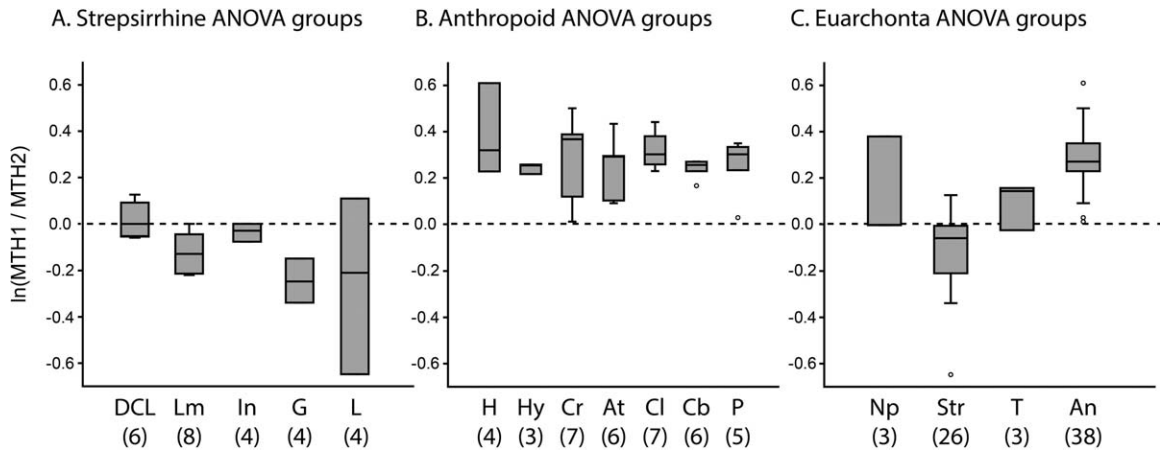

Fig. 8. Plots of group means for MTH1/MTH2 that were compared with ANOVAs and reported in Table 13. Figure symbology explanations and most abbreviations can be found in Figure 4 caption. New abbreviations include: An, Anthropoidea; Str, Strepsirrhini.

strepsirrhines transmit more weight through their MTF.

MTF proportional variables

ln[(MTFa$^{1/2}$)/(EFa$^{1/2}$)]. This variable represents the relative size of the MTF compared with the EF. Our logic for using this variable assumes that 1) joint surfaces transmitting more force will be larger than those transmitting less in order to balance joint stress, and 2) that inverted foot postures on narrow supports will direct more stress through the MTF, while everted postures on larger substrates will direct more force through the lateral side of the talus, and hence through the EF. If "prosimians" use more inverted foot postures, then our results support the suggestion that the distinctive morphology of the "prosimian" MTF facilitates this behavioral tendency. Some of the exceptions tend to help "prove the rule" here. In particular, *Daubentonia* and members of Cheirogaleidae have relatively low values. *Daubentonia* is not committed to using a hallucal grasp on small supports to the same extent as other strepsirrhines since its claws allow alternative mechanisms of gripping the substrate. Being small-bodied, cheirogaleids encounter relatively larger diameter supports and more varied support orientations than larger strepsirrhines, which may lead to less frequent use of inverted foot postures. The low values in *Lepilemur* are not as easily explained. Given that it is substantially larger than most cheirogaleids, and (as far as we know) typical among strepsirrhines in its use of hallucal grasping, we would have expected it to exhibit values closer to the Lemuridae, Indriidae, or Lorisiformes.

An alternative explanation for values of *Lepilemur* comes from consideration of its phylogenetic context and from fossil "prosimians". Recent phylogenetic assessments place *Lepilemur* as the sister to Cheirogaleidae (Springer et al., 2012). Thus, the low values it exhibits may be a primitive retention inherited from its common ancestor with cheirogaleids. Likewise, the low values in *Babakotia, Archaeolemur*, and *Megaladapis* may indicate that smaller MTFs are primitive for both Indrioidea and Lemuridae. The idea that major lemuriform groups had primitive members with smaller MTFs also is consistent with the interpretation of *Daubentonia's* low value as a primitive retention, and this state being homologous with that exhibited by fossil "prosimians" of the sample. This interpretation would suggest parallel increase in relative facet area in extant Indriidae, Lemuridae, and Lorisiformes. Such a pattern is supported by our ancestral reconstructions (Fig. 10B). As discussed in more detail below, it seems likely that demands both for greater specialization for inverted foot postures on small diameter supports and more emphasis on leaping from such postures could explain such parallelism.

Though leaping was not considered as an influence on MTF proportions in our primary hypotheses, variation in ln[(MTFa$^{1/2}$)/(BM$^{1/3}$)] and ln[(EFa$^{1/2}$)/(BM$^{1/3}$)] values appear to correspond to leaping to some degree. As a clade, strepsirrhines have larger MTFa relative to body mass, but this difference is not ubiquitous when using proportional ratios for the assessment. Only indriids, lemurids, and galagids are distinguished from anthropoids by larger MTFa relative to body mass. In contrast, lorises have some of the smallest MTFa. Rather than reflecting how much weight is borne by the MTF in particular, this value may better reflect the overall load experienced by the hindlimbs. Because lorises rarely move quickly or leap (and thus do not highly accelerate their masses), it seems likely that they transmit a smaller proportion of body mass through their ankle joints. The equivalence in ln[(MTFa$^{1/2}$)/(BM$^{1/3}$)] among *Daubentonia*, cheirogaleids, and most anthropoids would suggest that stress loads of this facet relative to body mass are fairly well matched among these taxa (allometric considerations aside). The large ln[(MTFa$^{1/2}$)/(BM$^{1/3}$)] in lemurids, indriids and galagids suggests increased forces relative to body mass. More frequent use of acrobatic grasp-leaping is the most straightforward explanation for why these groups would experience greater stress. The ln[(EFa$^{1/2}$)/(BM$^{1/3}$)] ratio provides support for the hypothesis that facet size relative to body mass represents the proportion of body mass transmitted through the hind limbs, because lorises again have exceptionally small EFs. Other strepsirrhines have higher ln[(EFa$^{1/2}$)/(BM$^{1/3}$)] ratios but are much less differentiated from each other, suggesting that variation in the degree of acrobatic behavior among strepsirrhines leads mainly to proportional variation in forces transmitted by the MTF.

The small MTFa of *Lepilemur* is potentially contrary to this idea. The observation that *Microcebus* is an adept

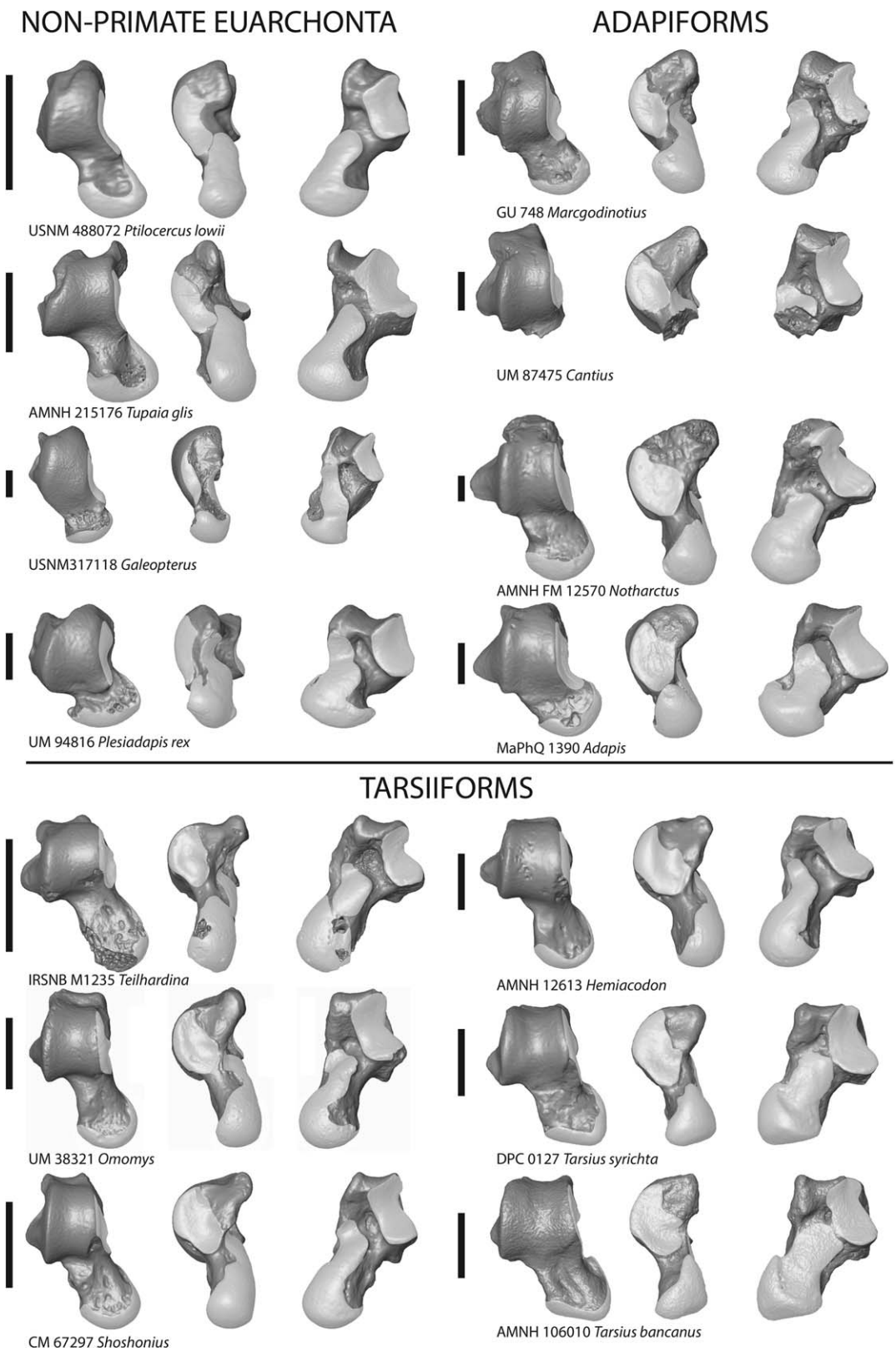

Fig. 9. Images of select tali showing MTF shape, and relationships between MTF, EF, and sustentacular facet. Views are dorsal, medial, and plantar. (**A**) Non-primate, fossil taxa and tarsiiforms. (**B**) Extant and subfossil strepsirrhines. (**C**) Extant and fossil anthropoids. Scale bars equal 3 mm. Note that some specimens have been inverted to make observation of morphological variation more straightforward.

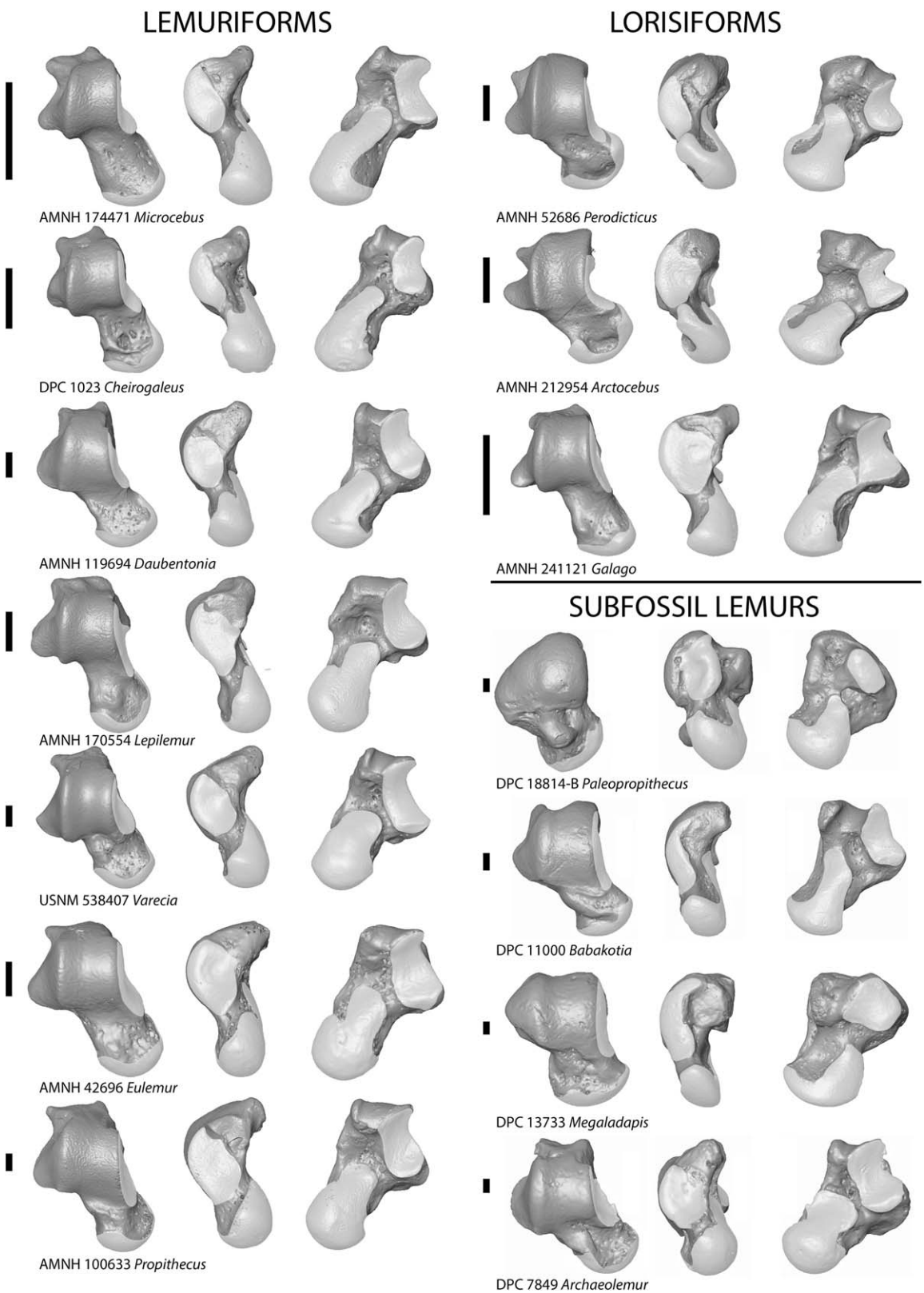

Fig. 9. (continued).

and frequent leaper with a small MTFa may also cast doubt on this explanation. However, it seems likely that for small-bodied taxa, highly acrobatic leaping does not stress the joints as much as it does for larger-bodied ones. The fact that lemuriforms are the only group to have a significant correlation between $\ln[(MTFa^{1/2})/$

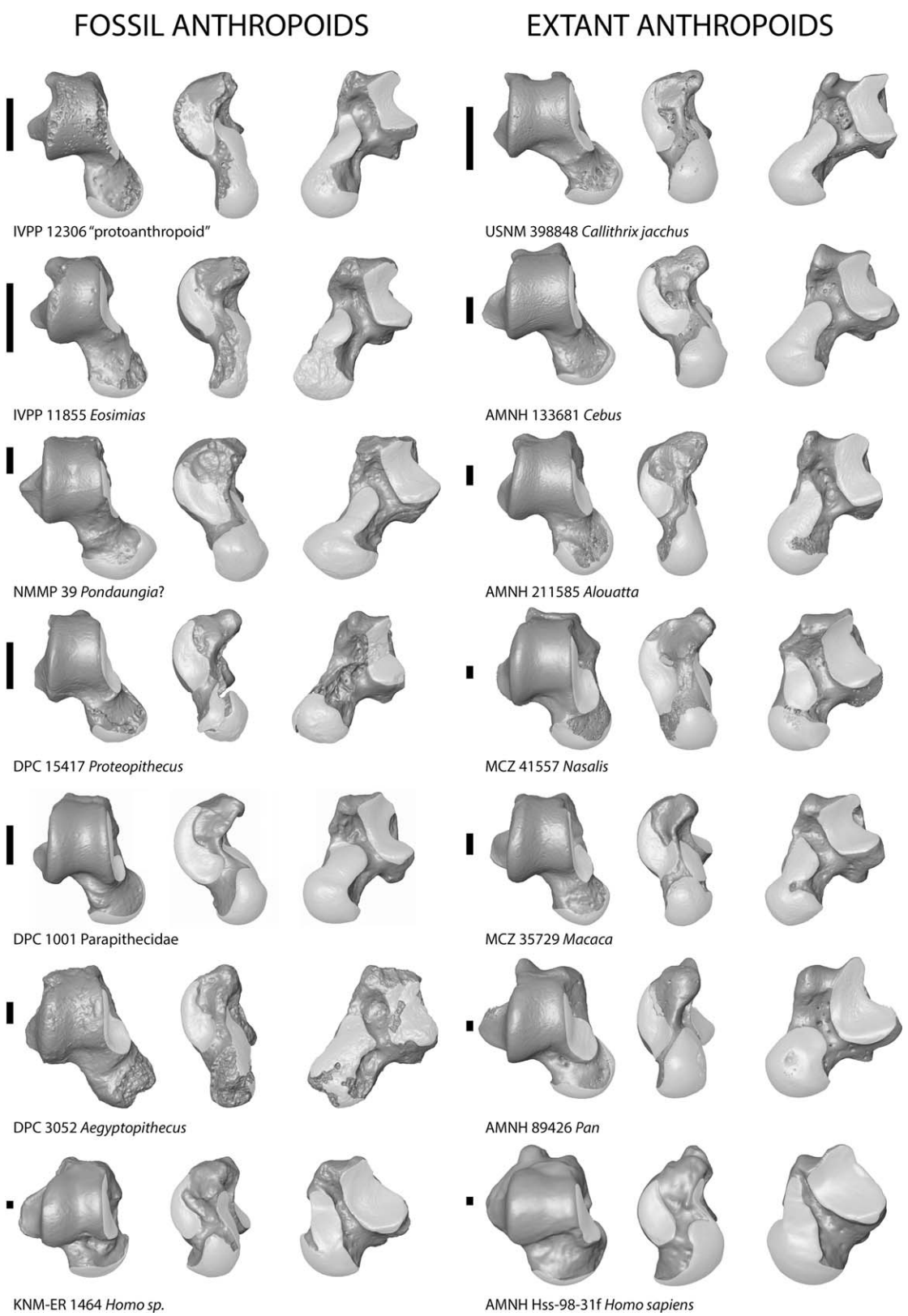

Fig. 9. (continued).

($BM^{1/3}$)] and BM (Table 6) would support our suggestion that allometry is part of the explanation here (further support is detailed below).

Among anthropoids, the only taxa that stand out as having consistently odd facet proportions are callitrichines, which generally have fairly small facets for their

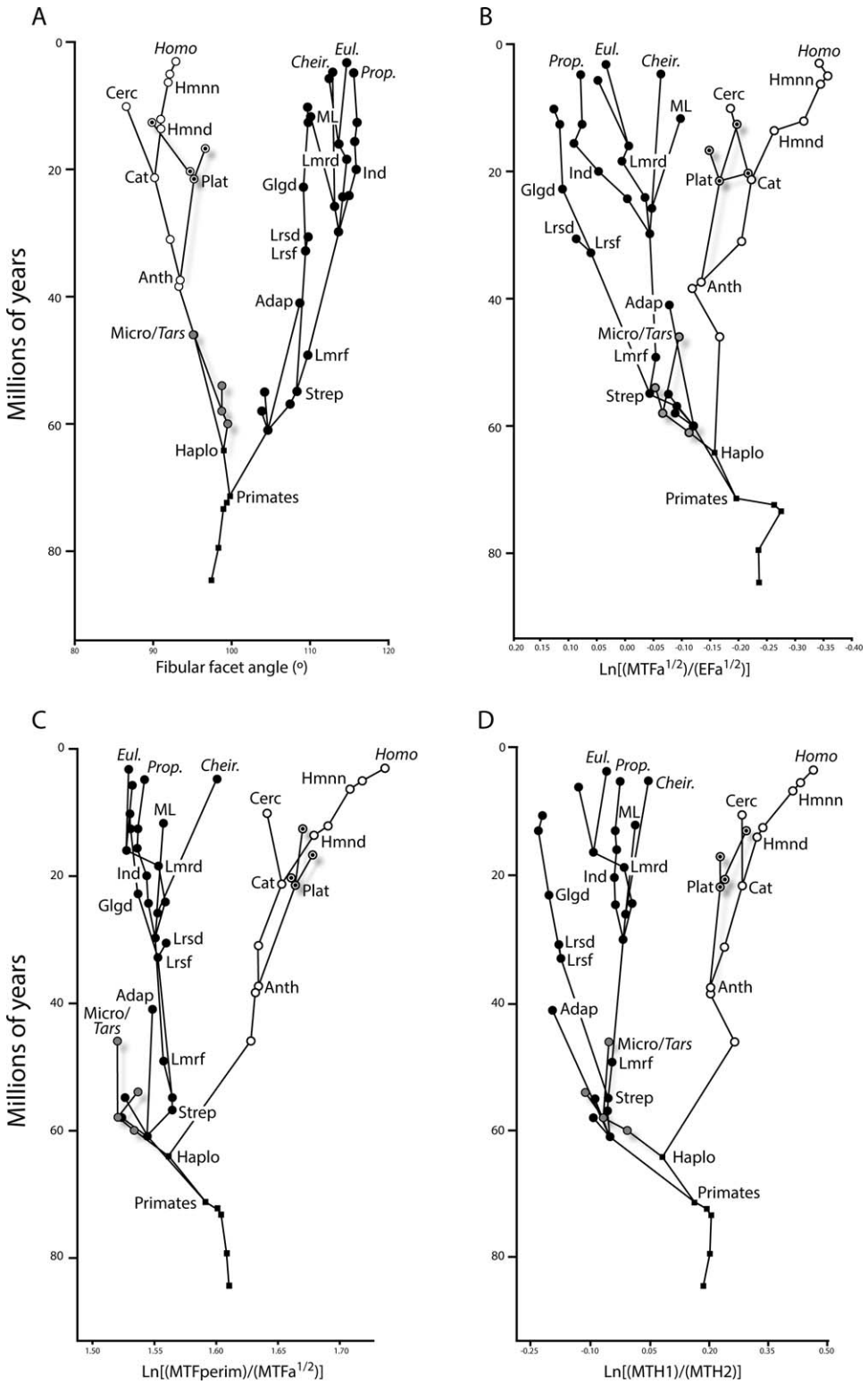

Fig. 10. ASR for select basal nodes of euarchontan tree. (**A**) FFa. (**B**) MTFa/EFa. (**C**) Pmtr/MTFa. (**D**) MTH1/MTH2. Values shown here and their confidence intervals can be found in Table 15. Time scale is based on divergence dates from Springer et al. (2012). See Methods and Supporting Information trees 2a–c. Stem primate nodes, the ancestral euprimate node, and the crown haplorhine node are represented by *black boxes*; stem and crown strepsirrhine nodes are represented by *black circles*; stem and crown tarsiiform nodes are represented by *gray circles*; stem anthropoid and catarrhine nodes are represented by *white circles*; stem and crown platyrrhine nodes are represented by *white circles* enclosing *black dots*. Abbreviations: Adap, Adapinae; Anth, crown Anthropoidea, Cat, crown Catarrhini, Cerc, crown Cercopithecoidea; *Cheir., Cheirogaleus*; *Eul., Eulemur*; Glgd, crown Galagidae; Haplo, crown Haplorhini; Hmnd, crown Hominoidea; Hmnn, crown Homininae; Ind, crown Indriidae; Lmrd, crown Lemuridae; Lmrf, crown Lemuriformes; Lrsd, crown Lorisidae; Lrsf, crown Lorisiformes; Micro/*Tars*, Microchoerinae + *Tarsius*; ML, mouse lemurs; Plat, crown Platyrrhini; *Prop., Propithecus*; Strep, crown Strepsirrhini.

TABLE 15. ASRs for select nodes

		Fibular facet angle			Ln[(MTFa$^{1/2}$)/(EFa$^{1/2}$)]			Ln[MTFP/(MTFa$^{1/2}$)]			Ln(MTH1/MTH2)		
Node	nd#	Mean	Lower	Upper	Mean	Lower	Upper	Mean	Lower	Upper	Mean	lower	Upper
Euarchonta root	1	97.42	91.84	103.03	−0.2322	−0.3441	−0.1269	1.6092	1.5346	1.6916	0.1785	−0.0097	0.3644
Scandentia	2	93.18	81.99	103.88	−0.2160	−0.3361	−0.0984	1.6466	1.5116	1.7826	0.1074	−0.1896	0.3973
Primatomorpha	3	98.32	92.12	104.33	−0.2309	−0.3505	−0.1135	1.6073	1.5273	1.6909	0.1946	0.0038	0.3781
Paromomyidae + Euprimateforms	4	98.95	92.83	104.81	−0.2708	−0.3823	−0.1614	1.6027	1.5256	1.6815	0.198	0.0458	0.3572
Euprimateforms (Plesiadapoidea + Primates)	5	99.38	93.42	105.38	−0.2596	−0.3762	−0.1481	1.5998	1.5236	1.6801	0.1869	0.0301	0.3341
Crown Primates (=Euprimates)	6	99.8	93.65	105.85	−0.1922	−0.3127	−0.0752	1.5902	1.5124	1.6708	0.1563	0.0028	0.3094
Crown Haplorhini	7	99	92.11	105.93	−0.1539	−0.2712	−0.0403	1.5619	1.4902	1.6357	0.077	−0.0817	0.2374
Tarsiiformes	8	99.5	92.75	106.58	−0.1095	−0.2109	−0.0082	1.5332	1.4660	1.6225	−0.01	−0.1507	0.1353
"Advanced" tarsiiforms (−*Teilhardina*)	9	98.74	91.77	105.53	−0.0631	−0.1559	0.0283	1.5205	1.4323	1.6108	−0.0696	−0.1995	0.0729
Microchoerinae + *Tarsius*	10	95.2	85.59	104.34	−0.0941	−0.2004	0.0116	1.5201	1.4045	1.6475	−0.0556	−0.2629	0.1405
Omomys + *Hemiacodon* + *Ourayia*	11	98.76	91.07	106.24	−0.0489	−0.1442	0.0465	1.5359	1.4394	1.6334	−0.114	−0.269	0.0313
Eosimiidae + 13	12	95.09	86.02	104.05	−0.1612	−0.2596	−0.0608	1.6264	1.5090	1.7378	0.2561	0.075	0.4339
Parapithecoidea + 14	13	93.27	83.85	102.06	−0.1125	−0.2180	−0.0032	1.6301	1.5123	1.7479	0.1964	0.0079	0.3765
Crown Anthropoidea	14	93.44	84.27	102.73	−0.1294	−0.2378	−0.0229	1.6325	1.5141	1.7544	0.1966	0.0158	0.3876
Crown Platyrrhini	15	95.2	84.48	105.41	−0.1631	−0.2685	−0.0505	1.6620	1.5277	1.7976	0.2201	0.0143	0.422
Atelidae–Cebidae	16	94.7	84.46	105.22	−0.2114	−0.3223	−0.0970	1.6587	1.5204	1.7909	0.2318	0.0291	0.4415
Pitheciidae	17	96.64	85.8	107.08	−0.1435	−0.2536	−0.0369	1.6759	1.5390	1.8148	0.2204	0.0135	0.4346
Callitrichidae	18	89.85	78.7	101.08	−0.1919	−0.3037	−0.0837	1.6681	1.5211	1.8067	0.2849	0.0651	0.5061
Crown Catarrhini	19	90.18	79.11	100.96	−0.2176	−0.3346	−0.0994	1.6324	1.5086	1.7629	0.275	0.0409	0.493
Aegyptopithecus + crown Catarrhini	20	92.16	82.2	102.24	−0.2048	−0.2981	−0.1059	1.6511	1.5146	1.7917	0.2308	0.0322	0.4259
Cercopithecoidea	21	86.56	75.17	98.34	−0.1809	−0.2969	−0.0706	1.6394	1.4990	1.7969	0.2744	0.0396	0.5053
Hominoidea	22	90.98	79.81	102.14	−0.2573	−0.3680	−0.1407	1.6769	1.5312	1.8173	0.3117	0.0865	0.5332
Hominidae	23	90.96	79.17	102.14	−0.3108	−0.4158	−0.2069	1.6882	1.5375	1.8295	0.3259	0.1049	0.5554
Homininae	24	91.91	80.33	103.29	−0.3397	−0.4345	−0.2349	1.7056	1.5596	1.8557	0.4002	0.1758	0.6166
Pan-Homo	25	92.12	80.61	103.66	−0.3524	−0.4470	−0.2585	1.7154	1.5686	1.8662	0.4192	0.2008	0.6388
Homo	26	92.89	81.14	104.29	−0.3390	−0.4269	−0.2501	1.7336	1.5799	1.8786	0.4512	0.231	0.6755
Crown Strepsirrhini	27	108.33	100.3	115.94	−0.0334	−0.1524	0.0811	1.5639	1.461	1.6659	−0.0573	−0.2302	0.1095
Crown Lemuriformes	28	109.71	100.4	118.82	−0.0483	−0.1641	0.0754	1.5568	1.4389	1.6728	−0.0476	−0.2616	0.1594
Crown Lemuriformes - *Daubentonia*	29	113.62	103.36	123.71	−0.0383	−0.1583	0.0810	1.5503	1.4225	1.6847	−0.0205	−0.2371	0.1953
Lepilemur + Cheirogaleidae	30	113.12	102.34	123.61	−0.0425	−0.1616	0.0666	1.5520	1.4144	1.6901	−0.0143	−0.2374	0.2104
Cheirogaleus	31	112.88	100.3	125.95	−0.0592	−0.1593	0.0362	1.5994	1.437	1.7623	0.0422	−0.2104	0.2883
Microcebus + *Mirza*	32	110.07	98.18	122.63	−0.0946	−0.1957	0.0123	1.5566	1.4009	1.7119	0.0097	−0.2332	0.2648
Megaladapis + crown Lemuridae	33	114.97	104.15	125.97	−0.0337	−0.1482	0.0783	1.5581	1.4235	1.7022	0.002	−0.2245	0.233
Crown Lemuridae	34	114.67	105.94	123.61	0.0104	−0.0937	0.1221	1.5527	1.4429	1.6675	−0.0178	−0.214	0.1813
Crown Lemuridae- *Varecia*	35	113.67	104.97	122.54	−0.0037	−0.1099	0.1057	1.5273	1.4167	1.6414	−0.0939	−0.29	0.1054
Eulemur	36	114.67	102.38	126.43	0.0385	−0.0633	0.1327	1.5288	1.373	1.6814	−0.0613	−0.2957	0.1595
Lemur-Prolemur-Hapalemur	37	112.43	100.82	125.02	0.0522	−0.0482	0.1537	1.5318	1.3733	1.6873	−0.1307	−0.3585	0.1068
Archaeolemur + Indrioidea	38	114.16	103.84	125.32	−0.0022	−0.1190	0.1106	1.5446	1.4058	1.6795	−0.0394	−0.2751	0.18
Indrioidea	39	115.88	104.68	127.1	0.0523	−0.0630	0.1679	1.5431	1.4042	1.6861	−0.0421	−0.2752	0.1886
Indriidae	40	115.69	103.99	127.03	0.0951	−0.0137	0.2041	1.5358	1.3861	1.6795	−0.0362	−0.2782	0.1936
Avahi + *Propithecus*	41	115.99	104.35	127.59	0.0795	−0.0228	0.1893	1.5362	1.3861	1.6869	−0.0398	−0.2822	0.1936
Propithecus	42	115.56	103.63	128.47	0.0813	−0.0149	0.1782	1.5415	1.3813	1.6980	−0.0276	−0.2656	0.2204
Crown Lorisiformes	43	109.42	98.84	120.15	0.0650	−0.0551	0.1879	1.5521	1.4165	1.6836	−0.1744	−0.4081	0.0626
Crown Lorisidae	44	109.75	99.17	120.79	0.0915	−0.0297	0.2088	1.5364	1.3913	1.6832	−0.1796	−0.4198	0.0522
Crown Galagidae	45	109.15	97.55	120.45	0.1175	0.0063	0.2354	1.5305	1.3799	1.6842	−0.2041	−0.4614	0.0428
Galagidae − *Euoticus*	46	109.76	97.31	121.73	0.1350	0.0242	0.2387	1.5298	1.3794	1.6926	−0.2303	−0.4812	0.014
Galago + *Otolemur*	47	109.68	97.42	122.32	0.1446	0.0408	0.2422	1.5588	1.4179	1.6947	−0.2202	−0.4675	0.027
Anchomomys + 27	48	107.45	100.01	114.83	−0.0848	−0.1899	0.0213	1.5639	1.4666	1.6621	−0.059	−0.2194	0.1015

TABLE 15. Continued

		Fibular facet angle			Ln[($MTFa^{1/2}$)/($EFa^{1/2}$)]			Ln[MTFP/($MTFa^{1/2}$)]			Ln(MTH1/MTH2)		
Node	nd#	Mean	Lower	Upper	Mean	Lower	Upper	Mean	Lower	Upper	Mean	lower	Upper
Adapiformes + 48	49	104.62	97.83	111.36	−0.1176	−0.2335	−0.0054	1.5439	1.4583	1.6345	−0.0526	−0.1983	0.0911
Asiadapinae	50	104.2	96.68	111.91	−0.0719	−0.1587	0.0146	1.5259	1.4241	1.6209	−0.0899	−0.2435	0.0521
Notharctinae	51	103.85	97	110.79	−0.0829	−0.1799	0.0137	1.5225	1.4325	1.6127	−0.094	−0.2316	0.0462
Adapinae	52	108.69	99.22	117.6	−0.0747	−0.1581	0.0101	1.5478	1.4272	1.6651	−0.1953	−0.3693	−0.018

Reconstructions based of Tables 3 and 4 and nexus file Tree 2a in Supporting Information documents. Supporting Information Figure S1 includes node numbers referenced in column "nd#". "Upper/Lower" refers the 95% HPD.

body mass, and *Homo sapiens*, which has an exceptionally large EFa. Given that *H. sapiens* is an extreme outlier to the rest of primates in its value for ln[($EFa^{1/2}$)/($BM^{1/3}$)], it seems safe to conclude that this is a functional correlate of striding bipedality. Evaluating this quantity with well-constrained body mass estimates for fossil hominins in the context of our comparative dataset would be interesting.

If an exceptionally large MTFa is a functional correlate of specialized grasp-leaping, the less-than-extreme values in *Tarsius* also require some explanation. Previous studies have noted various ways that joint mechanics and myological configurations of the tarsier foot differ from strepsirrhines (Jouffroy et al., 1984; Gebo, 1987a); this alternate anatomy may result in a different stress environment despite similar positional behaviors. In particular, Gebo (1987a) explains how foot inversion in *Tarsius* is accomplished without calcaneocuboid translation. Foot inversion, instead, appears to be primarily accomplished through "navicular rotation" and movements among unusually mobile naviculo-cuneiform joints. Therefore, the focus of inversion movements is shifted distally in tarsiers such that the stress environment of the talus is probably less affected by foot rotation. Maintaining ankle configurations that minimize force transmission through the MTF is probably aided by a long midtarsal region, which dictates that smaller angular excursions in abduction-adduction are needed to shift the foot a given distance from the midline.

If a moderately high ln[($MTFa^{1/2}$)/($EFa^{1/2}$)] ratio indicates use of inverted foot postures, while an exceptionally large MTF relative to body mass and/or EF reflects leaping specialization, then by these criteria it would be hard to argue for extreme leaping proclivity in any fossil "prosimians," since none exhibit the extreme proportions seen in indriids, lemurids, and galagids (though their ranges do overlap in some cases). However, the lack of extreme values in *Lepilemur* may indicate that there is strong phylogenetic signal in this trait relative to functional demand, as has been shown for calcaneal elongation (Boyer et al., 2013a). In that case, we would not expect a one-to-one mapping between behavioral tendencies and morphology among clades or between extant taxa and fossils. Furthermore, if any fossil taxa are like *Tarsius* in using grasp-leaping without strong inversion at the lower ankle joint or do not utilize abducted limb postures to achieve inversion (Boyer and Seiffert, 2013), then extant strepsirrhine morpho-functional patterns may not extend to them. This is a likely possibility for omomyiforms.

ln[(MTF-Perimeter)/($MTFa^{1/2}$)]. Higher values of this trait indicate a less circular facet. Anthropoids are traditionally characterized as having a less circular, more dorsoplantarly narrow facet; "prosimians" a more circular one. This perspective is upheld relatively well by our analyses. Some of the exceptions can be explained relative to known nuisance parameters. Lorisids have a narrower facet (higher value) than other strepsirrhines, but this is probably a correlate of also having a shallow body (Gebo, 1989b). The fact that atelids and hominids tend to have more circular facets than most other anthropoids, and thus appear more "prosimian"-like, might at first seem to be explained by allometry: they are the biggest members of their respective clades and have more circular facets. Though this idea is not supported by allometry tests in Table 6, the lack of a correlation between facet shape and

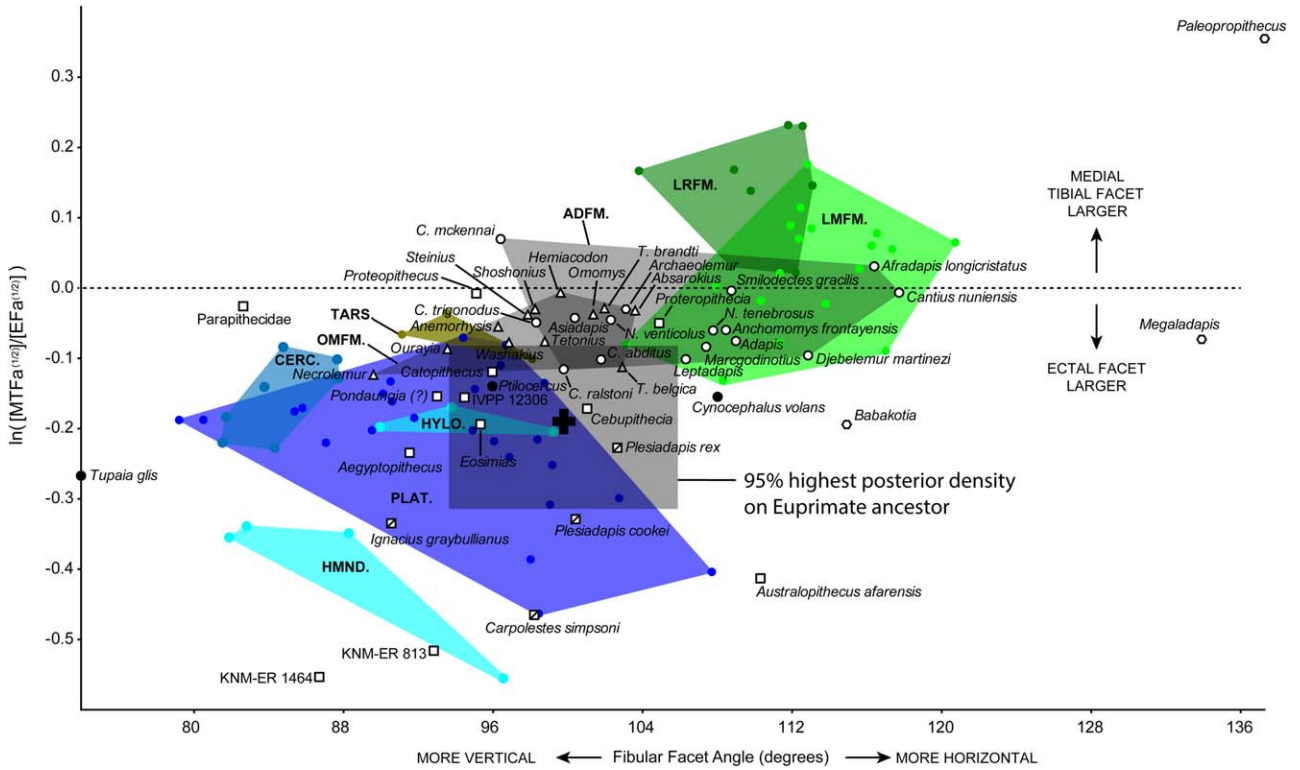

Fig. 11. Plot of species mean values of FFa (x-axis) and MTFa/EFa (y-axis). Note that although fossil taxa are also represented by species means when possible, they are more often represented by single individuals and may therefore display a different level of variance than extant data points. Abbreviations: TARS, tarsiiforms; OMFM, omomyiforms; ADFM, adapiforms; LRFM, lorisiforms; LMFM, lemuriforms; HYLO, hylobatids; PLAT, platyrrhines; CERC, cercopithecoids; HMND, hominoids. Phylogenetically corrected regression analysis of these two variables is broadly significant except when analyses are restricted to anthropoid groups (Table 14). Note that these two seemingly functionally correlated variables overlap most broadly among omomyiforms and adapiforms potentially indicating the region of overlap as the euprimate primitive condition. Alternatively, if one considers the similarity of the treeshrew *Ptilocercus*, stem-anthropoid *Eosimias*, and plesiadapiforms, their morphology can also be parsimoniously explained by primitive retention. In which case omomyiforms, adapiforms, and strepsirrhines may represent respectively independent derivations toward more "prosimian"-like morphology. ASRs are consistent with this latter interpretation. The mean value for the euprimate ancestral node is represented by a bold cross. The 95% bayesian highest probability density interval for the ancestral values on both variables is given by the gray bounding box.

body size may be influenced by fossil hominins KNM-ER 813 and KNM-ER 1464, which do not show circular facets despite being relatively large (Fig. 5). This variable may also reflect range of motion differences in flexion and extension, with a less circular facet in non-atelids reflecting a more proximodistally elongated facet and a greater range of mobility. However, given the scope of this study, it is difficult to move beyond speculation for this hypothesis. It is prudent to review Figure 5, which shows that despite average differences among species, there is substantial intraspecific variation and overlap among most groups. We would thus caution against overly general explanations for the apparent differences between atelids, hominids, and other anthropoids at this time. A much larger sample for all taxa involved would probably be necessary to identify meaningful differences within anthropoids or within non-lorisid strepsirrhines confidently, given the large intraspecific variation in our quantification of this feature.

The variation in this feature is not well correlated with proportional variation in MTFa or FFa (Table 14). This suggests an alternative, yet complementary, functional explanation. Gebo (1986) suggested the more elliptical shape in anthropoids is a consequence of distal migration of the deltoid ligament, possibly as a result of the ligament becoming more extensive or robust. If compressive stresses centered on the MTF are reduced among anthropoids compared with strepsirrhines, then potentially dislocating tensile stresses may be more frequent. In this case, a more extensive network of collateral ligaments would be beneficial to anthropoids and other taxa utilizing everted foot postures in which the animal's mass and movements do not maintain compressive loading along the medial margin of the talus.

ln[(MTH1)/(MTH2)]. MTH1 is a measure of the dorsoplantar depth of the medial side of the talar body, while MTH2 is a measure of the dorsoplantar depth of the MTF. In cases where the MTF extends onto the neck, it is possible for MTH2 to be greater than MTH1. This variable seems to have the clearest phylogenetic signal at the level of "prosimians" versus anthropoids, as these two groups are mostly non-overlapping (Figs. 7 and 8). Furthermore, though this variable is strongly correlated with both $\ln[(MTFa^{1/2})/(EFa^{1/2})]$ and MTF shape (Table 14), it is not correlated with FFa and does not differentiate any groups within Strepsirrhini or Anthropoidea. Therefore, it would appear to reveal little about diversity in functional demands

on the ankle within major radiations, unlike ln[(MTFa$^{1/2}$)/(EFa$^{1/2}$)], ln[(MTFa$^{1/2}$)/(BM$^{1/3}$)], and ln[(MTF-Perimeter)/(MTFa$^{1/2}$)]. It seems more likely that variation in this feature is only indirectly related to function and driven more directly by correlated traits. Interestingly, several species of anthropoids consistently evoke strepsirrhine-like values, mainly two macaque species. Visual inspection of these bones reveals indeed the MTF to be so plantarly extensive that it broadly contacts the sustentacular facet (Fig. 9c). Qualitative examination of several cercopithecoids not measured in this study reveal the condition also characterizes at least some individuals of *Miopithecus*.

Regression of shape variables and fibular facet against each other

We originally predicted that if MTF proportional variables were related to use of inverted foot postures, then they should correlate with FFa. This prediction was based on the findings of Boyer and Seiffert (2013) who concluded that FFa variation is related principally to variation in demands for inverted postures between haplorhines and strepsirrhines, as well as between small-bodied and large-bodied primates. Broadly speaking, ln[(MTFa$^{1/2}$)/(EFa$^{1/2}$)] and FFa show the predicted pattern of correlation for the hypothesis that both are explained by relative emphasis on inverted foot postures. The lack of a correlation in haplorhines, anthropoids, and platyrrhines is probably explained by the observations above that these groups also exhibit the "reverse from expected" correlation between ln[(MTFa$^{1/2}$)/(EFa$^{1/2}$)] and body mass. Again, the expectation stems from the hypothesis that variation in ln[(MTFa$^{1/2}$)/(EFa$^{1/2}$)] is driven by inversion demands. The lack of correlation between FFa and ln[(MTFa$^{1/2}$)/(EFa$^{1/2}$)] among anthropoids would suggest FFa is the more faithful reflector of pronograde inversion differences in Anthropoidea and its component clades than ln[(MTFa$^{1/2}$)/(EFa$^{1/2}$)] or other MTF variables.

The pattern of correlations between ln[(MTFa$^{1/2}$)/(BM$^{1/3}$)] and FFa tells a more complex story. Generally speaking, these variables are significantly correlated, which would appear to support a functional link in the sense that taxa using more inverted postures have both a larger MTF and a more obtuse FFa. However, because this correlation breaks down for "prosimians" and strepsirrhines, it may be that other behavioral and possibly allometric demands influence the pattern. As discussed above, cheirogaleids, *Daubentonia, Lepilemur* (the "DCL" group), and lorisids, have ln[(MTFa$^{1/2}$)/(BM$^{1/3}$)] ratios that are not different from most anthropoids. Only galagos, indriids and lemurids exhibit elevated values. We suggest that the correlation breaks down in strepsirrhines (and as a result among "prosimians") due to 1) differences in acrobatic hind limb driven leaping (which we argue above is driving MTFa beyond the effects of inversion); and 2) allometry (Table 6) (as discussed above as potentially explaining small MTFs in *Lepilemur* and *Microcebus* despite their proclivity for leaping).

Implications for adaptive trends in primate evolution

Results of recent comparative studies suggest greater parallelism in certain key primate characters than previously thought. While these results may indicate reduced phylogenetic valence for the traits in question, the new patterns often have tangible functional–adaptive implications that enrich understandings of primate evolution. Boyer and Seiffert (2013) and the current study show the ancestral euprimate to a have haplorhine- or plesiadapiform-like FFa, suggesting the "shallowly sloping" strepsirrhine condition is derived. These findings are not particularly surprising and largely confirm early qualitative works. More novel was Boyer and Seiffert's (2013) suggestion that a shallowly sloping fibular facet potentially evolved convergently in notharctine adapiforms, extant strepsirrhines, and other groups based on a haplorhine-like condition in basal notharctines. This pattern may suggest multiple increases of inverted foot postures in early primates, possibly associated with increasing body mass or increasing fine-branch niche specialization. In another example, Boyer et al. (2013a) showed repeated trends of allometrically-corrected elongation of the distal calcaneus that began among stem-primates and continued in parallel among strepsirrhine and haplorhine lineages. They argued these trends in ankle elongation reflect a consistent selective pressure for improved leaping during early primate evolution among multiple primate lineages.

Prior to the publication of these studies, it was reasonable to propose that low FFa is adaptive for, among other things, leaping (Gebo, 2011), and that calcaneal elongation is driven by demands of foot inversion and use of a fine-branch niche (Moyà-Solà et al., 2011). These hypotheses are now apparently refuted if Boyer et al. (2013a) have correctly identified evidence of a leaping signal in calcaneal elongation. If FFa was also explained by leaping, its pattern of variation in the primate clade should closely match that of calcaneal elongation, but it does not (Boyer and Seiffert, 2013; Fig. 10).

According to ASRs, the variables examined here covary more strongly with calcaneal elongation than FFa does. All three variables of this study show a parallel shift in basal strepsirrhines and haplorhines relative to the ancestral euprimate node, that indicate increasingly "prosimian" morphologies. The logic of Boyer et al. (2013a) suggests that these morphological trends represent adaptive responses to similar sets of functional demands in lineages that exhibit them. In discussion above, we are led to interpret our results as indicating that increased MTFa is a correlate of more inverted foot postures, with an added effect of increasing leaping proclivity within strepsirrhines, predicated on their habitual utilization of more strongly inverted postures.[2] A parallel morphological shift in haplorhines and strepsirrhines indicates that both were relying on inverted foot postures to an important degree. There are several additional potential behavioral explanations for these parallel morphological shifts, including 1) shifts into a fine-branch niche, 2) increasing specialization within a fine-branch niche, 3) increases in leaping, or 4) increasing body size that exaggerated the support size differential. Because there is little evidence for a change in body size within these basal lineages (Boyer et al., 2013a), fine-branch

[2]Admittedly, this interpretation should ultimately be tested more rigorously by coding leaping proclivity for taxa in the sample—as done by Boyer et al. (2013a)—and including an interaction term between leaping proclivity and FFa in a general linear model for MFa/BM variation. Given difficulties in coding behavior in an adaptively meaningful way, and due to limited power inherent in statistical analyses relying on the taxonomic and behavioral diversity of primates, we do not, however, see the hypotheses outlined in the discussion to follow as hinging on the results of such an analysis.

niche specialization and leaping increases are more likely alternatives, especially considering congruent evidence of the calcaneus (Boyer et al., 2013a). Nonetheless, the recognition of multiple ecological changes with similar functional-adaptive consequences presents the possibility that parallel morphological trends may reflect different ecological transitions in haplorhines and strepsirrhines. Unless character displacement fortuitously accentuated similar functional tendencies for different ecological demands in basal, sympatric haplorrhine and strepsirrhine lineages, it seems that at least this initial morphological parallelism is more likely to be reflective of behavioral parallelism. Future studies executing ASR of additional traits with different patterns of functional variation can help test this speculation.

If the ancestral euprimate occupied a fine-branch niche, and MTFa and calcaneal elongation have responded similarly to demands for leaping, we would expect broad correlation between the two variables. However, there is some important discordance between trends in calcaneal and MTFa data when more basal lineages on the tree are considered. Unlike the results for calcaneal elongation, MTF variables do not show a consistent trend on the branch leading from stem-primates to the ancestral euprimate node, as we would expect in response to increased (specialization for) leaping. PGLS regressions in *caper* (Orme et al., 2011) of MTF variables against calcaneal elongation values reported by Boyer et al. (2013a) are not significant whether the whole sample or just "prosimians" are analyzed, supporting the perspective that these variables are effectively decoupled in the stem primate lineage, at least.

Furthermore, we reconstruct the ancestral euprimate as having $\ln[(MTFa^{1/2})/(EFa^{1/2})]$ proportions similar to some plesiadapiforms, extant non-primate euarchontans, eosimiids, and most anthropoids. The absence of a trend in MTFa in the stem primate lineage and a relatively small MTFa at the euprimate ancestral node suggest that despite increases in leaping along the primate stem lineage (as indicated by calcaneal elongation), the talus did not reflect this behavioral trend. We postulate that the talus was not affected by these initial behavioral changes due to a lack of strongly inverted foot postures when leaping and landing prior to the radiation of crown primates. That this interpretation emerges is surprising, as it suggests that stem primates would have locomoted in an environment where larger supports and more everted foot postures could usually be relied upon. If primates did not inhabit environments requiring habitually inverted foot postures prior to the radiation of crown lineages, then parallel morphological trends in basal haplorhines and strepsirrhines can be explained as reflecting a transition to a fine branch niche (and potentially an increase in leaping as well), rather than as "refinements" to an already occupied terminal branch niche. To be clear, we do not mean to suggest that stem-primates were incapable of or did not utilize inverted foot postures. Strong evidence of this comes even from the most basal plesiadapiforms (Chester et al., in press). However, as for modern arboreal sciurids and scandentians, inversion was most likely critical mainly for hind foot reversal during downclimbing of large tree trunks (Jenkins, 1974). This interpretation may also imply that fine-branch grasping adaptations of the plesiadapiform *Carpolestes simpsoni* (Bloch and Boyer, 2002) were acquired in parallel to those in euprimates.

The increase in MTFa/EFa from the anthropoid node shared with *Eosimias* to that shared with parapithecoids is actually similar in magnitude to that between crown Haplorhini and Tarsiiformes, and could similarly be correlated with a shift toward greater inversion and/or leaping in early African anthropoids, perhaps reflecting adaptation to arboreal habitats the structure of which was different from those that were available to more basal anthropoids in Asia. Among early African stem anthropoids, both *Proteopithecus* (Simons and Seiffert, 1999; Seiffert and Simons, 2001) and *Apidium* (Fleagle and Simons, 1995) have been interpreted as adept leapers, and appear to be consistent with this hypothesis, though analysis of semicircular canal size suggests that *Apidium* might have been more slow-moving than its postcranial morphology would imply (Ryan et al., 2012).

Based on our results and other recently published studies, we propose the following scenario for primate adaptive origins, assuming that Euarchonta and primates are primitively arboreal radiations (Bloch et al., 2007; Chester et al., in press): 1) Proximal stem- and basal eu-primates experienced selection for more acrobatic locomotor capabilities and responded by increasing ankle elongation (manifested in the calcaneus). Due to retention of an acute FFa and small MTFa as revealed by ASRs of this study, these basal taxa likely did not rely upon small diameter supports and inverted foot postures in a manner or degree comparable to extant strepsirrhines. 2) In haplorhines and strepsirrhines, a shift to relatively smaller diameter supports led to the need for more inverted foot postures and improved hallucal grasping, while benefits of improved leaping were still important, as suggested by continued trends of ankle elongation as well as increasing MTFa. Fine branch clinging and leaping may have led to increased length and robustness of the hallux and increased pressure for improved foot prehensility, necessitating the shift to a tarsifulcrumating foot. Elongate metatarsals in the basal *Teilhardina*-like tarsiiform, *Archicebus* (Ni et al., 2013) and new evidence of similar proportions in *Teilhardina belgica* (Gebo et al., in press) suggest that increased robustness and length of the hallux preceded reduction in non-hallucal metatarsal lengths. While tarsiiforms remained small at this stage, adapiforms began to exploit a large-bodied niche, at which point they experienced selection for a more concave MTF, rotated medial malleolus, and more obtuse fibular facet (Dagosto, 1985).

As in our previous work (Boyer et al., 2013a), the primary biological role of improvements in acrobatics is not indicated by our study and thus we can only speculate on it. Predator escape seems the most generally defensible role (Crompton and Sellers, 2007); however, it would not be surprising if prey capture also drove improved agility in the primate stem and early haplorhines (Boyer et al., 2013b). Our ASRs show the anthropoid lineage would have split from the tarsiiform lineage before the latter obtained a fully "prosimian"-like $\ln[(MTFa^{1/2})/(EFa^{1/2})]$ value (Fig. 10). This suggests that other features implicated in this transition, such as the full expression of "prosimian" hallucal metatarsal morphology (Szalay and Dagosto, 1988) or a tarsifulcrumating foot, were not present at this stage either. Thus, these reconstructions support the notion that anthropoids are postcranially primitive in some aspects of their pedal morphology rather than convergently similar to nonprimate euarchontans. To clarify, our results suggest that eosimiids are unlikely to be derived from a taxon with a fully omomyiform-like talus and calcaneus, even though eosimiid talar morphology has been described as

intermediate between anthropoids and tarsiiforms in some respects (Gebo et al., 2001) (Fig. 11).

Furthermore, our data and interpretations suggest that small-bodied, dentally primitive asiadapines with strongly obtuse FFa and relatively large MTFa (Table 4) are not a good model for the ancestral euprimate, since ASRs predict more acute FFa and relatively small MTFa. Additionally, because asiadapines seem to be generalized arboreal quadrupeds occupying a fine-branch niche, they do not match the behavioral repertoire proposed for the ancestral euprimate based on our data. This is surprising since asiadapines are quite early occurring and primitive in other respects. It may suggest a particularly rapid initial radiation of euprimates, a significant ghost lineage, or that our scenario is incorrect. In contrast to MTFa/EFa ratios, ASR suggests that ln[(MTH1)/(MTH2)] and ln[(MTF-Perimeter)/($MTFa^{1/2}$)] do undergo a "full" reversal in anthropoid origins. Though Shanghuang "protoanthropoid" tali (IVPP V12305 and V12306) and an amphipithecid talus (NMMP 39) were not included in our ASR analyses, they support this hypothesis (if they are indeed basal members of the anthropoid lineage) by virtue of having lower (and more "prosimian"-like) ln[(MTH1)/(MTH2)] values than eosimiids or other anthropoids.

Perhaps the most provocative implication of our scenario is that basal anthropoids and basal euprimates were similar in their postcranial adaptations while many "prosimian" features evolved in parallel among strepsirrhines and tarsiiforms (including omomyiforms). The fact that both stepsirrhine and haplorhine stem lineages show a shift toward a more "prosimian"-like *bauplan* before anthropoids reverse or stop the trend speaks strongly to the role of available substrates (habitat geometry), which may be determined for a taxon as much by its body size as by substrate size and spatial arrangement. Previous scenarios for anthropoid origins positing the defining ecological context as a transition to a diurnal activity pattern in a small-bodied, previously nocturnal lineage that maintained its vision-guided, predatory dietary lifestyle (Ross, 1996) are not impacted by our results. Ross (1996) applied his scenario to the haplorhine stem lineage due to the implication that the common ancestor of tarsiers and anthropoids had already made this transition on account of the retinal foveas exhibited by both groups. The presence of small orbits in *Teilhardina* (Ni et al., 2004) may indicate that this shift happened very basally along the haplorhine stem (clearly even if *Teilhardina* was diurnal, other omomyiforms later radiated back into nocturnal niches [Rosenberger, 2011]). The loss or *cessation of accrual* of "prosimian"-like features may be explainable with regard to these shifts between diurnal and nocturnal lifestyles, if such shifts imposed different substrates, foraging opportunities, or predator risks. Alternatively, it is possible that changes in body size and habitat geometry explain the initial loss of incipiently "prosimian"-like features in the anthropoid stem, particularly if the stem lineage evolved smaller body mass compared with the last common ancestor with tarsiiforms as possibly indicated by the Shanghaung primate fauna (e.g., Gebo, 2004; Gebo et al., 2001, 2012a).

ACKNOWLEDGMENTS

We would like to thank many people for access to scans and specimens: the American Museum of Natural History and the Smithsonian Institution National Museum of Natural History for access to extant and fossil specimens, L. Marivaux (for scans of *Djebelemur* and *Necrolemur*), S. Moyà Solà (for scans of *Anchomomys*), K. D. Rose (for the loan of *Cantius* and Vastan material), K. C. Beard et al. (for scans of eosimiids), T. Smith (for access to new *Teilhardina* material), P. Holroyd (UCMP omomyids), H. Covert (UCM omomyids), G. Gunnell (for access to DPC holdings), Stephen Chester (for *Ptilocercus*, some plesiadapiforms, and access to his facilities), B. A. Patel and C. Orr (many catarrhine specimens), Anne Su (many hominoid specimens), C. Gilbert for access to his facilities, and E. Delson, Will Harcourt-Smith, and Lissa Tallman (for scans of hylobatids and *Homo*). The associate editor and two reviewers (one anonymous and one self-identified as Laurent Marivaux) read and provided helpful feedback on earlier versions of this manuscript, which greatly improved the result. Ian Wallace executed and processed scans at Stony Brook University's Center for Biotechnology, Morgan Hill executed scans at AMNH's Microscopy and Imaging Facility, and Jimmy Thostenson executed scans at MIF and Duke University's Shared Microscopy and Instrumentation Facility.

LITERATURE CITED

3D Systems Inc. 2013. Geomagic studio. Rock Hill: 3D Systems Inc.

Arnold C, Matthews LJ, Nunn CL. 2010. The 10kTrees website: a new online resource for primate phylogeny. Evol Anthropol 19:114–118.

Beard KC, Dagosto M, Gebo DL, Godinot M. 1988. Interrelationships among primate higher taxa. Nature 331(6158):712–714.

Beard KC, Tong YS, Dawson MR, Wang JW, Huang XS. 1996. Earliest complete dentition of an anthropoid primate from the late middle Eocene of Shanxi Province, China. Science 272(5258):82–85.

Bloch JI, Boyer DM. 2002. Grasping primate origins. Science 298:1606–1610.

Bloch JI, Silcox MT, Boyer DM, Sargis EJ. 2007. New Paleocene skeletons and the relationship of plesiadapiforms to crown-clade primates. Proc Natl Acad Sci USA 104:1159–1164.

Boyer DM, Seiffert ER. 2013. Patterns of astragalar fibular facet orientation in extant and fossil primates and their evolutionary implications. Am J Phys Anthropol 151:420–447.

Boyer DM, Seiffert ER, Simons EL. 2010. Astragalar morphology of *Afradapis*, a large adapiform primate from the earliest late Eocene of Egypt. Am J Phys Anthropol 143:383–402.

Boyer DM, Seiffert ER, Gladman JT, Bloch JI. 2013a. Evolution and allometry of calcaneal elongation in living and extinct primates. PLoS ONE 8(7):e67792. doi:10.1371/journal.pone.0067792

Boyer DM, Yapuncich GS, Chester SGB, Bloch JI, Godinot M. 2013b. Hands of early primates. Yearb Phys Anthropol 57:33–78.

Chester SGB, Bloch JI, Boyer DM, Clemens WA. in press. Oldest known euarchontan postcrania and affinities of Paleocene *Purgatorius* to Primates. Proc Natl Acad Sci USA doi:10.1073/pnas.1421707112

Crompton RH, Sellers WI. 2007. A consideration of leaping locomotion as a means of predator avoidance in prosimian primates.In: Gursky S, Nekaris K, editors. Primate anti-predator strategies. Berlin: Springer. p 127–145.

Dagosto M. 1985. The distal tibia of primates with special reference to the Omomyidae. Int J Primatol 6:45–75.

Dagosto M. 1988. Implications of postcranial evidence for the origin of euprimates. J Hum Evol 17:35–56.

Dagosto M. 1990. Models for the origin of the anthropoid postcranium. J Hum Evol 19:121–139.

Dagosto M. 2007. The postcranial morphotype of primates.In: Ravosa MJ, Dagosto M, editors. Primate origins: adaptation and evolution. Chicago: Springer. p 489–534.

Demes AB, Gunther MM. 1989. Biomechanics and allometric scaling in primate locomotion and morphology. Folia Primatol 53:125–141.

Engqvist L. 2005. The mistreatment of covariate interaction terms in linear model analyses of behavioral and evolutionary ecology studies. Anim Behav 70:967–971.

Fleagle JG. 1985. Size and adaptation in primates.In: Jungers WL, editor. Size and scaling in primate biology. New York: Plenum Press. p 1–19.

Fleagle JG, Simons EL. 1995. Limb skeleton and locomotor adaptations of *Apidium phiomense*, an Oligocene anthropoid from Egypt. Am J Phys Anthropol 97:235–289.

Franzen JL, Gingerich PD, Habersetzer J, Hurum JH, von Koenigswald W, Smith BH. 2009. Complete primate skeleton from the middle Eocene of Messel in Germany: morphology and paleobiology. PLoS ONE 4(5):e5723.

Freckleton RP. 2009. The seven deadly sins of comparative analysis. J Evol Biol 22(7):1367–1375.

Gebo DL. 1985. The nature of the primate grasping foot. Am J Phys Anthropol 67:269–277.

Gebo DL. 1986. Anthropoid origins - the foot evidence. J Hum Evol 15:421–430.

Gebo DL. 1987a. Functional anatomy of the tarsier foot. Am J Phys Anthropol 73:9–31.

Gebo DL. 1987b. Locomotor diversity in prosimian primates. Am J Primatol 13:271–281.

Gebo DL. 1988. Foot morphology and locomotor adaptation in Eocene primates. Folia Primatol 50:3–41.

Gebo DL. 1989a. Locomotor and phylogenetic considerations in anthropoid evolution. J Hum Evol 18:201–233.

Gebo DL. 1989b. Postcranial adaptation and evolution in Lorisidae. Primates 30(3):347–367.

Gebo DL. 1993. Functional morphology of the foot in Primates. In: Gebo DL, editor. Postcranial adaptation in nonhuman primates. DeKalb: Northern Illinois University Press.

Gebo DL. 2004. A shrew-sized origin for Primates. Yearb Phys Anthropol 47:40–62.

Gebo DL. 2011. Vertical clinging and leaping revisited: vertical support use as the ancestral condition of strepsirrhine primates. Am J Phys Anthropol 146:323–345.

Gebo DL, Schwartz GT. 2006. Foot bones from Omo: implications for hominid evolution. Am J Phys Anthropol 129:499–511.

Gebo DL, Dagosto M, Beard KC, Qi T, Wang JW. 2000. The oldest known anthropoid postcranial fossils and the early evolution of higher primates. Nature 404(6775):276–278.

Gebo DL, Dagosto M, Beard KC, Qi T. 2001. Middle Eocene primate tarsals from China: implications for haplorhine evolution. Am J Phys Anthropol 116(2):83–107.

Gebo DL, Dagosto M, Ni X, Beard KC. 2012a. Species diversity and postcranial anatomy of Eocene primates from Shanghuang, China. Evol Anthropol 21:224–238.

Gebo DL, Smith T, Dagosto M. 2012b. New postcranial elements for the earliest Eocene fossil primate *Teilhardina belgica*. J Hum Evol 65:305–218.

Gebo DL, Smith R, Dagosto M, Smith T. in press. Additional postcranial elements of *Teilhardina belgica*, the oldest European primate. Am J Phys Anthropol doi:10.1002/ajpa.22664

Gunnell GF. 2002. Notharctine primates (Adapiformes) from the early to middle Eocene (Wasatchian–Bridgerian) of Wyoming: transitional species and the origins of *Notharctus* and *Smilodectes*. J Hum Evol 43:353–380.

Hammer Ø, Harper DAT, Ryan PD. 2006. PAST: paleontological statistics software package for education and data analysis. 1.43 ed. Oslo: University of Oslo.

Hanna JB, Schmitt D, Griffin TM. 2008. The energetic cost of climbing in primates. Science 320:898.

Janečka JE, Miller W, Pringle TH, Wiens F, Zitzmann A, Helgen KM, Springer MS, Murphy WJ. 2007. Molecular and genomic data identify the closest living relative of primates. Science 318(5851):792–794.

Jenkins FA. 1974. Tree shrew locomotion and the origins of primate arborealism.In: Jenkins FA, editor. Primate locomotion. New York: Academic Press. p 85–115.

Jouffroy FK, Berge C, Niemitz C. 1984. Comparative study of the lower extremity in the genus *Tarsius*.In: Niemitz C, editor. Biology of the tarsiers. New York: Gustav Fischer. p 167–190.

Kay RF. 1975. The functional adaptations of primate molar teeth. Am J Phys Anthropol 43:195–216.

Kay RF. 2015. Biogeography in deep time - what do phylogenetics, geology, and paleoclimate tell us about early platyrrhine evolution? Mol Phylogenet Evol 82(Part B):358–374. dx.doi.org/10.1016/j.ympev.2013.12.002.

Kay RF, Ross CF, Williams BA. 1997. Anthropoid origins. Science 275:797–804.

Kirk EC, Williams BA. 2011. New adapiform primate of Old World affinities from the Devil's Graveyard Formation of Texas. J Hum Evol 61:156–168.

Maddison WP, Maddison DR. 2011. Mesquite: a modular system for evolutionary analysis. Version 2.75. http://mesquiteproject.org.

Marigó J, Minwer-Barakat R, Moyà-Solà S. 2013. *Nievesia sossisensis*, a new anchomomyin (Adapiformes, Primates) from the early Late Eocene of the southern Pyrenees (Catalonia, Spain). J Hum Evol 64:473–485.

Marigó J, Roig I, Seiffert ER, Moyà-Solà S, Boyer DM. in review. Astragalar and calcaneal morphology of the middle Eocene primate *Anchomomys frontanyensis* (Anchomomyini): implications for early primate evolution. J Hum Evol.

Marivaux L, Chaimanee Y, Ducrocq S, Marandat B, Sudre J, Soe AN, Tun ST, Htoon W, Jaeger JJ. 2003. The anthropoid status of a primate from the late middle Eocene Pondaung Formation (Central Myanmar): tarsal evidence. Proc Natl Acad Sci USA 100(23):13173–13178.

Moyà-Solà S, Kohler M, Alba DM, Roig I. 2012. Calcaneal proportions in primates and locomotor inferences in *Anchomomys* and other Palaeogene euprimates. Swiss J Paleontol 131:147–159.

Napier JR, Walker AC. 1967. Vertical clinging and leaping - a newly recognized category of primate locomotion. Folia Primatol 6:204–219.

Ni X, Wang Y, Hu Y, and Li C. 2004. A euprimate skull from the early Eocene of China. Nature 427:65–68.

Ni X, Gebo D, Dagosto M, Meng J, Tafforeau P, Flynn JJ, Beard KC. 2013. The oldest known primate skeleton and early haplorhine evolution. Nature 498(7452):60–64.

Orme CDL, Freckleton RP, Thomas G, Petzoldt T, Fritz SA, Isaac N, Pearse W. 2011. Caper: comparative analysis of phylogenetics and evolution in R. Meth Ecol Evol 3(1):145–151.

Pagel M, Meade A. 2013. BayesTraits v2 manual.

Rambaut A, Drummond A. 2009. Tracer v1.5.

Rasoazanabary E. 2010. The human factor in mouse lemur (*Microcebus griseorufus*) conservation: local resource utilization and habitat disturbance at Beza Mahafaly, SW Madagascar. Amherst: University of Massachusetts.

Roberts TE, Lanier HC, Sargis EJ, Olson LE. 2011. Molecular phylogeny of treeshrews (Mammalia: Scandentia) and the timescale of diversification in Southeast Asia. Mol Phylogenet Evol 60(3):358–372.

Rose KD, Chester SGB, Dunn RH, Boyer DM, Chew AE, Bloch JI. 2011. New fossils of the oldest North American euprimate *Teilhardina brandti* (Omomyidae) from the Paleocene-Eocene Thermal Maximum. Am J Phys Anthropol 146:281–305.

Rosenberger AL. 2011. *Strigorhysis*: another large-eyed Eocene North American fossil tarsiiform. Anat Rec 294:797–812.

Ross CF. 1996. Adaptive explanation for the origins of the Anthropoidea (Primates). Am J Primatol 40:205–230.

Ryan TM, Silcox MT, Walker A, Mao X, Begun DR, Benefit BR, Gingerich PD, Köhler M, Kordos L, McCrossin ML, Moyà-Solà S, Sanders WJ, Seiffert ER, Simons E, Zalmout IS, Spoor F. 2012. Evolution of locomotion in Anthropoidea: the semicircular canal evidence. Proc R Soc B 279:3467–3475.

Seiffert ER, Simons EL. 2001. Astragalar morphology of late Eocene anthropoids from the Fayum Depression (Egypt) and the origin of catarrhine primates. J Hum Evol 41:577–605.

Seiffert ER, Simons EL, Fleagle JG, and Godinot M (2010) Paleogene anthropoids. In: Werdelin L, Sanders WJ, editors Cenozoic Mammals of Africa. Berkeley: University of California Press. p 369–391.

Simons EL, Seiffert ER. 1999. A partial skeleton of *Proteopithecus sylviae* (Primates, Anthropoidea): first associated dental and postcranial remains of an Eocene anthropoidean. C R Acad Sci Paris IIA 329:921-927.

Smith RJ, Jungers WL. 1997. Body mass in comparative primatology. J Hum Evol 32:523–559.

Springer MS, Teeling EC, Madsen O, Stanhope MJ, de Jong WW. 2001. Integrated fossil and molecular data reconstruct bat echolocation. Proc Natl Acad Sci USA 98:6241–6246.

Springer MS, Meredith RW, Gatesy J, Emerling CA, Park J, Rabosky DL, Stadler T, Steiner C, Ryder OA, Janečka JE, Fisher CA, Murphy WJ. 2012. Macroevolutionary dynamics and historical biogeography of primate diversification inferred from a species supermatrix. PLoS ONE 7(11):e49521.

Strait DS, Grine FE. 2004. Inferring hominoid and early hominid phylogeny using craniodental characters: the role of fossil taxa. J Hum Evol 47(6):399–452.

Szalay FS, Dagosto M. 1980. Locomotor adaptations as reflected on the humerus of Paleogene primates. Folia Primatol 34:1–45.

Szalay FS, Dagosto M. 1988. Evolution of hallucal grasping in the Primates. J Hum Evol 17(1-2):1–33.

Tacutu R, Craig T, Budovsky A, Wuttke D, Lehmann G, Taranukha D, Costa J, Fraifeld VE, de Magalhães JP. 2013. Human Ageing Genomic Resources: integrated databases and tools for the biology and genetics of ageing. Nucleic Acid Res 41:D1027–D1033.

Tornow MA. 2008. Systematic analysis of the Eocene primate family Omomyidae using gnathic and postcranial data. Bull Peabody Mus Nat Hist 49:43–129.

Visualization Sciences Group. 2009. AVIZO, version 6.0. Burlington: Mercury Computer Systems.

White TD, Folkens PA. 2010. The Human Bone Manual. Amsterdam: Elsevier.

Winchester JM, Boyer DM, Cooke SE, St. Clair EM, Ledogar JA, Gosselin-Ildari AD. 2014. Dental topography of platyrrhines and prosimians: convergence and contrasts. Am J Phys Anthropol 153(1):29–44.

Yapuncich GS, Boyer DM. 2014. Interspecific scaling patterns of talar articular surfaces within Euarchonta. J Anat 224(2): 150–172.